Università di Pisa

Department of Physics

Master's Degree in Physics
Curriculum of Theoretical Physics

Topological properties of

Shiba chain

with orbital degrees of freedom

Graduation Session July 21st, 2016
Academic Year 2015/2016

Candidate:
Gian Marcello Andolina

Supervisor:
Prof. Pascal Simon

Internal Supervisor:
Prof. Ettore Vicari

Abstract

Topological superconductors are new materials that can host exotic quasiparticles at their edges called **Majorana fermions** (MFs). MFs are particles which are their own antiparticles. They may be useful for quantum computation since they obey non-abelian statistics. In order to achieve experimentally topological superconductivity a convenient direction is to combine well established materials to engineer this exotic superconductivity. One promising approach is to utilise magnetic impurities on top of a superconductor that can host MFs. This system can be theoretically described using the **Shiba chain Hamiltonian** in the dilute limit, or using the **quantum wire Hamiltonian** in the dense limit. In the literature, the intermediate regime has not been studied. In this work, we aim to filling this gap.

In this thesis, we study more complex and realistic models to describe a chain of magnetic atoms on top of a superconductor by taking into account the different impurity orbital degrees of freedom. Therefore, due to the impurity orbital overlap one has a 1D conduction band on top of the superconductor coexisting with the magnetic moments that can create a 1D Shiba band into the superconductor. The main original result of this thesis is the derivation of an effective low-energy *Kitaev-like* Hamiltonian that describes the system as two 1D coupled channels.

Thanks to this model we achieved the main goal of this thesis: we are able to derive the **phase diagram** of the system by computing numerically the winding number w that shows that the system has different topological phases characterized by the presence (or absence) of multiple MFs. We discuss the role of disorder showing that the existence of multiple MF is related with the presence of the effective time-reversal symmetry. Finally, we study how the phase diagram changes in the small magnetization limit $J'S \ll t_w$. Our final statement is that the system can be topological and can host multiple MFs for certain conditions.

Acknowledgements

I would like to thank Prof. Pascal Simon for the opportunity he gave me to work in the frame of his team. I was delighted in trying to solve the physical problem he assigned to me and I am very grateful with him for all the time and effort he employed to improve my work. I would like to thank all the members of the Pascal team, foremost Olesia, for her strong will to help me in the improvement of the present thesis. I would like to thank Sebastien for the useful chats we had in the time I spent in the team and for the attempt to make me properly learn French, without success. I would also like to thank Mircea for the nice chats we had.
I would like to thank the internal Director of the present Thesis, Prof. Vicari, for his advice despite the bureaucratic nuisances he suffered to let me live this wonderful experience at Paris. Moreover, I want to thank all the students of the LPS for the nice moments we shared together. The hospitality you showed me during these months provided me with the opportunity to spend a really nice permanence in the Laboratory; it is not an obvious achievement, given the complete absence of proper coffee deserving this name.
I want to thank my family. You gave me all the support a son could ask for during his first permanence in a faraway country. I want to thank all the people who spent with me some time along the last six years in Pisa. I must definitively start thanking the Spezia gang: in these years we have studied, we have eaten, we have even slept, we have (disputed) argued, constantly together. I want to also thank Alessandro and the whole bunch of friend from La Spezia for their friendship and the support they provided to me. I want to finally thank Giulia: this thesis would never have existed without you.

Finally, I would like the Physics department of Pisa for the Erasmus grant that supported me while I was working on this project.

Contents

Chapter 1

Introduction

In the last couple of decades, condensed matter theory experiences huge developments on the relatively new field of topological materials.
Before the discovery of topological order, it was believed that all phases could be characterized by spontaneous symmetry-breaking. All of the symmetry-breaking orders can be understood in terms of Landau's approach: the phase transition can usually be characterized by a local order parameter $\phi(x)$, which is not invariant under the relevant symmetry of the Hamiltonian. The expectation value of this parameter has to be zero outside the ordered phase, while it is non-zero in the ordered phase. Landau's symmetry breaking theory points out that different phases are different because they have different symmetry. Over the past 30 years, the study of the quantum Hall effect led to a different classification paradigm based on the notion of topological order [1].

The notion of topological order was developed when it became clear that the criterium of symmetry breaking was not sufficient to characterize all phases when quantum systems are concerned. A topological system contains different phases at zero temperature which have the same symmetry. Thus, those phases cannot be distinguished by symmetries and cannot be described by Landau's symmetry breaking theory.
The first discovered example of a topologically ordered phase is the quantum Hall effect [2]. As the name suggests, such a phase has a Hall conductance quantized in integer multiplied by the constant $e^2/\hbar$ and cannot change unless the perturbations become sufficiently large. In order for a state to be robust against any local perturbations, two conditions must be satisfied: first, should exist an energy gap separating the ground-state from the excited states, i.e. the Hamiltonian of the system is gapped; second, long-range correlations within the system are also

necessary. The energy gap prevents the perturbation from exciting the particles away from the ground-state, while the long-range correlations protect the phase of the system from local perturbations. The topological order provides this two ingredients and protect the ground state against local perturbations.

In this thesis, we will only deal with a specific one-dimensional (1D) system and analyze its topological properties. It turns out that the intrinsic topological order can only exist in dimensions higher than one [3, 4]. Nevertheless, a weaker topological order - the so-called symmetry-protected topological (SPT) order - can be found in one dimension (as well as higher dimensions). A system is said to have SPT order if it has a gap and the Hamiltonian has some discrete symmetries. The SPT order is characterized by the following properties:

- Two copies of the system, each in different SPT phases, cannot be smoothly transformed into each other while preserving the symmetries unless the energy gap closes.
- All phases can be continuously transformed into the same trivial state equivalent to the vacuum by breaking the symmetries [46].

Two systems with the same symmetries are said to be topologically equivalent if there exists a path between their respective Hamiltonians in the space of all Hamiltonian' s parameters such that the gap does not close at any point along the transformation.
The most common classification scheme of SPT phases is the one introduced by Schnyder, et al based on the Altland-Zirnbauer symmetry classes in random matrix theory [5–7]. Materials are classified into ten different categories depending on three discrete symmetries: time reversal symmetry (TRS), particle-hole symmetry (PHS) and chiral or sub-lattice symmetry (SLS). These symmetries restrict the form of a real-space Hamiltonian as follows:

$$\begin{aligned} &\text{TRS:} \quad \mathcal{T}H^T\mathcal{T}^{-1} = H \qquad \mathcal{T}^\dagger\mathcal{T} = 1, \\ &\text{PHS:} \quad \mathfrak{C}H^T\mathfrak{C}^{-1} = -H \qquad \mathfrak{C}^\dagger\mathfrak{C} = 1, \\ &\text{SLS:} \quad C_sHC_s^{-1} = -H \quad C_s^\dagger C_s = 1, \end{aligned} \tag{1.1}$$

where $\mathcal{T}$ and $\mathfrak{C}$ are anti-unitary operators and C_s is a unitary matrix.

In SPT ordered materials the non-trivial phases are characterized by the presence of quasiparticle excitations at their edges. In the next section, we shall discuss a

	TRS	PHS	SLS	$d = 1$
A(unitary)	0	0	0	-
AI (orthogonal)	+1	0	0	-
AII (symplectic)	-1	0	0	-
AIII	0	0	1	$\mathbb{Z}$
BDI	+1	+1	1	$\mathbb{Z}$
CII	-1	-1	1	$\mathbb{Z}$
D	0	+1	0	$\mathbb{Z}_2$
C	0	-1	0	-
DIII	-1	+1	1	$\mathbb{Z}_2$
CI	1	-1	1	-

Table 1.1: Classification of topological insulators and superconductors in one dimension. In the first three columns, 0 indicates the absence of the symmetry, whereas ± 1 indicates presence of a symmetry with the symmetry operator squaring to ± 1. In the last column, the symbol indicates the number of topologically distinct phases; a dash indicates a trivial system, whereas $\mathbb{Z}_2$ allows two different phases and $\mathbb{Z}$ any integer number. In this thesis, we will treat only systems in the BDI and the D class. (in red)

specific type of zero-energy quasiparticle that occurs as a localized edge state in some topological materials, namely the Majorana fermions (MFs).

To see how zero-energy modes can appear in topological phases, we will exploit the following argument: two gapped systems are topologically equivalent if we can adiabatically map the Hamiltonians of the two systems without any gap closing. Let us now imagine a system made up of two subsystems in different topological phases with an interpolating region in between. By definition, we cannot smoothly go from one subsystem to the other without closing the gap somewhere between them. This means that there must be a zero-energy mode at the interface separating them. The vacuum can also be thought as topologically trivial. We thus expect zero-energy states to localize at the edges of any topologically non-trivial sample, with *open boundary conditions*. This is called the *bulk-boundary correspondence*: a topologically non-trivial bulk comes with edge modes when the sample has open boundary conditions. Regardless of the nature of these edge states, we can conclude that since they follow from the topology of the system, they are robust and they only vanish if the system is driven out of its non-trivial phase.

1.1 Majorana fermions

The Dirac equation describes fermionic particles (such as electrons) and it predicts the existence of their antiparticles (such as positrons). In 1937, Ettore Majorana

showed that is possible to find a real solution to the Dirac equation. A real solution describes a particle, which is its own antiparticle [8].
This can be understood rewriting the Dirac equation in the Majorana representation, where all Γ matrices are purely imaginary.
In this representation, the Dirac equation

$$\left(i\partial_\mu \Gamma^\mu_M - \frac{mc}{\hbar}\right)\Psi_M = 0, \tag{1.2}$$

becomes a real differential equation for Ψ_M , the Dirac spinor in Majorana representation.
Since in this representation the Dirac equation Eq:(1.2) is invariant under the complex conjugation, if Ψ_M is a solution of this equation, so is its complex conjugate Ψ^*_M. In quantum field theory, a real solution $\Psi_M = \Psi^*_M$ represents its own antiparticle, and has been dubbed a Majorana fermion after its proposer. Since Majorana fermions are their own antiparticles, they have to be uncharged, but do carry a momentum and spin.
In the second quantization formalism it can be shown that every ordinary fermions can be decomposed in two Majorana operators. As a first step, we consider some ordinary (i.e. non-Majorana) fermions that are created by the second-quantized operators $c_i^\dagger$. Being fermions, these operators obey the anticommuting relation $\{\, c_i^\dagger, c_j \,\} = \delta_{i,j}$. From every such operator, two independent Majorana fermions can be constructed:

$$\begin{aligned} \gamma_{i,1} &= c_i^\dagger + c_i, \\ \gamma_{i,2} &= i(c_i^\dagger - c_i). \end{aligned} \tag{1.3}$$

These new operators satisfy the relation:

$$\begin{aligned} \gamma_{i,n}^\dagger &= \gamma_{i,n}, \\ \{\, \gamma_{i,n}, \gamma_{j,m} \,\} &= \delta_{i,j}\delta_{n,m}, \end{aligned} \tag{1.4}$$

and thus describe fermionic particles that are their own antiparticles. As a result, every regular fermion can be decomposed into two Majorana fermions. Vice versa, two Majorana fermions can be combined into one regular fermion. In case the initial fermion is charged, such as an electron, its charge must be absorbed into some other degrees of freedom as one goes from electronic operators to Majorana

operators. Superconductors, where particle number and charge are not conserved, are thus natural candidates for hosting Majorana fermions, as charge can simply be absorbed into the superconducting condensate. As we will discuss, MFs can be found as edge states of certain exotic superconductors.
Despite the intense effort from generations of physicists, the experimental detection of Majorana fermions remained elusive for a long time. At this moment, none of the elementary particles of the standard model is currently supposed to be a Majorana fermion.
Nevertheless, the neutrino is usually suspected to be Majorana fermion in nature. There are indeed key aspects of the neutrino that are still unknown (such as its mass) because of its weak interactions and the relative difficulties in quantitative observations. Furthermore, the weak interaction violates parity and therefore right-handed neutrinos (and left handed anti-neutrinos) have no interaction. Therefore, it is unknown if those states are unobservable or if they simply do not exist. [23]

1.1.1 Majorana fermions in condensed matter

Recently the idea of Majorana fermions was resurrected in the context of condensed matter. The MF can be realized as a quasiparticle excitation in a superconductor. A superconductor is a natural environment for Majorana because quasiparticle contains both electron and hole degrees of freedom. Holes can be viewed as electrons antiparticles.
We will introduce in details the Bogoliubov-de Gennes (BdG) mean field formalism for superconductivity in the section 2.2. For now it is sufficient to say that an excitation in a superconductor can be described with the Bogoliubov quasiparticle:

$$\gamma_E = \sum_i u_{E,i} c_i + v_{E,i} c_i^\dagger, \tag{1.5}$$

where i runs over all the sites and spins index. $u_E(v_E)$ is the electron (hole) components. The BdG formalism also provides the so-called particle-hole symmetry (PHS) (see section 2.2.2), which it can be expressed as:

$$\gamma_E^\dagger = \gamma_{-E}. \tag{1.6}$$

It seems that a good candidate is a quasiparticle with zero energy (a so-called zero mode). However, it is not always possible to impose the Majorana condition for a

zero mode. For example in a spin-singlet superconductor we have:

$$\gamma_\sigma = \sum_i u_i c_{i,\sigma} + v_i c^\dagger_{i,-\sigma}, \tag{1.7}$$

where σ is the spin index $\uparrow, \downarrow$ and i is the site index. For this kind of excitation the PHS reads $\gamma^\dagger_{E,\sigma} = \gamma_{-E,-\sigma}$, so the quasiparticle and the anti-quasiparticle do not contain the same electron-hole operator and then it is not possible to create a Majorana fermion. In conclusion, a spin singlet superconductor does not allow the formation of Majorana fermions.
From this, it seems that the most natural context where we can find MFs is exotic superconductivity e.g. p-wave or spinless superconductivity.
As we will discuss in detail in section 2.1, Kitaev [9] showed in 2001 that a 1D Hamiltonian of spinless fermions with superconductivity can host Majorana zero mode excitation, on finite system. In this model, the Majorana excitations at the end of the superconducting chain $\gamma_{1,1}$ and $\gamma_{N,2}$ form a very delocalized electron $c_M = \gamma_{1,1} + i\gamma_{N,2}$, which seems robust to any small perturbation.
On more practical purposes, MFs have non-abelian statistics meaning that particle exchanges are non-trivial operations which in general do not commute. The braiding of MFs can thus offer a natural platform for fault-tolerant quantum computation [11]. In contrast with ordinary quantum computation, quantum computation would require less quantum error corrections since MFs are immune to local noise due to their non local topological nature.

1.1.2 Physical realisation

Even if the Kitaev model in Eq.(2.1) is a toy model, we can still ask ourself if there is a realistic system that can be described by the Kitaev model at low-energy. We can enumerate the main properties that characterize the Kitaev Hamiltonian:

1. A 1D system
2. An effective band of spinless fermions
3. Superconductivity

We are looking for a realistic system that share these three fundamental proprieties with Kitaev Hamiltonian.

- **Spin-orbit nanowire**: One of the most promising proposal having these three ingredients is a semiconducting nanowire with a large spin-orbit coupling on top of a s-wave superconductor and under the effect of a magnetic

field. The spin-orbit coupling and the Zeeman field provide an effective spinless band. The superconductivity is provided by proximity effect: if the contact between the wire and the superconductor is clean, a Cooper pair can tunnel between the two systems. Such model has received a lot of attention due its simple ingredients. In 2012, the Kouwenhoven's group [12] conducted measurements on InSb nanowires contacted by a normal and a superconducting electrode, see Fig.1.1.2. Through tunnelling spectroscopy, they detected a zero-bias peak (ZBP) in the conductance $G = \frac{dI}{dV}$ for intermediate-strength magnetic fields, as seen in Fig. 1.1.2 .The conductance in this case can be seen as a direct measure of the density of states DOS. The peak was observed only when the theoretical requirements for the presence of Majorana bound states were fulfilled, indicating a possible discovery of the Majorana quasiparticles. However, various alternative explanations for the observed ZBPs have been suggested, such as zero-bias Kondo peaks [13, 14] and disorder [15, 16], and the experiment is therefore not fully conclusive.

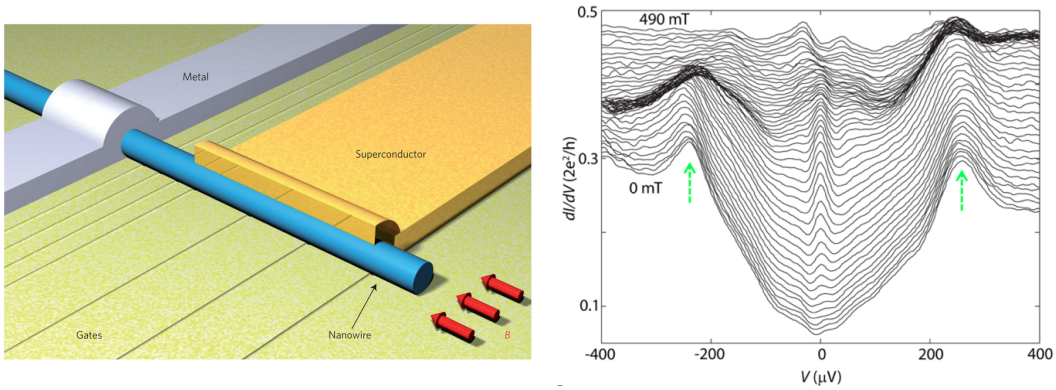

Figure 1.1: Experimental setup (on the left) and differential conductivity (on the right)of an InSb nanowire on an s-wave superconductor with Rashba spin-orbit as a function of gate voltage and magnetic field. Different lines correspond to magnetic fields from 0 to $490mT$in steps of $10mT$, with offset added for clarity; the green arrows indicate the edges of the gap. Relevant parameters are $T = 70mK$, $\Delta \approx 250\mu eV$ Figure taken from ref. [12].

- **Magnetic nanowire**: another realistic system can be a nanowire with magnetic spin texture: instead a strong spin-orbit coupling an helical magnetic field $B_h(x)$ provide the same spectrum and the same zero energy edge state.The helical field can be engineered by nano magnets or can emerge from helical spin chains due to RKKY interaction. [34, 36] This system is equivalent to spin-orbit nanowire after an unitary transformation which transforms one in the other.

- **Shiba band**: Isolated magnetic impurities in a superconductor give rise to so-called Shiba states, a bound state whose energy is inside the superconducting gap [24]. The spatial extent of their long-range wavefunction has been recently characterized experimentally [32] in 2D superconductors. Magnetic impurities can be regarded as the building blocks to engineer topological superconductivity in a controlled way. The presence of an array of helical magnetic impurities, in the dilute limit these bound states give rise to bands which can be in some topological phase supporting Majorana fermions [26]. In addition to the fact that their energy is zero, another property of Majorana bound states in one-dimensional systems is that they are expected to be localized at the ends of the wire, which should also be observable experimentally. In 2014, the Yazdany's group [17] conducted a new experiment in which they measured the spatially resolved differential conductance, which can be seen as a direct measure of the local density of states LDOS in Fe-based atomic chains on a Pb superconductor. They also observed ZBPs, which, as seen in Fig. 1.1.2 are clearly located at the ends of the wires. However, the topological nature of the zero-bias peaks is to be proven [18]: in particular, under certain conditions zero-bias peaks may be located at the ends of the chain even in the absence of Majorana modes [19].

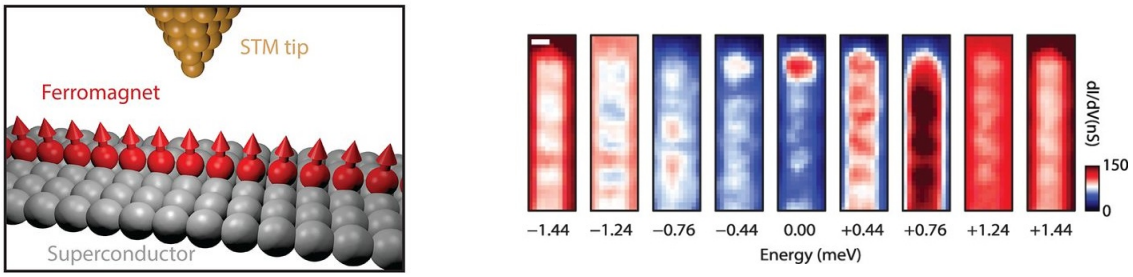

Figure 1.2: Experimental setup (on the left) and conductance map (right) of a Fe atomic chain on top of a Pb superconductor. Relevant parameters are $\Delta = 1.36meV$, $T = 1.45K$ The grey scale bar is of length 10Å. The conductance shows a zero-bias peak localized at the end of the chain, while higher-energy modes are delocalized. Figures taken from ref. [17]

However, there is not general agreement in how this experimental setup has to be theoretically described. Yazdani's group [17] describes it using a Shiba Hamiltonian [26], i.e. taking the diluite limit. In this situation the low-energy Hamiltonian is focused on the electrons in the superconductor.

Another approach is to take the dense limit to describe the same situation and model the magnetic impurities as a local Zeeman field [20]. In this case the low-energy model take in account only the electron localized on the magnetic impurities. Nowadays, the same experimental setup is described with two very different models and the question is still debate. Both predict the presence of MFs. The Shiba Hamiltonian predict a MF localized on the superconductors, the dense limit Hamiltonian host the MF on the electron on the magnetic impurity at the edge. Nowadays the experimental accuracy required to distinguish the two cases is not yet achieved. Another important problem is that most of the parameter that are important to chose correctly the model are not experimentally accessible. The whole interpretation of the experimental result is *model dependent*. In this thesis, we try to fill this gap between this two models.

1.1.3 Our theoretical model

In this thesis, we investigate more complex and realistic models to describe a chain of magnetic atoms on top of a superconductor by taking into account the different impurity orbital degrees of freedom. These orbitals may play an important role in the intermediate regime between the dilute and the dense limit. Due to the overlap between impurities orbital, these electrons form a 1D conduction band on top of the superconductor (forming effectively a 1D conducting wire). This band coexists also with the magnetic moments (formed in another orbitals) that creates a 1D Shiba band into the superconductor. Therefore, our starting point is that these two 1D conducting channels are present. In some limits we will derive an effective model to describe these two 1D coupled channels. In the literature the experimental setup of Yazdany's group [17] is described in the dilute limit with the Shiba chain Hamiltonian [26], or with the magnetic wire [39], in the dense limit. The model that we shall derive in the following can be a good description in the intermediate regime. We will try to answer to the following questions:

- Are there any values of the Hamiltonian's parameters that make the system topologically non-trivial?
- Can this system support pairs of Majorana fermions at its edges or does two MFs annihilate each others?
- Are these Majorana excitations robust against perturbations? Is there any kind of small perturbations that can easily destroy the MFs?

We will give our answers in the final chapter 7.

1.2 Outline of the work

In the follow we will explain the structure of this thesis chapter by chapter.

Chapter 2 In this chapter, we give an overview of the literature of topological superconducting systems. In section:2.1 we introduce the Kitaev model, as a paradigm for one dimensional systems that can host MFs. After an introduction of this toy model we give an overview of the main realistic systems: in section 2.3 we introduce the **spin-orbit nanowire**, this system made by a one dimensional semiconducting wire proximitized with a superconductor is one of the most promising setup to realize MFs. After that, we proceed to introduce the **Shiba bound state** that will be the environment of the entire thesis: a single magnetic impurity on top of a superconducting substrate give rise of a quasiparticle bounded to the impurity, the so-called *Shiba state*. After that we show that, taking some limits, a 1D chain of magnetic impurities can be described by an effective Kitaev-like Hamiltonian and can host MFs.
The goal of this chapter to summarise the literature relevant for the next chapter.

Chapter 3 This chapter is the core of this thesis and is devoted to describe a chain of magnetic atoms on top of a superconductor by taking into account the different impurity orbital degrees of freedom. We start from the case of a single adatom in section 3.1, in order to understand the scale of the relevant energy in this problem. Then we explain in section 3.2 details of our starting model of a chain of magnetic impurities. Its originality is to taking into account more orbital degrees of freedom. In section 3.3, we derive an effective model that can describe the system at low-energy respect to the superconducting gap $\epsilon \ll \Delta$. The derivation of the effective model in Eq:(3.36) is one of the main goal of the thesis. In section 3.4, we comment on the behaviour of our effective model, discussing how it depends of main parameters. After that we discuss the topological class of the system and how the relaxation of our main hypotheses can affect our system. In section 3.4.2, we discuss the role of the disorder, showing that some kind of disorder in the orientation of the magnetic impurities can affect strongly the system, destroying multiple MFs.

Chapter 4 In this chapter, we study numerically the Shiba chain and the orbital (or wire) part as non-interacting. This is a study of the models already used in the literature. For our system this case does not have any physical meaning, however this two uncoupled models are studied in literature and the goal of this chapter is to introduce and to test the numerical tools that we will use in the following two chapters. In section 4.1, taking periodic boundary conditions we are able to take the Fourier transform of our Hamiltonian. In $k-$space we are able to calculate the winding number w, a topological index, that classifies the phases of the system. Thanks to the bulk-boundary correspondence the number w is equal to the number of edge states (MFs, in our case).

Chapter 5 This chapter, together with chapter 3, represents the main new result of this thesis: using numerics we will explore the phase diagram of the Hamiltonian in Eq:(3.36). Because this is a original model all the results are unprecedented. Calculating the winding number we are able to classify the distinct phase of the system. Looking at the spectrum we show that the number of the crossing between the energy $h(k)$ and the Fermi level is related to the winding number and can be a simple criteria to understand the phase transition. In conclusion we find that the system can be topological and can host multiple MFs, when the helical magnetic order is perfect and disorder does not affect the system. Our model can accommodate up to three Majorana excitation: two localized on the Shiba chain and one on the orbital wire.

Chapter 6 In this chapter, we discuss how the relaxation of large magnetization limits can affect our result: previously we assumed that the magnetic impurities polarize the orbital electrons. Now we study the case where the orbital wire is a spinful system. A spinful system is affected by proximity s-wave superconductivity and the presence of the s-wave gap, will affect the system avoiding any topological gap inversion. The conclusion of this chapter is that this system is topologically trivial in the orbital sector.

Conclusions In chapter 7, we summarize our main result about our system and try to answer to the initial questions.

1.2.1 Original contents

Here we shall list the most relevant original results of this thesis:

- The contents of chapter 3.2 where we derive an effective low-energy Hamiltonian Eq:(3.36) that describes the low-energy excitations.
  The whole Hamiltonian reported in appendix F is original. The initial study of a single adatoms is original.
- All the phase diagrams and numerics of the chapters 6 and 5 are new.
- In the appendix E.0.1 we derived the Shiba tight-binding Hamiltonian [26] as a projection on the wavefunction. The result is already know in the literature but the procedure it is original and it is also used in the derivation of the Hamiltonian Eq:(3.36) in the chapter 3.2 .

Chapter 2

Topological superconductivity: an overview

In this chapter, we will give an overview of topological superconducting systems, which can host Majorana fermions (MFs). In section 2.1, we will start from a toy model introduced by Kitaev [9] which is the paradigm of one dimensional systems that can host Majorana excitations.
After that, in order to treat more realistic systems, in section 2.2 we will introduce the BCS theory for a superconductor and the Bogoliubov-de Gennes (BdG) mean-field description.
Once we have introduced the formalism and main concepts of superconductivity, we can analyse the main realistic system which can emulate a Kitaev-like Hamiltonian. The main experimental proposals are:

- **Nanowire** : in section 2.3, we will give an overview about nanowires. These systems are made by a one dimensional semiconducting wire in proximity of a superconductor are one of the most promising setup to realize MFs.

- **Shiba chain**: in the section 2.4, we introduce the so-called **Shiba Physics**. A single magnetic impurity on top of a superconducting substrate gives rise of a quasiparticle bounded to the impurity, the so-called **Shiba state**. After that we show that, in some limits, a 1D chain of magnetic impurities can be described by an effective Kitaev-like Hamiltonian able to host MFs.

In conclusion, the main goal of this chapter is to summarize the literature relevant for the following of the thesis.

2.1 Kitaev Hamiltonian

2.1.1 Fermionic and Majorana operators

In this section, we will study the Kitaev model, which describes some spinless fermions with a mean-field pairing term Δ and a hopping t. We will show that this model has two different topological phases: one trivial and other one is characterized by the presence of Majorana zero modes, when open boundary conditions are taken. These two different phases can be distinguished also in a large system with periodic boundary conditions by the topological index w.

The following Kitaev model arises as a paradigm for 1D systems supporting Majorana fermions (see [9]):

$$H = \sum_{j=1}^{L-1}\Big(-t(a_{j+1}^{\dagger}a_j + a_j^{\dagger}a_{j+1}) + \Delta a_j a_{j+1} + \Delta^* a_{j+1}^{\dagger}a_j^{\dagger}\Big) - \sum_{j=1}^{L}\mu\Big(a_j^{\dagger}a_j - \frac{1}{2}\Big). \tag{2.1}$$

This Hamiltonian describes a chain of spinless electron a_j with a chemical potential μ, a hopping t and a superconducting term Δ. It was argued that such system can host Majorana zero-energy excitations localized at the edge of the system. We can formally define Majorana operators as:

$$\gamma_{2j-1} = a_j + a_j^{\dagger}, \quad \gamma_{2j} = i(a_j^{\dagger} - a_j) \qquad (j = 1, ..., L), \tag{2.2}$$

which satisfy the relations:

$$\gamma_j = \gamma_j^{\dagger}, \quad \{\,\gamma_j, \gamma_k\,\} = 2\delta_{j,k}, \qquad (j, k = 1, ..., 2L). \tag{2.3}$$

The Kitaev Hamiltonian can be recast in the form:

$$H = \frac{i}{4}\sum_{m,n=1}^{2N} A_{m,n}\gamma_m\gamma_n, \tag{2.4}$$

Note that, at this level, any quadratic Hamiltonians can be written in terms of Majorana operator. We can start to study two simple case:

a)

$$\Delta = t = 0, \qquad\qquad \mu < 0,$$

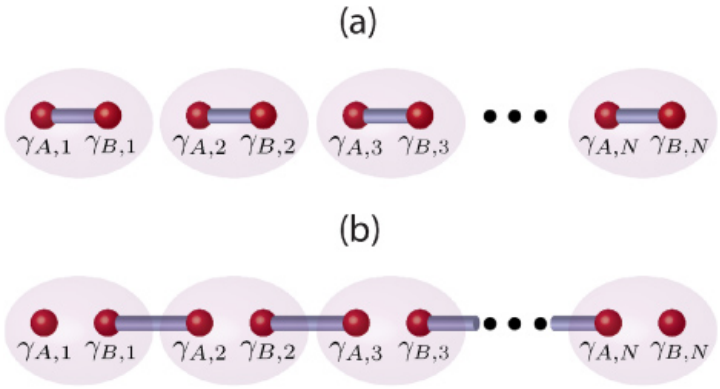

Figure 2.1: Figure from [10]: a pictorial representation of the two phases of the system. Red balls represent the Majorana operators. Pink cloud represents the electron formed by the combination of two Majorana operators.

Then the Hamiltonian reads:

$$H = -\sum_{j=1}^{L} \mu(a_j^\dagger a_j - \frac{1}{2}) = \frac{i}{2}\sum_{j=1}^{2L}(-\mu\gamma_{2j-1}\gamma_{2j}),$$

The ground state has zero occupation number and represent the vaacum, and the Hamiltonian couples γ_{2j-1} and γ_{2j} from the same site j in a single isolated electron.

b)

$$\Delta = t > 0, \qquad \mu = 0,$$

The Hamiltonan reads:

$$H = \frac{it}{2}\sum_{j=1}^{2L-1}(\gamma_{2j}\gamma_{2j+1}), \tag{2.5}$$

This Hamiltonian couples the Majorana operators from different sites, we can define new fermionic operators $\tilde{a}$, which combine c from different sites: $\tilde{a}_j = \frac{1}{2}(\gamma_{2j} + i\gamma_{2j+1})$ and $\tilde{a}_j^\dagger = \frac{1}{2}(\gamma_{2j} - i\gamma_{2j+1})$. The Hamiltonian becomes:

$$H = 2t\sum_{j=1}^{L-1}(\tilde{a}_j^\dagger\tilde{a}_j - \frac{1}{2}),$$

The energy cost to create a fermion $\tilde{a}_j$ is $2t$. Then, we have a ground state

with zero occupation number, but the fermion $\tilde{a}_L = \frac{1}{2}(\gamma_{2L} + i\gamma_1)$ is totally missing from the Hamiltonian, so occupying this states requires zero energy. Therefore, we have a two degenerate ground state (GS). The application of the operator γ_{2L} or γ_1 shift between the two GS. This states are highly nonlocal since γ_{2L} and γ_1 operators are localized on opposite ends of the chain.

We are tempted to define something like a single Majorana quasiparticle counted by a Majorana number operator $\hat{n}_i^{MF} = \gamma_i^\dagger \gamma_i$. With this definition we find that $\hat{n}_i^{MF} \equiv 1$, independently of the state, which makes no sense [21].

These previous two cases represent two different phases, with similar bulk properties. The boundary properties are clearly different: only the latter has unpaired Majorana fermions at the ends of the chain.

2.1.2 General solution and winding number

Here we follow the analysis of [29]: in order to study the bulk properties in the general case, we take the Fourier transform of the fermionic operators:

$$a_j = \frac{1}{\sqrt{L}} \sum_k e^{ikj} a_k, \quad k = n\frac{\pi}{L}, \tag{2.6}$$

We have take periodic boundary condition ($a_0 = a_{L+1}$) in order to restore traslational invariance which makes k a good quantum number. That operation removes edge states. However, we can still introduce a topological invariant that reveals the presence of edge state, thanks to the bulk-boundaries correspondence. Without the trivial constant $\sum_j \frac{\mu}{2}$ the Hamiltonian becomes:

$$\begin{aligned} H &= \frac{1}{2} \sum_k \begin{pmatrix} a_k^\dagger & a_{-k} \end{pmatrix} \begin{pmatrix} -\mu - 2t\cos(k) & 2i\Delta\sin(k) \\ -2i\Delta\sin(k) & \mu + 2t\cos(k) \end{pmatrix} \begin{pmatrix} a_k \\ a_{-k}^\dagger \end{pmatrix}, \\ &= \frac{1}{2} \sum_k \begin{pmatrix} a_k^\dagger & a_{-k} \end{pmatrix} H_k \begin{pmatrix} a_k \\ a_{-k}^\dagger \end{pmatrix} \end{aligned} \tag{2.7}$$

.

The bulk spectrum is:

$$E_{\pm}^2(k) = (2t\cos(k) + \mu)^2 + 4\Delta\sin^2(k),$$

The gap closes when $k = 0$ and $\mu = -2t$ or $k = \pi$ and $\mu = 2t$.
We can rewrite the Hamiltonian in the Pauli matrices basis τ:

$$H_k = h_2(k)\tau_2 + h_3(k)\tau_3, \tag{2.8}$$

Where $h_2(k) = 2\Delta\sin(k)$ and $h_3(k) = -\mu - 2t\cos(k)$. The Hamiltonian unit vector $\hat{\mathbf{h}}(k) = \mathcal{N}\begin{pmatrix} h_2(k) & h_3(k) \end{pmatrix}$ define a map $T^1 \longrightarrow S^1$, so we can characterize that with a winding number w.
The winding number of a two dimensional vector $\mathbf{r} = \Big(x(t), y(t)\Big)$ parametrised by $t \in [0, 2\pi)$, with $\mathbf{r}(0) = \mathbf{r}(2\pi)$, is:

$$w = \frac{1}{2\pi}\int_0^{2\pi} dt \frac{\dot{y}x - y\dot{x}}{r^2}, \quad r^2 = y^2 + x^2. \tag{2.9}$$

The computation of the winding number is simply the counting of how many times the two dimensional vector $\mathbf{r}(\mathbf{t})$ wraps the origin.

In our case we can simplify the expression using the Brouwer degree of curves [29] defined by:

$$\begin{aligned} w &= -\frac{1}{2}\sum_{k\in\ker(h_2(k))} sgn[\partial_k h_2(k) h_3(k)], \\ &= \frac{1}{2}[sgn(2t+\mu) + sgn(2t-\mu)], \end{aligned} \tag{2.10}$$

When $|2t| < |\mu|$ the winding number is zero and there are no edge states. When $|2t| > |\mu|$ the winding number is one and there are Majorana edge states. If $|2t| = |\mu|$ the gap closes and the winding number is not defined. See Fig:2.2
We have found the edge states in the case $w = \Delta, \mu = 0$, that is in the phase characterized by $|2t| > |\mu|$. But changing adiabatically the Hamiltonian we cannot remove this edge states without closing the gap. Then we can conclude that the phase $w = 1$ is characterized by edge states. [1]

[1] Few words for the follow: if the Kitaev Hamiltonian is chosen with only real parameters, it posses both particle-hole symmetry and time-reversal symmetry. Then the Hamiltonian is in the BDI class Tab:1 with a $\mathbb{Z}$ invariant. Nevertheless, we can use the $\mathbb{Z}_2$ invariant because in the absence of long-range coupling both invariants will give the same result.

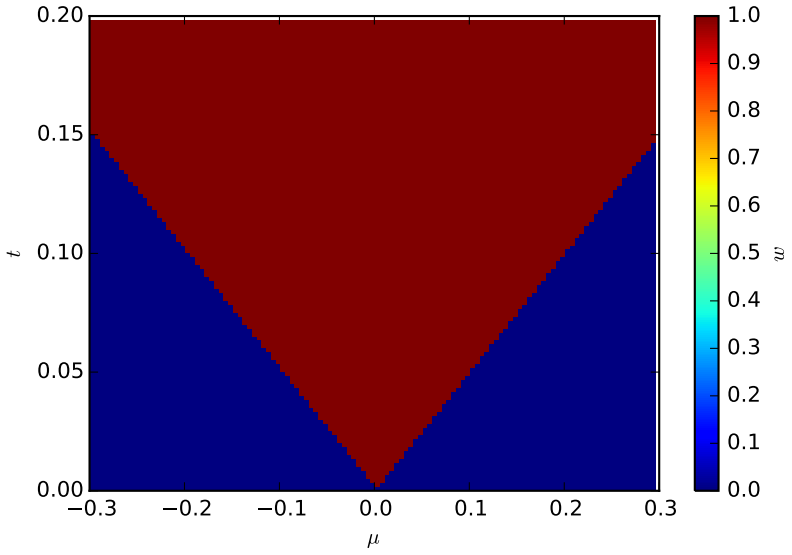

Figure 2.2: The winding number w as a function of μ and t. Red part is the topological non-trivial phase.

There is another way to distinguish the topological phase form the trivial one, we can calculate a Majorana number $\mathcal{M}(H)$ associated with the Hamiltonian. [9, 22] $\mathcal{M}(H)$ is $+1$ if the Hamiltonian is in a trivial phase and -1 if it is in topological one. Kitaev proves that [9]:

$$\begin{aligned} \mathcal{M}(H) &= sgn\{\, Pf(A)\,\}, \\ P(H) &= sgn\{\, Pf(A)\,\}, \end{aligned} \tag{2.11}$$

Where A is skew-symmetric matrix in Eq:2.4, and P is the fermion parity of ground state. If we take a translation invariant system, and define the Fourier Transform of A as $A\tilde{(k)}$, we have:

$$\mathcal{M}(H) = sgn\{\, Pf(A\tilde{(0)})Pf(A\tilde{(\pi)})\,\}, \tag{2.12}$$

Kitaev showed that this equation can be simplified as:

$$\mathcal{M}(H_0) = (-1)^{\nu(\pi)-\nu(0)}, \tag{2.13}$$

where $\nu(k)$ is number of negative eigenvalues of H_0 at point k . The interval $[0, \pi/a]$ is half Brillouin zone (BZ) arising from discrete Fourier transform. Then, $\nu(\pi) - \nu(0)$ correspond to number (mod (2)) of Fermi points, the intersection points between the Fermi level and the energy bands, in the half BZ. See Fig: 2.3 Now, we can summarize the condition to get Majorana fermions:

1. Spinless or triplet superconductivity.
2. Bulk gap.
3. Odd number of Fermi points in half the BZ.

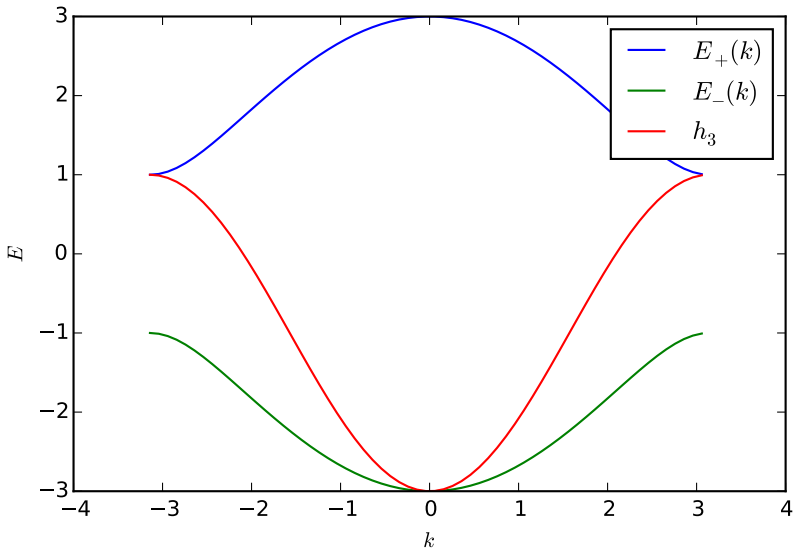

Figure 2.3: The spectrum of the Kitaev Hamiltonian in k-space for $t = \Delta = \mu = 1$, h_3 has one zero in half BZ.Then, we are in non-trivial topological phase.

2.2 Brief introduction to superconductivity

In this section, we introduce the microscopic theory of the superconductivity, the BCS theory. We also introduce the formalism of mean field theory in this context: the Bogoliubov-de Gennes (BdG) approximation. This will be the framework of the entire thesis. This formalism artificially doubling the degree of freedom and this redundancy introduces a new "symmetry": the particle-hole symmetry (PHS). This introduction does not aim at a detailed presentation of superconductivity but only introduce the few concepts necessary for the understanding of the rest of the thesis.

Superconductivity is a phenomenon of zero electrical resistance and expulsion of magnetic fields occurring in certain materials when cooled below a characteristic critical temperature. It was discovered by Heike Kamerlingh Onnes on 1911 in Leiden. In 1957 Bardeen, Cooper, and Schrieffer published an article [40,41] which contains what is now know as the BCS theory of superconductivity. The BCS theory is related to an idea of Cooper: he showed that an attractive interaction between a pair of electrons with energies close to Fermi energy, would condense in a so-called Cooper pair, with lower energy than free electrons. The BCS theory extend this idea to all the electrons close to Fermi energy, because all electrons near the Fermi surface condense in Cooper pairs with lower energy. This open a gap between the Fermi energy and highest occupied energy. This gap Δ is a priori empty of single particle states.In order to create excitations in the material, the energy needed must be larger than the superconducting gap.

2.2.1 Bogoliubov-de Gennes Hamiltonian

The BCS theory can be formulated in the second quantization formalism by defining the fermionic creation operator $a^\dagger_{\mathbf{k},\sigma}$ and $a_{\mathbf{k},\sigma}$ for an electron with momentum $\mathbf{k}$ and spin $\sigma =\uparrow,\downarrow$. These operator satisfy the commutation rules:

$$\{\, a^\dagger_{\mathbf{k},\sigma}, a_{\mathbf{k}',\sigma'} \,\} = \delta_{\mathbf{k},\mathbf{k}'}\delta_\sigma\sigma', \quad \{\, a_{\mathbf{k},\sigma}, a_{\mathbf{k}',\sigma'} \,\} = 0. \tag{2.14}$$

In absence of phonon coupling the free Hamiltonian is given by:

$$T = \sum_{\mathbf{k},\sigma}\left(\frac{k^2}{2m} - \mu\right) a^\dagger_{\mathbf{k},\sigma} a_{\mathbf{k},\sigma}, \tag{2.15}$$

where μ is chemical potential, which describes the energy cost of adding a particle in the system. To obtain the BCS Hamiltonian, we also add the phonon coupling:

$$H = T + \sum_{\mathbf{k},\mathbf{k}'}\left(U_{\mathbf{k},\mathbf{k}'} a^\dagger_{\mathbf{k},\uparrow} a^\dagger_{-\mathbf{k},\downarrow} a_{\mathbf{k}',\downarrow} a_{\mathbf{k}',\uparrow}\right), \tag{2.16}$$

The interaction is phonon mediated and is an attractive potential when $|\xi_{\mathbf{k}}| = |\frac{k^2}{2m} - \mu| < \omega_D$ and $|\xi_{\mathbf{k}'}| < \omega_D$, where ω_D is the Debye frequency. At a temperature below the critical one, electrons condense in Cooper pairs giving a non-zero ground-state expectation value $\langle a^\dagger_{\mathbf{k},\uparrow} a^\dagger_{-\mathbf{k}}\rangle$. Neglecting the fluctuations around this expectation value, we can rewrite our Hamiltonian as:

$$H = T - \sum_{\mathbf{k}} \Delta_{\mathbf{k}} a^{\dagger}_{\mathbf{k},\uparrow} a^{\dagger}_{-\mathbf{k},\downarrow} + h.c., \tag{2.17}$$

$$\Delta_{\mathbf{k}} = \sum_{\mathbf{k}'} U_{\mathbf{k},\mathbf{k}'} \left\langle a_{\mathbf{k}',\uparrow} a_{-\mathbf{k}',\downarrow} \right\rangle . \tag{2.18}$$

In the mean-field description, the electron number $\hat{N}$ is evidently no longer conserved. However, the parity operator $\mathcal{P} = (-)^{\hat{N}}$ is still conserved. This Hamiltonian can be diagonalized by the introduction of the so-called Nambu spinors. Permuting the ladders operators, we can rewrite the Hamiltonian as:

$$H = \frac{1}{2} \sum_{\mathbf{k}} \begin{pmatrix} a^{\dagger}_{\mathbf{k},\uparrow} & a_{-\mathbf{k},\downarrow} \end{pmatrix} \begin{pmatrix} \xi_{\mathbf{k}} & \Delta_{\mathbf{k}} \\ \Delta^{*}_{\mathbf{k}} & -\xi_{-\mathbf{k}} \end{pmatrix} \begin{pmatrix} a_{\mathbf{k},\uparrow} \\ a^{\dagger}_{-\mathbf{k},\downarrow} \end{pmatrix} + \frac{1}{2} \sum_{\mathbf{k}} \xi_{\mathbf{k}}, \tag{2.19}$$

where $\Psi^{T}_{\mathbf{k}} = \begin{pmatrix} a^{\dagger}_{\mathbf{k},\uparrow} & a_{-\mathbf{k},\downarrow} \end{pmatrix}$ is the Nambu spinor. Neglecting the constant, we can rewrite the Hamiltonian in terms of Pauli matrix τ_i, acting on Nambu spinors.

$$\begin{aligned} H &= \frac{1}{2} \sum_{\mathbf{k}} \Psi^{\dagger}_{k} \mathcal{H}^{\mathrm{BdG}}_{\mathbf{k}} \Psi_{k} + \mathrm{cost}, \\ \mathcal{H}^{\mathrm{BdG}}_{\mathbf{k}} &= \xi_{\mathbf{k}} \tau_z - \Delta_{\mathbf{k}} \tau_x . \end{aligned} \tag{2.20}$$

Squaring the Hamiltonian we obtain the spectrum $E_k = \pm\sqrt{\xi^2_{\mathbf{k}} + \Delta^2_{\mathbf{k}}}$ These eigenvalues tell us two important things about the superconductor: first, as long as $\Delta_{\mathbf{k}}$ is non vanishing, it defines an energy gap separating the valence (negative energies) and conductance (positive energies) bands. Second, for each energy level E, there is a corresponding energy level at $-E$, which is due to the artificial doubling the degrees of freedom. This redundancy is usually named particle hole symmetry (PHS). Let us analyse in a more general system the meaning of PHS.

2.2.2 Particle-hole symmetry

Taking the mean field approximation, the Hamiltonian of a superconductor can always be written in the BdG form:

$$H_{BdG} = \frac{1}{2} C^{\dagger} \mathcal{H} C, \tag{2.21}$$

where $C = \begin{pmatrix} \mathbf{c} \\ \mathbf{c}^\dagger \end{pmatrix}$ and $\mathbf{c}$ is a column which contains annihilation operators of all sites. The more general Bogoliubov-deGennes Hamiltonian is

$$\mathcal{H} = \begin{pmatrix} H_0 & \Delta \\ \Delta^\dagger & -H_0^* \end{pmatrix}, \tag{2.22}$$

where H_0 is the single particle Hamiltonian and Δ is the superconducting coupling in mean field approximation. We define $\mathfrak{C}$, the charge conjugation operator as:

$$\mathfrak{C} c \mathfrak{C}^{-1} = c^\dagger, \tag{2.23}$$

$\mathfrak{C}$ transforms a particle in a hole and vice versa. Charge conjugation is a symmetry of the Hamiltonian:

$$[\mathfrak{C}, H] = 0, \tag{2.24}$$

with hermiticity of the Hamiltonian we have :

$$\begin{aligned} &\mathfrak{C} = \tau_1 K \\ &\{\, \mathcal{H}, \mathfrak{C} \,\} = 0, \end{aligned} \tag{2.25}$$

where K is the complex conjugate operator and τ_1 is a Pauli matrix acting on the Nambu space. For this symmetry any states has a particle-hole conjugate with opposite energy. We are explicitly considering the hole states by artificially doubling the spectrum. Then the particle-hole symmetry (PHS) [2] relates the particle and hole states, preserving the correct number of independent states. We take the Shrodinger equation $\mathcal{H}\Psi = E\Psi$ with $\Psi = \begin{pmatrix} \mathbf{u} \\ \mathbf{v} \end{pmatrix}$.

If Ψ is an eigenfunction with energy E, then $\mathfrak{C}\Psi = \begin{pmatrix} \mathbf{v}^* \\ \mathbf{u}^* \end{pmatrix}$ is an eigenfunction with energy $-E$. Another representation of solution is Bogoliubov quasiparticle operator:

$$\gamma_E^\dagger = \sum_i \left(v_{i,E} c_i + u_{i,E} c_i^\dagger \right), \tag{2.26}$$

[2] Despite the name PHS is not a proper symmetry: the relation between the state at energy E and $-E$ is due to a mathematical artifact to resolve BdG Hamiltonian and it is a redundancy rather than a proper Symmetry.

Due to PHS, for a spin-less electron we have $\gamma_E^\dagger = \gamma_{-E}$. Because the ground state is defined by $\gamma_E |GS\rangle = 0, \forall E > 0$, we can write the gound state in terms of vacuum of usual electrons $|0\rangle$:

$$|GS\rangle = \prod_{E<0} \gamma_E^\dagger |0\rangle . \tag{2.27}$$

We did not consider zero energy quasiparticle. Due the PHS this is a Majorana operator:

$$\gamma_0^\dagger = \gamma_0. \tag{2.28}$$

In presence of zero mode, γ_0 shifts one ground state to the other:

$$|GS'\rangle = \gamma_0 |GS\rangle \quad \text{and} \quad |GS\rangle = \gamma_0 |GS'\rangle . \tag{2.29}$$

Therefore we cannot speak about a quasiparticle because we cannot count it: due to the anticommutation $\hat{n}_{\gamma_0} = \gamma_0^\dagger \gamma_0 \equiv 1$, independently to the state. In that sense γ_0 is not really a fermionic operator. A better name would be Majorana zero modes rather than Majorana fermion.

2.3 Realistic setup: quantum nanowire

As we wrote in the introduction, there are some systems which can be described by the Kitaev Hamiltonian, as a low-energy effective Hamiltonian. In this section, we describe in details how the spin-orbit coupling (SOC) and a Zeeman field can provide an effective spinless band. We derive how effective p-wave superconductivity can arise as low-energies description. After that, we will discuss the equivalence between SOC and the helical magnetic field in 1D. Finally, we mention how this helical spin texture can arise in a realistic system.

2.3.1 Spin-orbit nanowire

Here we follow [29] for a description of the spin-orbit wire.
The continuum version of the Kitaev Hamiltonian (2.1) is:

$$H = \int dx \Psi^\dagger(x) \left(\frac{p_x^2}{2m} - \mu \right) \Psi(x) + \Psi^\dagger(x) p_x \Delta \Psi(x) + h.c, \tag{2.30}$$

Where $\Psi(x)$ creates an electron at the position x. p_x is the momentum operator, m and μ are the effective mass and the chemical potential. Δ is the p-wave superconducting gap.
A p-wave spinless superconductor is described by that Hamiltonian. As we showed this system can host Majorana Fermions. We show below that a semiconductor with strong spin-orbit coupling, in a presence of a magnetic Zeeman field B, proximitized by a s-wave superconductor can be described by an effective Hamiltonian like (2.30) for some parameters.
The system is described by the Hamiltonian:

$$H_{wire} = \int dx \Psi^\dagger(x) \left(\frac{p_x^2}{2m} - \mu + \tilde{\alpha} p_x \sigma_y + \tilde{B}_z \sigma_z \right) \Psi(x), \tag{2.31}$$

where we have taken $\hbar = 1$, and $\tilde{\alpha}$ is strength of Rashba spin-orbit, and $\tilde{B}_z = g\mu_B B_z$ is the applied Zeeman field. The pairing Hamiltonian reads

$$H_\Delta = \Psi_\uparrow(x) \Delta \Psi_\downarrow(x) + h.c, \tag{2.32}$$

H_Δ crudely models the tunnelling of Cooper pairs from the superconductor into the wire. It can be shown that it arises as an effective low-energy coupling (see the Appendix A and [25] for a more detailed discussion). We can rewrite the Hamiltonian in BdG form, doubling the number of degrees of freedom:

$$\begin{aligned} &H_{BdG} = \frac{1}{2} \int \Phi(x)^\dagger \mathcal{H} \Phi(x) dx, \\ &\text{with } \Phi(x)^\dagger = \left(\Psi_\uparrow^\dagger(x), \Psi_\downarrow^\dagger(x), \Psi_\downarrow(x), -\Psi_\uparrow(x) \right), \\ &\mathcal{H} = \left(\frac{p^2}{2m} - \mu + \tilde{\alpha} p \sigma_2 \right) \tau_1 + \tilde{B} \sigma_3 - \Delta \tau_1, \end{aligned} \tag{2.33}$$

Squaring twice, the Hamiltonian we find the bulk spectrum:

$$E_\pm^2 = \xi_p^2 + \alpha^2 + B^2 + \Delta^2 \pm 2(\xi_p^2 \alpha^2 + \xi_p^2 B^2 + \Delta^2 B^2)^{\frac{1}{2}}, \tag{2.34}$$

with $\xi_p = \frac{p^2}{2m} - \mu$. We note that E_+ and E_- are related by PHS. For now we set μ to zero. Now we try to justify how it is possible that the low-energy description of this system is a Kitaev-like Hamiltonian. When there is no magnetic field and no superconductivity the effect of the spin-orbit coupling is to shift the two parabolas of the free electron gas into two separate parabolas, whit the spin along y as a good quantum number$|k, s_y = \pm\rangle$. The Zeeman field along x-axis open a

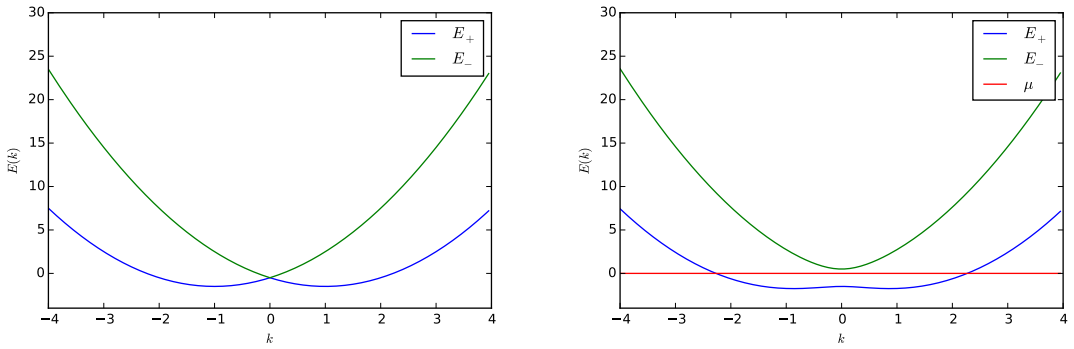

Figure 2.4: Left: The spectrum of free electron gas with a spin-orbit coupling α which splits the two parabolas. Right: Magnetic field B opens a gap at $k = 0$. When μ is between the two bands it is possible to project on the lower band $E_-(k)$.

gap at $k = 0$ and with the opportune tuning of the chemical potential the system can be described as spinless. There are two gaps in the system one at the Fermi momentum p_F , $\Delta(p_F) \sim \Delta$ and one at $p = 0$: $\Delta(0) = B - \sqrt{(\mu^2 + \Delta^2)}$. When $\Delta(0)$ change sign we are in a topological phase. More formally, it can be shown on the lattice, with spacing a, that:

$$\mathcal{M}(H) = sgn(\mu^2 - B^2 + \Delta^2)sgn((t-\mu)^2 - B^2 + \Delta^2), \tag{2.35}$$

For experimental consideration $t \sim \frac{1}{ma^2}$ is typically much larger than other parameters so the condition to have a topological phase reduces to $B^2 > \mu^2 + \Delta^2$. Setting $\Delta = 0$, our Hamiltonian and associated eigenfunctions in k-space read:

$$H = \frac{k^2}{2m} + \alpha\sigma_x k - B\sigma_z, \qquad E_\pm(k) = \frac{k^2}{2m} \pm \sqrt{(\alpha k)^2 + B^2}, \tag{2.36}$$

$$|\chi_+\rangle = \left(\sin(\tfrac{\gamma(k)}{2}), \cos(\tfrac{\gamma(k)}{2})\right), \qquad |\chi_-\rangle = \left(\cos(\tfrac{\gamma(k)}{2}), -\sin(\tfrac{\gamma(k)}{2})\right),$$

where $\gamma(k) = \arctan(\frac{k\alpha}{B})$. Assuming that the pairing is very weak with respect to $|E_+ - E_-|$ we can project the entire Hamiltonian on the lower band $(-)$, in the limit $\alpha \ll Bk_F$ $(\sin(\gamma(k)) \approx \frac{\alpha k}{B})$,we can write the projected Hamiltonian as:

$$H = \int \frac{dk}{2\pi}\left(E_-\psi_-(k)^\dagger\psi_-(k) + \Delta\frac{\alpha}{B}\psi_-(k)k\psi_-(-k) + h.c.\right), \tag{2.37}$$

Thus, we have obtained an effective 1D p-wave superconductivity for spinless electrons as a low-energy projection. Therefore, we can expect that this system can host MFs with the appropriate choice of parameters.
Indeed, a numerical calculation (with $B^2 > \mu^2 + \Delta^2$) shows MF in local DOS as depicted in Fig: 2.5.

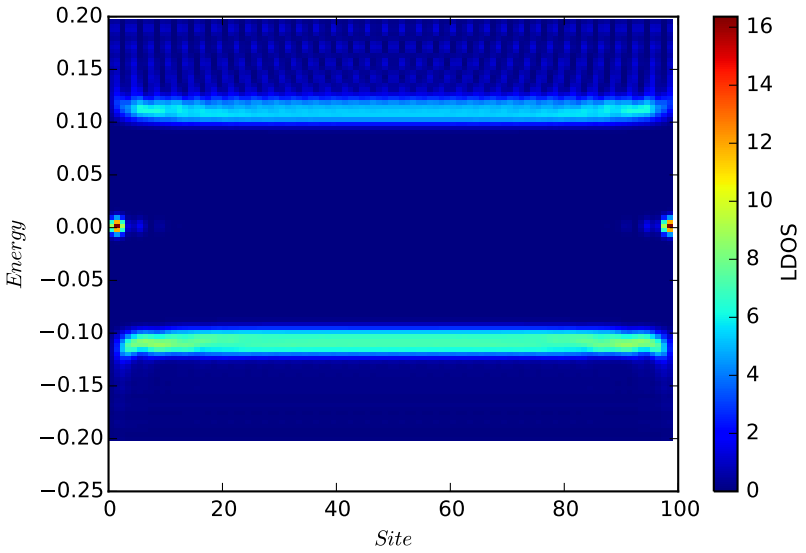

Figure 2.5: LDOS of the Hamiltonian (2.33), with $t = 1, B = 0.4, \Delta = 0.3, \alpha = 0.2, \mu = 0$. We can see MF as zero-energy states localized at the end of the wire.

2.3.2 Equivalence between spin-orbit and helical magnetic field

Another possible realisation of Eq:(2.30) is performed by a spiral magnetic field $B(x)$. Following the reference [34] we show that a non-uniform magnetic field is equivalent in 1D (for the spectrum) to both spin-orbit coupling and uniform Zeeman field. Starting from the previous Spin-orbit Hamiltonian:

$$H_0 = \int dx \Psi^\dagger(x) \left(\frac{p_x^2}{2m} + \frac{k_{SO}}{m} p_x \sigma_z - B\sigma_x \right) \Psi(x), \tag{2.38}$$

we can perform an unitary transformation in order to remove the spin-orbit coupling:

$$\Psi(x) = U(x)\Phi(x), \text{ with } \quad U(x) = e^{-ik_{SO}x\sigma_z}, \tag{2.39}$$

The Hamiltonian becomes:

$$\begin{aligned} H_0 &= \int dx \Phi^\dagger(x) \left(\frac{p_x^2 - k_{SO}^2}{2m} - \mathbf{B}(x)\boldsymbol{\sigma} \right) \Phi(x), \\ \text{with } \mathbf{B}(x) &= \left(\cos(2k_{SO}x)\hat{\mathbf{x}} + \sin(2k_{SO}x)\hat{\mathbf{y}} \right), \end{aligned} \tag{2.40}$$

Except a trivial constant, we have shown that a 1D electron gas with spin-orbit and uniform Zeeman field has the same spectrum as 1D electron gas with spiral Zeeman field. In presence of the proximity effect, we have to transform also the superconducting pairing term. In the BdG representation the pairing term is invariant under U because is proportional to τ_x, without any spin matrix. Therefore, we have proven that the Hamiltonian of a wire with helical magnetic field is equivalent to the spectrum of a wire with spin-orbit coupling and uniform magnetic field.

We note also that U leaves unchanged the observable without an explicit dependence on p and σ, hence the LDOS is the same in both wires models.

2.3.3 RKKY model

For now we simply assumed the helical magnetic field, but it is not clear how the spin texture of Eq:(2.40) can arise in a real system. Such a field can be engineered by nano-magnets or can emerge in magnetic impurities interacting via the Ruderman-Kittel-Kasuya-Yoshida (RKKY) interaction mediated by a 1D electronic conductor. [35]
In this thesis, we do not focus on the physical conditions where this kind of spin texture can be present. We only assume fixed helical orientation of the spins. However, there is a literature about this mechanism and we try to outline the main argument for the formation of an helical texture. Here we follow [36].

As a prototype for our model we consider a semiconducting nanowire with magnetic atoms or nuclear spins placed on top of a bulk s-wave superconductor. The interaction between the magnetic impurities is mediated by electrons of the 1D conductor and it can be described by RKKY interaction:

$$H_{\text{RKKY}} = -\sum_{i,j} J_{i,j} \mathbf{S}_i \mathbf{S}_j, \tag{2.41}$$

where $\mathbf{S}$ is the spin of the impurities and the coupling J is essentially the spin susceptibility χ of the 1D proximitized conductors. $J_{i,j} \sim \chi(\mathbf{r}_i - \mathbf{r}_j)$. Is convinient

to analyze the Fourier transform of the spin susceptibility $\chi(q)$. Under certain conditions [3] $\chi(q)$ has a positive peak at $q = 2k_F$. In order to minimize the magnetic energy $\langle H_{\text{RKKY}} \rangle$, we want to maximize χ and this happens exactly at momentum $q = 2k_F$. This creates an helical texture of magnetic moments with a momentum q. In conclusion, the helical spin texture rather ferromagnetism (or anti-ferromagnetism) can minimize the free energy of the 1D system under certain conditions.

2.4 Realistic setup: Shiba physics

Another realistic setup to produce MFs consist of an array of magnetic impurities on top of a 2D superconductor. In this section, we introduce the Shiba physics that will be the context of the entire thesis. A generic superconductor with magnetic impurities give rise to the so-called Shiba bound state, a localized electron bound state with energies within the superconducting gap. This part is based on the article [26] with a 2D superconductors rather than 3D. Because we did not find a derivation in the literature[4] for a 2D superconductors with only helical magnetic order, we report the entire detailed calculation in Appendix D. In the following, we summarize the main results.

2.4.1 One impurity

We start analyzing only one magnetic impurities in a 2D superconductors. We will derive the allowed energies ϵ_α for a state bound to the impurity, the so-called Shiba state [24]. This will be useful to derive a new energy scale α which tell us how deep is bound state [5] with respect to the gap Δ.

In this work we treat the magnetic impurities only in the classical limit $S \gg 1$, where S is the spin of the impurity. This spin is supposed to be fixed. The only action of that variable is to polarize the electron in the superconductor: the

[3] $\Delta < \mu_F$, where μ_F is the chemical potential of the superconductor.

[4] We find [44] which treats ferromagnetic order with spin-orbit, also the Glazman's article [26] did our calculation (i.e. for helical order) in a 3D superconductors. These systems are quite similar and the calculation are done in a similar way, however I think that can be useful for someone find all the calculation in details.Also [30] is a good reference where the details of [26] are well explained. I would like to thank Prof. Teemu Ojanen,who I met personally in LPS, for the segnalation of the thesis of two his student [30, 31], that are really detailed introductions in the Shiba physics, and that were extremely useful at the beginning of this work for learn the concept of the Shiba chain and for the thesis writing himself.

[5] When we speak about bound states, in this context we mean $|E| < |\Delta|$, with this constrain the wavefunction of this state is localized on the impurities and has a $e^{-r/\xi(E)}/\sqrt{k_F r}$ tail. In this thesis, we only consider the case $r \ll \xi$ and with $e^{-r/\xi(E)} \approx 1$we can't see explicitly the difference between a bound states and a continuum state.

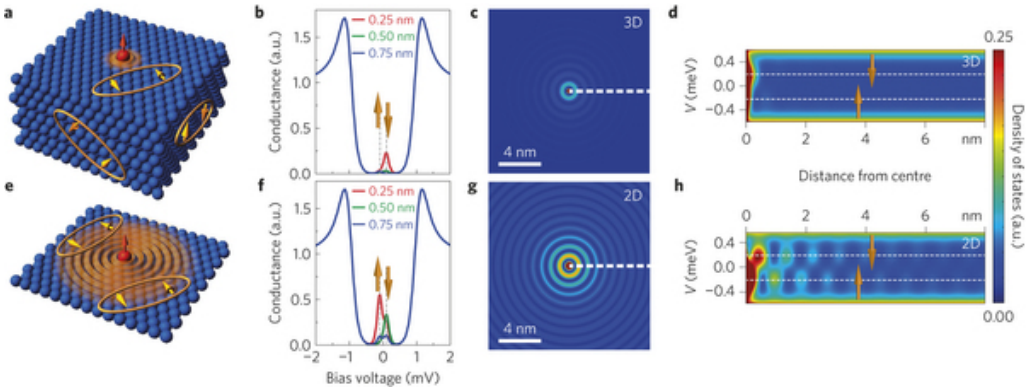

Figure 2.6: Figure from [32] : The spatial extent of the Shiba state long-range wavefunction has been characterized experimentally in [32]. The figure shows the decay of the wavefunction for a single impurity in a 3D superconductor and in a 2D superconductor.

magnetic moments are nothing but local magnetic field. In that limits the impurity is described by the Kondo Hamiltonian:

$$H_{\text{Kondo}} = -J \sum_{\alpha,\beta} \psi^{\dagger}_{\alpha}(\mathbf{r_0}) \mathbf{S} \boldsymbol{\sigma}_{\alpha,\beta} \psi_{\beta}(\mathbf{r_0}), \tag{2.42}$$

where this Hamiltonian describes the effect of a magnetic impurity placed at position $\mathbf{r}_0$. $\psi^{\dagger}_{\alpha}(\mathbf{r_0})$ creates an electron in the superconductor with spin α . And $\boldsymbol{\sigma}_{\alpha,\beta}$ is the spin operator quantized along $\hat{\mathbf{S}}$.
Such Kondo Hamiltonian can be derived by the more fundamental Anderson model using the Schrieffer-Wolf transformation, this procedure and the Anderson model are discussed in the Appendix B.
Our system is described by the follow BdG Hamiltonian:

$$\mathcal{H} = \Big(\xi_p \tau_z - J \mathbf{S} \boldsymbol{\sigma} \delta(\mathbf{r}) + \Delta \tau_x \Big), \tag{2.43}$$

$$\Psi(\mathbf{r})^{\dagger} = \Big(\psi^{\dagger}_{\uparrow}(\mathbf{r}), \psi^{\dagger}_{\downarrow}(\mathbf{r}), \psi_{\downarrow}(\mathbf{r}), -\psi_{\uparrow}(\mathbf{r}). \Big)$$

Where $\xi_p = \frac{p^2}{2m} - \mu$ is the kinetic term, p is the momentum, m is the effective mass of the electron in the superconductor. τ_i are the Pauli matrices acting in the Nambu space. We can choose the classical impurity spin along z-axis $\mathbf{S} = S\hat{\mathbf{z}}$. In this case the (4×4) Hamiltonian (D.1) separates into two decoupled (2×2)

Hamiltonians .

After some work (AppendixD), we have an equation to determine the allowed energies:

$$\left(1 \mp \alpha \frac{E + \Delta\tau_x}{\sqrt{\Delta^2 - E^2}}\right)\Psi(0) = 0, \tag{2.44}$$

where $\alpha = \pi\nu_0 JS$, and ν_0 is the density of states of the substrate when the superconductivity is not present. The allowed energies with the constrain $|E| < |\Delta|$ are:

$$\epsilon_\pm = \pm\Delta\frac{1-\alpha^2}{1+\alpha^2}. \tag{2.45}$$

We write explicitly the relative eigenvectors for a generic orientation of spin $\mathbf{S} = S\hat{\mathbf{S}}$:

$$\Psi_+(0) = \frac{1}{\sqrt{2\mathcal{N}}}\begin{pmatrix}|\uparrow\rangle_{\hat{\mathbf{S}}}\\ |\uparrow\rangle_{\hat{\mathbf{S}}}\end{pmatrix}, \Psi_-(0) = \frac{1}{\sqrt{2\mathcal{N}}}\begin{pmatrix}|\downarrow\rangle_{\hat{\mathbf{S}}}\\ -|\downarrow\rangle_{\hat{\mathbf{S}}}\end{pmatrix}. \tag{2.46}$$

The normalization factor $\mathcal{N}$ is determined by normalization $\int d\mathbf{x}|\Psi|^2 = 1$. We also note that particle hole symmetry $\mathfrak{C} = \tau_y\sigma_y K$ [6] relates the two eigenvectors: $\mathfrak{C}\Psi_+ = \Psi_-$.

We have shown that the main effect of a magnetic impurity in a superconductor is to create a quasiparticle bounded to it. The magnetic moment of the impurity polarizes the superconducting electrons and decrease their energy.
However, we just derived the allowed energies and the existence of bound states. Now we want to characterize the spatial wave function of those impurities. Our system is described by the following BdG Hamiltonian:

$$\mathcal{H} = \left(\xi_p\tau_z - J\mathbf{S}\boldsymbol{\sigma}\delta(\mathbf{r}) + \Delta\tau_x\right) = \mathcal{H}_0 - J\mathbf{S}\boldsymbol{\sigma}\delta(\mathbf{r}). \tag{2.47}$$

Inverting the Shrodinger equation we can show that the spinors solution only

[6] This representation of $\mathfrak{C}$ is a little bit different than 2.25 because we are dealing explicitly with spin.

depends on the free propagator $\mathcal{G}_E^0(\mathbf{r}) = (E - \mathcal{H}_0)^{-1}$:

$$\Psi(\mathbf{r}) = -\mathcal{G}_E^0(\mathbf{r}) J \mathbf{S}\boldsymbol{\sigma}\Psi(0). \tag{2.48}$$

Because we are interested in an effective low-energy description of our system we focus on the case where the Shiba energy is far from the gap, $\epsilon_\alpha \ll \Delta$, the so-called deep Shiba limit.
In this limit it is easy to derive an asymptotic wave function for the Shiba bound state:

$$\Psi_+(0) = \sqrt{\frac{\Delta}{2JS}} \begin{pmatrix} |\uparrow\rangle_{\hat{\mathbf{S}}} \\ |\uparrow\rangle_{\hat{\mathbf{S}}} \end{pmatrix}, \tag{2.49}$$

$$\Psi_+(\mathbf{r})_{k_F r \gg 1} = \sqrt{\frac{2\Delta}{\pi J S k_F r}} e^{-r/\xi} \begin{pmatrix} \cos(k_F r)\,|\uparrow\rangle_{\hat{\mathbf{S}}} \\ \sin(k_F r)\,|\uparrow\rangle_{\hat{\mathbf{S}}} \end{pmatrix}.$$

where k_F is the Fermi momentum of the superconducting substrate, ξ is the coherence length of the substrate and $|\uparrow\rangle_{\hat{\mathbf{S}}}$ is the spin polarised along the $\hat{\mathbf{S}}$-direction. Because the BdG formalism provides the particle-hole symmetry (PHS), $\mathfrak{C} = \tau_y \sigma_y K$, we have another solution $\Psi_- = \mathfrak{C}\Psi_+$ with opposite energy.

2.4.2 Shiba chain

We just treated a single magnetic impurity in the classical limit. Now we want to treat the more complex situation of a chain of impurities $\mathbf{S}_n$ at site $\mathbf{r}_n = na\mathbf{e}_1$, where a is the spacing between impurities. A single impurity creates a bound state below the gap Δ. Following [26] we show that a 1D chain creates an entire band below the gap, with a reference energy ϵ_α and a band width $\Delta/\sqrt{k_F a}$.
Because we are interested in the low-energy limit with respect to the gap energy Δ, is natural to take the so-called Shiba limit $\epsilon_\alpha \ll \Delta$ (i.e. $\alpha \sim 1$) and also to take a small band width $\Delta/\sqrt{k_F a} \ll \Delta$, i.e. the dilute limit $k_F a \gg 1$.
In this case we analytically know the wave function and we can project on these quasiparticle states. In a realistic system we can also take $\xi \gg a$.
We start considering the BdG Hamiltonian for a chain of magnetic impurities

placed at the position $\mathbf{r}_n$:

$$\mathcal{H} = \Big(\xi_p \tau_z - J \sum_n \mathbf{S}_n \boldsymbol{\sigma} \delta(\mathbf{r} - \mathbf{r}_n) + \Delta \tau_x \Big). \tag{2.50}$$

We suppose, for the magnetic impurities, a perfect planar helical order:

$$\mathbf{S}_n = \Big(\cos(2k_h na), \quad \sin(2k_h na), \quad 0\Big). \tag{2.51}$$

First, we separate the impurity terms from the rest:

$$\Big(E - \xi_{\mathbf{p}} \tau_z - \Delta \tau_x\Big)\Psi(\mathbf{r}) = -J \sum_n \mathbf{S}_n \boldsymbol{\sigma} \delta(\mathbf{r} - \mathbf{r}_n)\Psi(\mathbf{r}_n). \tag{2.52}$$

After some manipulation, it becomes clear that we can rewrite the entire equation in terms of the free propagator.

$$\Psi(\mathbf{r_m}) = -JS \sum_n \mathcal{G}_E^0(\mathbf{r}_m - \mathbf{r}_n)\hat{\mathbf{S}}_n \boldsymbol{\sigma} \Psi(\mathbf{r}_n). \tag{2.53}$$

Taking the deep Shiba limit and the dilute one we obtain a simple expression for the propagator. Then we approximate the Eq. (2.53) by expanding in terms of $(1-\alpha)$, E/Δ and $1/\sqrt{k_F r}$, keeping only the terms up to linear order in all three. Now this equation can be written as an *effective tight-binding Hamiltonian* that describes the Shiba chain:

$$\tilde{\mathcal{H}}^{\text{eff}}_{m,m} = \begin{pmatrix} \Delta(1-\alpha) & 0 \\ 0 & -\Delta(1-\alpha) \end{pmatrix}, \tag{2.54}$$

$$\mathcal{H}^{\text{eff}}_{m\neq n} = \Delta \sqrt{\frac{2}{\pi k_F r_{mn}}} e^{-r_{mn}/\xi} \tag{2.55}$$

$$\times \begin{pmatrix} -\cos(k_F r_{mn} - \frac{\pi}{4})\cos(k_H(x_m - x_n)) & -i\sin(k_F r_{mn} - \frac{\pi}{4})\sin(k_H(x_m - x_n)) \\ -i\sin(k_F r_{mn} - \frac{\pi}{4})\sin(k_H(x_m - x_n)) & \cos(k_F r_{mn} - \frac{\pi}{4})\cos(k_H(x_m - x_n)) \end{pmatrix}.$$

We can easily rewrite this Hamiltonian so that we can show the similarity with the Kitaev model. Thus we define $c_i^\dagger$ the creation operators of a Shiba bound

quasiparticle at site i. In this way the Hamiltonian reads:

$$H_{\text{ShibaChain}} = \sum_n \epsilon_\alpha c_n^\dagger c_n + \sum_{n \neq m} \Big(h_{m,n} c_m^\dagger c_n + \Delta_{m,n} c_m^\dagger c_n^\dagger + h.c. \Big), \tag{2.56}$$

This Hamiltonian is reminiscent of the Kitaev Hamiltonian in Eq.(2.1) but there are some important differences:

- The hopping $h_{m,n}$ is long range term and it falls like $1/\sqrt{k_F r}$; this behavior is due to the extension of Shiba wave function.
- The pairing $\Delta_{m,n}$ is odd and it gives a p-wave superconductivity, but it also involves a long range contributions.

In order to study the topological property of this Hamiltonian, we analyse its symmetries: the Hamiltonian is invariant under PHS. Moreover, for a spinless Hamiltonian the time reversal symmetry is $\mathcal{T} = K$, where K is the complex conjugation. But the Hamiltonian Eq:2.54 can be made real after a gauge $c_i \longrightarrow e^{i\pi/4} c_i$.

Because this system is invariant under the effective time-reversal $\mathcal{T}$, with $\mathcal{T}^2 = 1$ and PHS $\mathfrak{C}$, this system is in BDI class [7, 37], with a $\mathbb{Z}$ topological index, see Table (1).

2.5 Conclusions to the chapter

In this chapter, we give an overview of topological superconductors. Starting from the Kitaev model [9], we showed that this toy model can host Majorana fermions. Then, we studied the main proposals to engineer the Kitaev model. In section 2.3 we will gave an overview about nanowires. These systems are made of one dimensional semiconducting wire in proximity of a superconductor are one of the most promising setup to realize MFs. In section 2.4, we introduce the so-called **Shiba physics**: a single magnetic impurity on top of a superconducting substrate gives rise of a quasiparticle bounded to the impurity, the so-called **Shiba state**. Finally, we show that in some limits a 1D chain of magnetic impurities can be described by an effective Kitaev-like Hamiltonian able to host MFs.

Chapter 3

Chain of magnetic adatoms with orbital degrees of freedom

In this chapter, we describe a chain of magnetic atoms on top of a superconductor by taking into account the different impurity orbital degrees of freedom. These orbitals may play an important role in the intermediate regime between the dilute and the dense limit. Due to the impurity orbital overlap, one has a 1D conduction band on top of the superconductor (forming effectively a 1D conducting wire). The band coexists with the magnetic moments which can create a 1D Shiba band into the superconductor. In this chapter, we derive an effective Hamiltonian that describe the system as two coupled Kitaev-like channels. This chapter represents the core of this thesis since this effective two channels Hamiltonian is still unprecedented in the literature.

3.1 Single adatom

We start by considering a single magnetic adatom put on top of a 2D superconductor, we consider one conducting electron of the external shell of the impurity. This procedure will be useful for the later discussion.Let us analyse the important energy scales in the problem.
We try to improve the physical description of a magnetic impurity: we include several orbitals to the impurity. We include the electrons in the core shell, and one orbital in the external shell. The contribution of the core electrons is to give rise to a classical spin S, which makes the adatom magnetic. The orbital electron are still treated quantum mechanically. This orbital electron is described by the operator $a_\sigma^\dagger$, where σ is the spin index. Moreover, the spin of the orbital electron

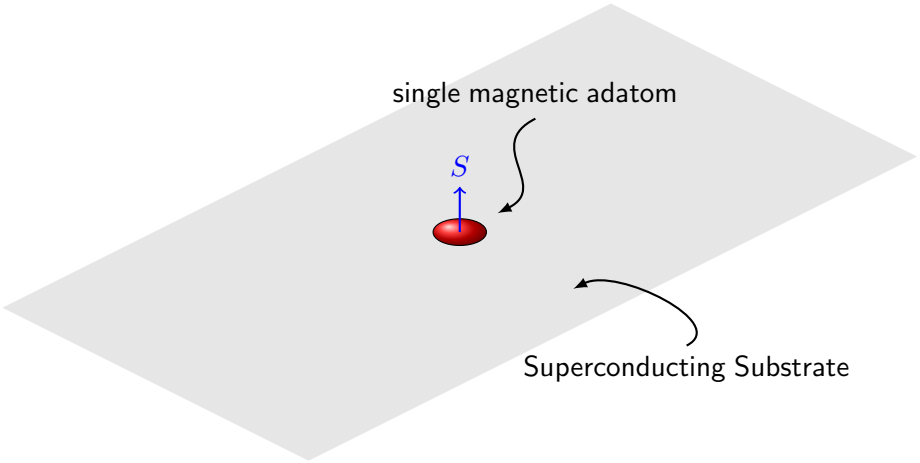

Figure 3.1: A single magnetic adatom, with a spin S, on a superconducting substrate. In this section we study this situation.

interact with the core classical spin S, with a coupling J'. Dealing with a single classical impurity we can take without a loss of generality $\hat{\mathbf{S}} = \hat{\mathbf{z}}$, which describes the core electrons.

We write the Hamiltonian of adatom with the Nambu spinors in the form:

$$\begin{aligned} H_{\text{adatoms}} &= \frac{1}{2} A^\dagger \Big(\epsilon_0 \tau_z - J' S \sigma_z \Big) A, \\ \text{with } A^\dagger &= \left(a_\uparrow^\dagger, \quad a_\downarrow^\dagger, \quad a_\downarrow, \quad -a_\uparrow \right), \end{aligned} \tag{3.1}$$

then we rewrite the Hamiltonian of 2D substrate as:

$$\begin{aligned} H_{\text{2D}} &= \frac{1}{2} \int d\mathbf{r} \Psi(\mathbf{r})^\dagger \Big(\xi_p \tau_z - JS\sigma_z \delta(\mathbf{r}) + \Delta \tau_x \Big) \Psi(\mathbf{r}), \\ \text{with } \Psi(\mathbf{r})^\dagger &= \left(\psi_\uparrow^\dagger(\mathbf{r}), \psi_\downarrow^\dagger(\mathbf{r}), \psi_\downarrow(\mathbf{r}), -\psi_\uparrow(\mathbf{r}) \right). \end{aligned} \tag{3.2}$$

The two Hamiltonians are coupled by a tunneling term, because an electron in the superconductor can tunnel in the external shell of the impurity (and vice versa):

$$H_{\text{Tunneling}} = -\frac{1}{2} \int d\mathbf{r} \delta(\mathbf{r}) t \Big(\Psi(\mathbf{r})^\dagger \tau_z A + A^\dagger \tau_z \Psi(\mathbf{r}) \Big), \tag{3.3}$$

writing the Shrodinger equation we have:

$$\begin{aligned} &\Big(\xi_p \tau_z - JS\sigma_z \delta(\mathbf{r}) + \Delta \tau_x \Big) \Psi(\mathbf{r}) - t\delta(\mathbf{r}) \tau_z A = E\Psi(\mathbf{r}), \\ &\Big(\epsilon_0 \tau_z - J' S \sigma_z \Big) A - \int d\mathbf{r} t \delta(\mathbf{r}) \tau_z \Psi(\mathbf{r}) = EA. \end{aligned} \tag{3.4}$$

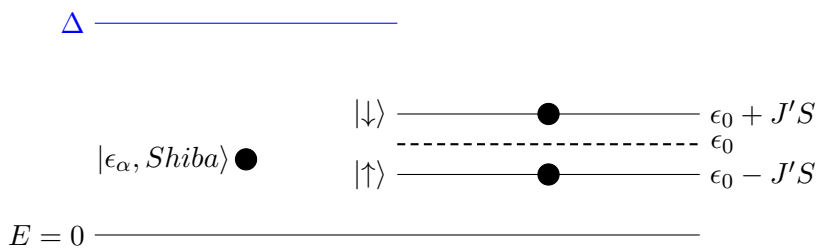

Figure 3.2: Spectrum of a single adatom, with Shiba state, without any tunnelling: $t = 0$. On the left we show the energy of Shiba states ϵ_α, on the rigth the energy of the orbital states $\epsilon_0 \pm J'S$.

We should pay attention that A and Ψ are not operators, but the Nambu wavefunction of quasiparticles, explicitly : $A^T = \Big(u_\uparrow, \quad u_\downarrow, \quad v_\downarrow, \quad v_\uparrow\Big)$.
Defining $\alpha_t = t\nu_0\pi$, we try to study the limit of large tunnelling between the impurity and superconductor, $\alpha_t \gg \alpha$. Setting $\alpha = 0$ and $\epsilon_0 = 0$ we find the energies:

$$E^{(1)}_{\text{Adatoms}} = \pm\left(\frac{-J'S - \alpha_t t}{1 + \frac{\alpha_t t}{\Delta}}\right), \quad E^{(2)}_{\text{Adatoms}} = \pm\left(\frac{-J'S + \alpha_t t}{1 + \frac{\alpha_t t}{\Delta}}\right), \tag{3.5}$$

where the $\pm$ is due as usual to PHS symmetry. We want to remember that $\alpha_t t \sim \nu_0 t^2 = \Delta'$ where Δ' is the induced superconductivity gap on adatoms (see Appendix A for the derivation of this equality). As expected we do not have any Shiba state $\alpha = 0$. On the other hand we find some bound state localized on the impurity, affected by proximitize superconductivity.

In the limit $\alpha_t \ll \alpha$ we have usual Shiba states $E_{\text{Shiba}} = \pm\Delta(1 - \alpha)$ and another decoupled state on the adatom $E = (\epsilon_0 \pm J'S)$. However, we want to treat the limit $t \ll J$ without neglecting the first order, therefore in Eq:(3.4) we keep only the terms linear in α_t, $1 - \alpha$ and E/Δ .

We can find the energies for $t \ll J'S$ and $\epsilon_0 = 0$:

$$\begin{aligned} E^{(1)} &= -J'S - \frac{\Delta\alpha_t t}{J'S}, \quad E^{(2)} = (1-\alpha)\Delta + \frac{\Delta\alpha_t t}{J'S}, \\ E^{(3)} &= +J'S + \frac{\Delta\alpha_t t}{J'S}, \quad E^{(4)} = (\alpha+1)\Delta - \frac{\Delta\alpha_t t}{J'S}, \end{aligned} \tag{3.6}$$

and the PHS conjugate. Not all of those energies are allowed. For the procedure used in the evaluation of the propagator only the values which respect the constrain $|E| < |\Delta|$ are acceptable. We note that the superconductivity correction are related

with $\Delta' = \frac{\Delta \alpha_t t}{J'S}$. We can treat that as perturbation if $\alpha_t t \ll J'S$. We will use again this condition in the section 3.3.2.

3.2 Chain of magnetic adatoms

This section is the core of this thesis. We start detailing our model: we want to study a chain of magnetic atoms on top of a superconductor by taking into account the different impurity orbital degrees of freedom. First we introduce the Hamiltonian of the superconductor. Then we focus on the impurity electrons.

3.2.1 The superconducting Hamiltonian

Our starting point is the Hamiltonian of a 2D s-wave superconductor. We assume that the superconductor is in the clean limit but it hosts an array of magnetic impurities placed at locations r_n:

$$H_{\mathrm{SC}} = \int dr^2 \sum_{\alpha,\beta} \Psi^\dagger_\alpha(\mathbf{r}) \left((-\frac{\nabla^2}{2m} - \mu)\delta_{\alpha,\beta} - \sum_n J\mathbf{S}_n \boldsymbol{\sigma}_{\alpha,\beta} \delta(\mathbf{r} - \mathbf{r}_n) \right) \Psi_\beta(\mathbf{r}) \\ + (\Delta \Psi^\dagger_\uparrow(\mathbf{r}) \Psi^\dagger_\downarrow(\mathbf{r}) + h.c.), \tag{3.7}$$

Here $\mathbf{r}$ denote the electron's position, m and μ are the effective mass and the chemical potential in the superconductor, Δ is the superconducting gap, and $J > 0$ denotes the strength of the exchange coupling between the magnetic impurity with spin S and the electrons in the superconductor. The Pauli matrices $\sigma^j_{\alpha,\beta}$ acts in the spin space. The electron field $\Psi^\dagger_\alpha(\mathbf{r})$ creates an electron in the position $\mathbf{r}$ and with spin α. We assume that the magnetic moments, provided by the core orbital electrons, are classical $S \gg 1$ and arranged along a linear chain with lattice spacing a. We can parametrize the impurity spins $\mathbf{S}_n$ through spherical coordinates,assuming a perfect helical order, characterized by the helical momentum k_h:

$$\mathbf{S}_n = \Big(\cos(2k_h n a), \quad \sin(2k_h n a), \quad 0 \Big). \tag{3.8}$$

We assume the spin of the core of the impurity as frozen into a given spin texture $\mathbf{S}_n$. We do not focus on how this kind of given spin texture can arise, but we take it for granted. This is one of the strongest assumption of this work.

3.2.2 The orbital electrons

Now we take into account the different impurity orbital degrees of freedom of the electrons on the impurities. We suppose to have two kinds of different orbitals. One core orbital strongly localized on the impurity will gives rise to a well defined magnetic moment S. We also take in account a second type of electron orbital, created by $a^{\dagger}_{n,\alpha}$, which is supposed to have a broaden extension of its wavefunction. These electrons form a delocalized band. For this kind of orbital electron we can write the Hamiltonian as:

$$H_{\text{Orbital}} = \sum_{n,\alpha}\Bigg((\epsilon_g + t_w)a^{\dagger}_{\alpha,n}a_{\alpha,n} - (\frac{t_w}{2}a^{\dagger}_{\alpha,n}a_{\alpha,n+1} + h.c)\Bigg), \tag{3.9}$$

where ϵ_g is the energy of the orbital level and t_w is the hopping between two neighbouring impurities, and α, β are the spin index. Also the large spin of the core electrons S affects the conducting electron favouring the alignment of the spin $\boldsymbol{\sigma}$ with the classical spin $\mathbf{S}$ with the strength $J' > 0$. [1]:

$$H_{\text{Imp}} = -\sum_{n,\alpha,\beta} J'\mathbf{S}_n a^{\dagger}_{\alpha,n}\boldsymbol{\sigma}_{\alpha,\beta}a_{\beta,n}. \tag{3.10}$$

This last equation shows how the energy cost of flipping the spin in the opposite direction of the classical spin $\mathbf{S}$ is $2J'S$.
This Hamiltonian corresponds as the Hamiltonian for the electrons in a nanowire with a Zeeman magnetic field $J'S$. Thus, we will refer on that as the wire Hamiltonian. Finally, we consider that an electron in the superconductor can tunnel in the orbital part (and vice versa) with a hopping energy t:

$$H_{\text{Tunneling}} = -t\int d^2r \sum_{n,\alpha}\Bigg(\Psi^{\dagger}_{\alpha}(\mathbf{r})a_{\alpha,n}\delta(\mathbf{r}-\mathbf{r}_n) + h.c.\Bigg), \tag{3.11}$$

3.3 Effective Hamiltonian

Now we are interested to derive an effective Hamiltonian for the low-energies below the gap $E \ll \Delta$. For the electrons in the superconductors the presence of magnetic impurity creates a Shiba quasiparticle states with energy ϵ_α bound to the impurity. In the case of deep Shiba state ϵ_α and in the dilute limit $k_F a \gg 1$ we can project out the states above the gap Δ and derive [26] an effective Kitaev-like

[1] Here we assume J, J' having a positive value (ferromagnetic exchange). Taking both as negative (anti-ferromagnetic exchange) would not alter the conclusion of this work.

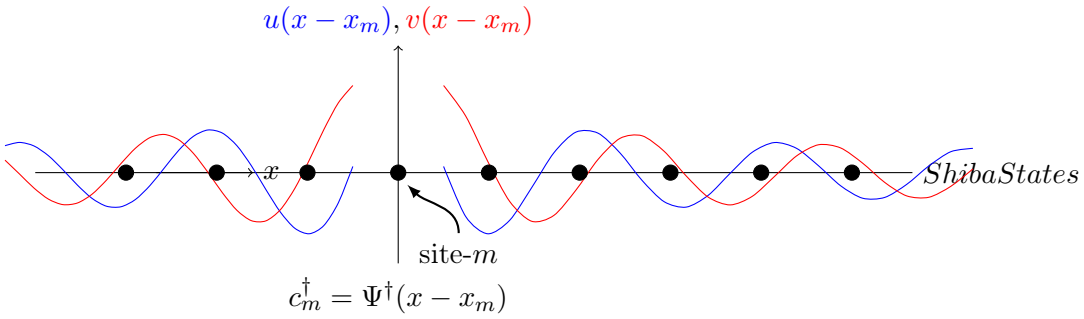

Figure 3.3: In this figure, we sketch the long range tail of electron (hole) wave function $u(x)(v(x))$ of a single Shiba state placed in site m. As we can see the tail is oscillating and long range. In presence of many impurities, in the dilute limit $k_F r \gg 1$ we can project the entire Hamiltonian on the wave function of a single Shiba state placed in a generic site n. After the projection we obtain a tight-binding Hamiltonian Eq: (E.10). Because of the long range tale of the single state on which we project it we obtain a long range hopping between the states.

Hamiltonian.

In the large magnetization regime $J'S \sim \epsilon_w \gg t_w$ the orbital electron spin is polarised along $\hat{\mathbf{S}}$. We take the large magnetization limit because we want first to analyse the simplest Hamiltonian and it's topological features. After this analysis, we will discuss the spinful case. The Hamiltonian can be projected onto the lowest spin band, taking in account virtual transitions to the higher spin band contribute [39].

3.3.1 Projection on the Shiba states

First of all we want to project on the states below the gap, i.e. the Shiba bound states and the orbital electrons states. This means that we project out the superconducting excitations above the gap but we want to take into account that the orbital electrons can virtually visit these states.

This process provides proximity effect on the orbital electrons: a Cooper pair can tunnel in the states below the gap.

In the following section, we will take in account these virtual processes. Let us first project the superconducting sector of the Hamiltonian i.e. Eq: (3.7) on the Shiba states. We just did that in the chapter 2.4 when we treated the Shiba chain. Another method to obtain the same resulting effective model is to project directly on the Shiba states is treated in the Appendix E.0.1.

In the following lines we briefly summarize this approach. We take the super-

conducting Hamiltonian in Eq: (3.7) and project on the Shiba states $\Psi_+^{(n)}, \Psi_-^{(n)}$ bounded to the impurity at position $\mathbf{r}_n$. Projecting on this kind of bound states we are neglecting the states in the continuum above the gap. This is a good approximation if our energies are very small compared to energy gap $E \ll \Delta$. The reference energy of the Shiba state is given by ϵ_α, we need to take the deep Shiba limit $\epsilon_\alpha \ll \Delta$. Moreover, we expect a band with of $\Delta/\sqrt{k_F a}$, thus we suppose $\sqrt{k_F a} \gg 1$, the so-called dilute limit. These are the same approximations of the section 2.4 but they arise more naturally asking the low-energy limit $\epsilon_\alpha \ll \Delta$.
After that we obtain the previous result: the Shiba chain is described by the following equation (we are just reminding the Eq: D.37):

$$\tilde{\mathcal{H}}^{\text{eff}}_{m,m} = \begin{pmatrix} \Delta(1-\alpha) & 0 \\ 0 & -\Delta(1-\alpha) \end{pmatrix} = \begin{pmatrix} \epsilon_\alpha & 0 \\ 0 & -\epsilon_\alpha \end{pmatrix}, \tag{3.12}$$

$$\begin{aligned} \tilde{\mathcal{H}}^{\text{eff}}_{m\neq n} &= \Delta\sqrt{\frac{2}{\pi k_F r_{mn}}} \\ &\times \begin{pmatrix} -\cos(k_F r_{mn} - \frac{\pi}{4}) \langle\uparrow, m| \uparrow, n\rangle & -\sin(k_F r_{mn} - \frac{\pi}{4}) \langle\uparrow, m| \downarrow, n\rangle \\ -\sin(k_F r_{mn} - \frac{\pi}{4}) \langle\downarrow, m| \uparrow, n\rangle & \cos(k_F r_{mn} - \frac{\pi}{4}) \langle\downarrow, m| \downarrow, n\rangle \end{pmatrix}. \end{aligned} \tag{3.13}$$

3.3.2 Self-energy and proximity effect

Now we want to describe how the states above the gap can influence the orbital electrons. We shall derive the proximity effect by evaluating the self-energy.
We try to understand how to take into account the effect of the substrate. [33] We define the projector on Shiba states and on orbital electrons $\mathcal{P}$ as :

$$\mathcal{P} = \sum_m \Big(|m, \pm\rangle_{\text{Shiba}} \langle m, \pm|_{\text{Shiba}} + |\text{Orbital}\rangle \langle \text{Orbital}| \Big), \tag{3.14}$$

and $\mathcal{H}^{\text{proj}} = \mathcal{P}\mathcal{H}\mathcal{P}$. Taking in account virtual processes, we obtain for the Schrodinger equation:

$$\begin{aligned} &E\mathcal{P}\Psi = \mathcal{H}^{\text{eff}}\mathcal{P}\Psi, \\ &\mathcal{H}^{\text{eff}} = \Big(\mathcal{H}^{\text{proj}} + \Sigma(E) \Big). \end{aligned} \tag{3.15}$$

The Hamiltonian has acquired a self-energy $\Sigma_E = \mathcal{H}^{\text{eff}} - \mathcal{H}^{\text{proj}}$, in order to take in

account the high energy states. Using second order perturbation theory we can write Σ_E as:

$$\Sigma_E(x,x') = \int dydy' \, \langle x|^C \mathcal{H}_{\text{Tunneling}}|y\rangle \, , \mathcal{G}_E^{\text{SC}}(y,y') \, \langle y'|\mathcal{H}_{\text{Tunneling}}|x'\rangle^C \, , \quad (3.16)$$

where $|x\rangle^C$ is a state on chain and $|y\rangle$ a state on superconductor, and $\mathcal{G}_E^{\text{SC}}(y,y')$ is the propagator for the superconducting states. Because we keep the Shiba states in our Hilbert space, we are projecting on $\mathcal{Q}$ which contains only states in the continuum, which are not strong affected to magnetic impurities. Then we can safely calculate the propagator in the free case, when there is not any impurities so $\mathcal{G}_E^{\text{SC}}(y,y') \approx \mathcal{G}_E^0(y,y')$ and:

$$\Sigma_E(x,x') = t^2 \mathcal{G}_E^0(|x-x'|), \quad (3.17)$$

On the lattice form we have:

$$\Sigma(E)_{n,m} = -\delta_{n,m}\alpha_t t \frac{E+\Delta\tau_x}{\sqrt{\Delta^2-E^2}} + O(\frac{\alpha_t t}{\sqrt{k_F r_{mn}}}), \quad (3.18)$$

we neglect terms $O(\frac{\alpha_t t}{\sqrt{k_F r_{mn}}})$ because we are interested in the small coupling limit. This is a second order in two small terms t^2 and $1/\sqrt{k_F r_{mn}}$. We linearize for small energy $E \ll \Delta$:

$$\Sigma(E)_{n,m} = -\delta_{n,m}\alpha_t t \tau_x. \quad (3.19)$$

This is nothing else than the proximity term (see Appendix (A)). We report that for energy out the gap $E > \Delta$, we have a pure imaginary Self-Energy $\Sigma(E) \sim it^2$ which describe the escape of electron in the superconductor.

We have recovered the induced superconductivity, demanding $E \ll \Delta$. This requires that the energy scale of the wire must be greater than t (we have treated that as small perturbation) i.e. $\epsilon_w, \alpha_t t \ll \Delta$. However, this terms coupling both spins on wire meanwhile we know that one of spins is inessential (in the large magnetization limit) . Thus, we want to project out this spin. This operation (as Eq: (2.37)) will give us p-wave superconductivity on the wire. We will derive this in next section.

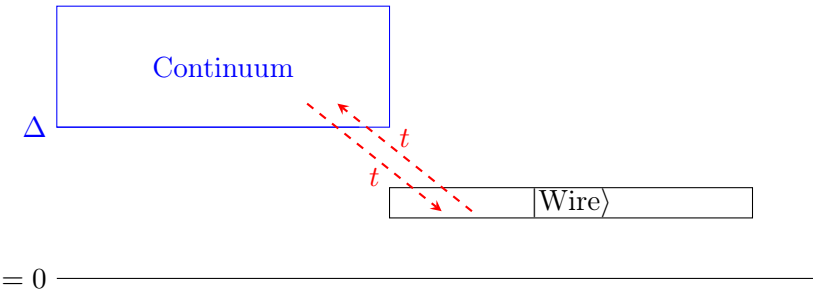

Figure 3.4: A cooper pair can tunnel from the superconductor to wire, or vice versa two electron on the wire can tunnel in the superconductor forming a Cooper pair. t is the tunnelling coupling. Assuming $E_{\text{Wire}} \ll \Delta$, after the projection we obtain an effective superconductivity on the wire $\Delta' = \alpha_t t$. In this section we take into account virtual processes showed in the figure.

3.3.3 Projection on $|\uparrow\rangle_n$ and p-wave superconductivity.

Now we project out the $|\downarrow\rangle_n$ to wire states. This is valid when $J'S \sim \mu \gg t_w, \Delta'$. In this case we will have two well spacing bands we can project safely onto the lower.The upper band still has a role for virtual transition and we cannot simply neglecting $|\downarrow\rangle_n$. Another time we use second order of perturbation theory to take in account the upper band. We follow Ref. [39].
First we write our discretized Hamiltonian as:

$$\begin{aligned} H_{\text{Wire}} = \sum_{n,\alpha,\beta} a^\dagger_{n,\alpha}\Big((\epsilon_g + t_w)I_{\alpha,\beta} - J'\sum_n \mathbf{S_n}\boldsymbol{\sigma}_{\alpha,\beta}\Big)a_{n,\beta} \\ -\frac{t_w}{2}\sum_{n,\alpha} a^\dagger_{n,\alpha}a_{n+1,\alpha} - \sum_n \Delta' a^\dagger_{n,\uparrow}a^\dagger_{n,\downarrow} + h.c. \end{aligned} \tag{3.20}$$

Where $\Delta' = \alpha_t t$ is induced superconductivity. We explicitly write the helical Zeeman term as:

$$\mathbf{S_n} = \Big(\cos(2\phi_n), \quad \sin(2\phi_n), \quad 0\Big), \tag{3.21}$$

where $\phi_n = k_H x_n$. Now we locally align the spin to the Zeeman field by unitarty transformation.[2]:

$$\begin{aligned} \begin{pmatrix} a_{n,\uparrow} \\ a_{n,\downarrow} \end{pmatrix} &= U_n \begin{pmatrix} \tilde{a}_{n,\uparrow} \\ \tilde{a}_{n,\downarrow} \end{pmatrix}, \\ U_n &= \frac{1}{\sqrt{2}} \begin{pmatrix} e^{-i\phi_n} & e^{-i\phi_n} \\ e^{i\phi_n} & -e^{i\phi_n} \end{pmatrix}, \end{aligned} \tag{3.22}$$

The Hamiltonian transforms to:

$$\begin{aligned} H_{\text{Wire}} = &\sum_{n,\alpha,\beta} \tilde{a}^\dagger_{n,\alpha} \Big((\epsilon_g + t_w) I_{\alpha,\beta} - J' S \sigma^{(z)}_{\alpha,\beta} \Big) \tilde{a}_{n,\beta} \\ &- \frac{t_w}{2} \sum_{n,\alpha,\beta} \tilde{a}^\dagger_{n,\alpha} \Omega_{\alpha,\beta} \tilde{a}_{n+1,\beta} - \sum_n \Delta' \tilde{a}^\dagger_{n,\uparrow} \tilde{a}^\dagger_{n,\downarrow} + h.c, \end{aligned} \tag{3.23}$$

The unitary Matrix $\Omega_{\alpha,\beta} = U_n^\dagger U_{n+1}$ has elements:

$$\Omega = \begin{pmatrix} \cos(k_H a) & -i \sin(k_H a) \\ -i \sin(k_H a) & \cos(k_H a) \end{pmatrix}, \tag{3.24}$$

where a is the lattice spacing. In the continuum limit the Ω-matrix reproduces a kinetic energy and a spin-orbit coupling. Now, we separate the Hamiltonian in two parts: H_{mix} which contains the coupling between different spins, and H_0 which contains only the decoupled spins.

$$\begin{aligned} H_0 = &\sum_{n,\alpha,\beta} \tilde{a}^\dagger_{n,\alpha} \Big((\epsilon_g + t_w) I_{\alpha,\beta} - J' S \sigma^{(z)}_{\alpha,\beta} \Big) \tilde{a}_{n,\beta} \\ &- \frac{t_w}{2} \sum_{n,\alpha} \tilde{a}^\dagger_{n,\alpha} \cos(k_H a) \tilde{a}_{n+1,\alpha} + h.c, \end{aligned} \tag{3.25}$$

Using second order perturbation theory and project on $|\uparrow\rangle$ (or equivalently using the Schrieffer-Wolf transformation) we obtain:

$$H_W^{\text{eff}} = H_0 + H_{\text{indirect}}. \tag{3.26}$$

[2]We use this transformation to be coherent with section:3.2

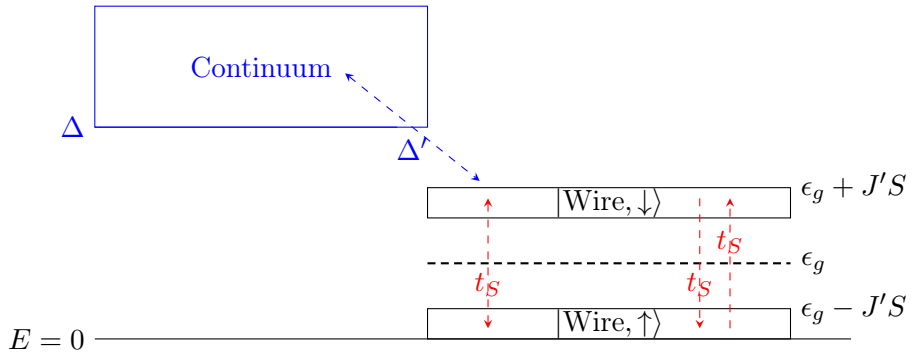

Figure 3.5: ϵ_g is the average energy of the wire without Zeeman splitting $J'S$. In this section we project out the states $|\text{Wire}, \downarrow\rangle$, this is possible when these states have a big energies i.e. when $\epsilon_g \approx J'S \gg t_w, \Delta'$. Before the projection we have to take in account the virtual processes showed in the figure. An electron can virtually spin-flip two times with amplitude $t_S = t_w \sin(k_H a)$, go from $|\text{Wire}, \uparrow\rangle$ to $|\text{Wire}, \downarrow\rangle$ and comes back. Another possibility is that a Cooper pair can tunnelling from the superconducting continuum in the wire with amplitude Δ'. One electron in lowest band and one in the upper. After that the upper band's electron $|\text{Wire}, \downarrow\rangle$ can spin flip and fall in the lowest band. This process give us a p-wave effective superconductivity term.

Let us calculate H_{indirect}. We will consider $+\Delta'$-term later, first we focus only on virtual processes mediated by the coupling t_w. Using the appendix formula Eq:(C.8), we obtain:

$$\begin{aligned} \langle n-2, \uparrow | H_{\text{indirect}} | n, \uparrow \rangle &= \frac{t_w^2 \sin^2(k_H a)}{8J'S}, \\ \langle n, \uparrow | H_{\text{indirect}} | n, \uparrow \rangle &= -\frac{t_w^2 \sin^2(k_H a)}{4J'S}. \end{aligned} \tag{3.27}$$

Where we have taken $E_{\uparrow,m} - E_{\downarrow,n} \cong -2J'S$ in the limit of large Zeeman effect $J'S \gg t_w$. Taking into account the Δ' term, we rewrite the coupling in Nambu formalism. Using $E_{\downarrow,n} - \mathfrak{C}E_{\uparrow,m} \cong 2\epsilon_g$, where $\mathfrak{C}E_{\uparrow,m} = -E_{\uparrow,m}$ is the PHS conjugate. In the limit $\epsilon_g \sim J'S \gg \Delta', t_w$, we obtain:

$$\begin{aligned} H_{\text{indirect}} = &\sum_n \left(\tilde{a}^\dagger_{n,\uparrow} \left(-\frac{t_w^2 \sin^2(k_H a)}{4J'S} \right) \tilde{a}_{n,\uparrow} + \tilde{a}^\dagger_{n,\uparrow} \left(\frac{t_w^2 \sin^2(k_H a)}{8J'S} \right) \tilde{a}_{n+2,\uparrow} \right) \\ &- \left(\frac{1}{J'S} + \frac{1}{\epsilon_g} \right) \frac{\Delta' i t_w \sin(k_H a)}{4} \sum_n \tilde{a}^\dagger_{n,\uparrow} \tilde{a}^\dagger_{n+1,\uparrow} + h.c. \end{aligned} \tag{3.28}$$

In principle $H_{\text{Tunneling}}$, the coupling between the wire and Shiba chain will be

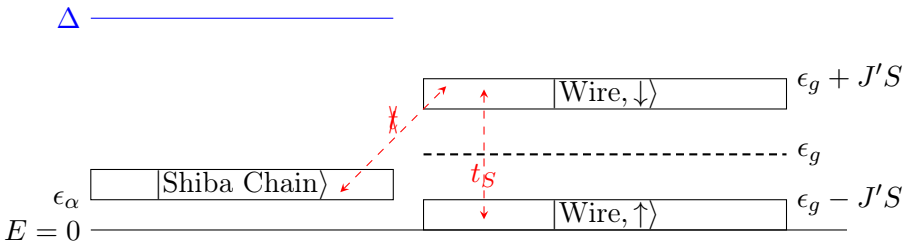

Figure 3.6: Virtual processes: In principle an electron on lower band on the wire can spin-flip and go to upper band and than tunnel in the Shiba chain, but we will ignore this kind of processes because this will simply produces a small renormalization of our constant .

affected by H_{indirect}. This correction will be of the order:

$$H_{\text{indirect}}^{\text{Wire}\leftrightarrow\text{Shiba}} \sim \Gamma\sqrt{\frac{\Delta}{JS}}\frac{t_w}{J'S}. \tag{3.29}$$

Only $\frac{t_w}{J'S}$ is small, therefore $H_{\text{indirect}}^{\text{Wire}\leftrightarrow\text{Shiba}}$ is a first order term, and we cannot neglect it. But direct inspection shows that local tunnelling between the Shiba State $|n, 1-\alpha\rangle$ and the upper band of the wire $|n,\uparrow\rangle$ is impossible due the orthogonality of spins $\langle n,\uparrow|H_{\text{Tunneling}}|n,\downarrow\rangle = 0$. Only a non-local tunnelling to from site n to site m is possible. This effect is suppressed by an order $1/\sqrt{k_F r}$, and we can neglect it. There are many terms of this form, we can ignore them because they will simply renormalizes the previous couplings.
At the end $H_{\text{Wire}}^{\text{eff}}$ reads:

$$\begin{aligned} H_{\text{Wire}}^{\text{eff}} = &\sum_n \tilde{a}_{n,\uparrow}^\dagger\left(\epsilon_g + t_w - J'S - \frac{t_w^2\sin^2(k_H a)}{4J'S}\right)\tilde{a}_{n,\uparrow} \\ &+ \sum_n [\tilde{a}_{n,\uparrow}^\dagger \frac{t_w^2\sin^2(k_H a)}{8J'S}\tilde{a}_{n+2,\uparrow} - \tilde{a}_{n,\uparrow}^\dagger\frac{t_w}{2}\cos(k_H a)\tilde{a}_{n+1,\uparrow} \\ &-\left(\frac{1}{J'S}+\frac{1}{\epsilon_g}\right)\frac{\Delta' i t_w \sin(k_H a)}{4}\tilde{a}_{n,\uparrow}^\dagger\tilde{a}_{n+1,\uparrow}^\dagger + h.c.] \end{aligned} \tag{3.30}$$

After that we will ignore the t_w^2 coupling, which does not give any particular topological features.

3.3.4 Tunnelling coupling

After that, we want to focus on the tunnelling term $H_{\text{Tunneling}}$ in Eq:(3.11). This terms couples the electrons in the superconductor with orbital electrons. We want to project this term on the low-energy states: the Shiba bound state $\Psi_{+,n}$ and the

lower band orbital electron $\tilde{a}_{n,\uparrow}$. In order to write this term in the BdG formalism we define $\langle n|^w$ the lower band orbital electron in the site-n.

We write the orbital electrons Hamiltonian (or wire Hamiltonian) in BdG form.

$$H_{\text{Wire}} = \frac{1}{2}\sum_n A_n^\dagger \Big((\epsilon_g + t_w)\tau_z - J' \sum_n \mathbf{S_n}\boldsymbol{\sigma} \Big) A_n - \frac{t_w}{4}\sum_n A_n^\dagger \tau_z A_{n+1} + h.c. \tag{3.31}$$

The effect of J' is to remove spin degeneracy, separating the energy in two bands with a gap $E_{\text{gap}} \approx 2J'S$. We have then two bands $(-)$ and $(+)$. Similarly at Eq: (2.37), we can project on the lower band corresponding to the wire's eigenvector $|n,\uparrow\rangle^W$ and his PHS conjugate.

$$|n,+\rangle^W = \begin{pmatrix} |\uparrow\rangle_{\hat{\mathbf{S}}_\mathbf{n}} \\ 0 \end{pmatrix} \quad |n,-\rangle^W = \begin{pmatrix} 0 \\ -|\downarrow\rangle_{\hat{\mathbf{S}}_\mathbf{n}} \end{pmatrix}. \tag{3.32}$$

Now we consider both $\mathcal{H}_{\text{Wire}}$ and $\mathcal{H}_{\text{SC}}$, coupled by $\mathcal{H}_{\text{Tunneling}}$.

$$\mathcal{H}^{\text{proj}} = \mathcal{H}_{\text{Wire}} + \mathcal{H}_{\text{SC}} + \mathcal{H}_{\text{Tunneling}}, \tag{3.33}$$

$$H_{\text{Tunneling}} = -\frac{1}{2}\int d\mathbf{r} \sum_l \delta(\mathbf{r}-\mathbf{r}_l) t \Big(\Psi(\mathbf{r})^\dagger \tau_z A_n + A_n^\dagger \tau_z \Psi(\mathbf{r}) \Big).$$

First of all, we will derive the coupling between the Shiba states and the states on the wire. For do that, we project $H_{\text{Tunneling}}$ on $|n,\pm\rangle^W$ (on wire) and $|n,\pm\rangle$ (on Shiba states), but $H_{\text{Tunneling}}$ only depends on the overlap of the wavefunction. After the projection, the coupling reads:

$$\langle n|^W \mathcal{H}_{\text{Tunneling}} |n\rangle = -t\sqrt{\frac{\Delta}{2JS}} \begin{pmatrix} 1 & 0 \\ 0 & -1 \end{pmatrix}. \tag{3.34}$$

$$\langle m|^W \mathcal{H}_{\text{Tunneling}} |n\rangle_{m\neq n} = -t\sqrt{\frac{\Delta}{2JS\pi k_F r}} \tag{3.35}$$
$$\times \begin{pmatrix} \cos(k_F r_{mn})\cos(k_H(x_m - x_n)) & i\sin(k_F r_{mn})\sin(k_H(x_m - x_n)) \\ i\sin(k_F r_{mn})\sin(k_H(x_m - x_n)) & -\cos(k_F r_{mn})\cos(k_H(x_m - x_n)) \end{pmatrix}.$$

The tunnelling is made by two terms, the first one is a local tunnelling: an electron can tunnel between the two systems at the same site n. The second is due to the long range of the wave function. We want to underline that the matrix elements are naturally coming from the wave function of Shiba state.Eq:(D.16).

3.4 Summary: The effective spinless Hamiltonian

In this brief section we summarise the effective Hamiltonian after the projection, in Nambu formalism the total Hamiltonian is:

$$\mathcal{H}^{\text{eff}} = \mathcal{H}_{\text{Shiba}} + \mathcal{H}_{\text{Wire}} + \mathcal{H}_{\text{Tunneling}}. \tag{3.36}$$

The full expression of this Hamiltonian is in the Appendix F.
We report a few comments about this effective Hamiltonian.

- $\mathcal{H}_{\text{Shiba}}$ The *Shiba band* has a reference energy of $\epsilon_\alpha = \Delta(1-\alpha)$ and a band width $\Delta/\sqrt{k_F a}$. Further the long range couplings allow to have multiple MFs in this sector.

- $\mathcal{H}_{\text{Wire}}$ The *Wire (or orbital) band* has a reference energy of $\epsilon_g - J'S$ and a band width of t_w. On that bands there is also a weak proximate superconductivity that can be safely ignored in the spinless case.

- $\mathcal{H}_{\text{Tunneling}}$ The *tunnelling Hamiltonian* is made by two terms: one local term with a strength $t\sqrt{\Delta/JS}$ and another non-local term with $t\sqrt{\Delta/JSk_F a}$ strength.

In order to study the topological property of this Hamiltonian we analyse the Symmetries: the Hamiltonian is invariant under PHS. Further for a spinless Hamiltonian the time reversal symmetry is $\mathcal{T} = K$, where K is the complex conjugation. But the Hamiltonian Eq:3.36 can be made real with the gauge

$a_i \longrightarrow e^{i\pi/4}a_i$ and $c_i \longrightarrow e^{i\pi/4}c_i$, which makes real the only complex term:

$$\begin{pmatrix} 0 & i \\ i & 0 \end{pmatrix} \rightarrow \begin{pmatrix} 0 & -1 \\ 1 & 0 \end{pmatrix}. \tag{3.37}$$

Because this system is invariant under the effective time-reversal symmetry $\mathcal{T}$, with $\mathcal{T}^2 = 1$ and PHS $\mathfrak{C}$, this system is in BDI class, with $\mathbb{Z}$ topological index (1).

3.4.1 Spinful case

What happen if we do not take the large Zeeman field limit $J'S \sim \epsilon_w \gg t_w$ for the orbital electrons? In this case we cannot ignore the spin of the orbital electrons. We know that a spinful system does not have any Majorana topological properties so we can guess that a spinful orbital electrons does not add anything to the physics of the Shiba chain.
An explicit calculation (3.38) shows that the Tunnelling coupling t :

$$\langle\downarrow, n|^W \mathcal{H}_{\text{Tunneling}} |n\rangle = -t\sqrt{\frac{\Delta}{2JS}} \begin{pmatrix} 0 & 1 \\ -1 & 0 \end{pmatrix}, \tag{3.38}$$

$$\begin{aligned} \langle\downarrow, n|^W \mathcal{H}_{\text{Tunneling}} |m\rangle_{n\neq m} &= -t\sqrt{\frac{\Delta}{2\pi k_F r_{n,m} JS}} \\ &\times \begin{pmatrix} -i\cos(k_F r_{mn})\sin(k_F(x_n - x_m)) & \sin(k_F r_{mn})\cos(k_F(x_n - x_m)) \\ -\sin(k_F r_{mn})\cos(k_F(x_n - x_m)) & -i\cos(k_F r_{mn})\sin(k_F(x_n - x_m)) \end{pmatrix}. \end{aligned} \tag{3.39}$$

We shall see below Chap:6 that this case is topologically less rich: if the orbital band is degenerate the proximity effect is not suppressed and then the s-wave gap protect the orbital system to any topological gap inversion. In this case only the Shiba part can host topological features and the orbital degree of freedom does not add any interesting new effect.

3.4.2 Effective time-reversal symmetry protection

Because the winding number w can assume a priori any integer number, we can expect more than one MF. On the contrary, we can think Majorana fermion as an half of electron, so we can expect that two MFs can be coupled each other to form an ordinary Bogoliubov quasiparticle with non-zero energy.
We can show that the effective time-reversal symmetry $\mathcal{T}$, i.e. the conjugation, can avoid this process and two MFs can survive in the same sites. For do that we take the most simple model which can describe this process. We take two decoupled Kitaev chain Eq: 2.1 A and B and we focus to a one edge: we call a_A (a_B) the electron on the edge in the system A (B). We remind that we can write an electron in the Majorana representation as $a_A = \gamma_{A,1} + i\gamma_{A,2}$. We take the simple case $\mu = 0$, $t = \Delta$, in this case each system has a Majorana as excitation: $\gamma_{A,1}$ and $\gamma_{B,1}$.
Now we can couple the Majorana with an effective low-energy Hamiltonian. We can consider only the excitation below the gap, so our degrees of freedom are $\gamma_{A,1}$ and $\gamma_{B,1}$ and we can write:

$$H^{\text{Eff}} = i2\epsilon(\gamma_{1,B}\gamma_{1,A}). \tag{3.40}$$

This kind of coupling mix the MFs in a Bogoliubov excitation with energy ϵ. This kind of effective Hamiltonian corresponds to some coupling between the two Kitaev chain, which destroy the MFs. Now we ask what kind of coupling corresponds of this effective Hamiltonian.
The simplest way to couple the two Kitaev models is a local tunnelling t_c:

$$H_{\text{Tunneling}} = t_c a_B^\dagger a_A + h.c. \tag{3.41}$$

Where we take t_c as real parameter. Rewriting $H_{\text{Tunneling}}$ in the Majorana representation we obtain:

$$H_{\text{Tunneling}} = i2t(\gamma_{1,B}\gamma_{2,A} + \gamma_{1,A}\gamma_{2,B}). \tag{3.42}$$

We can see in the previous equation that there is not any coupling $\gamma_{1,B}\gamma_{1,A}$ (is cancelled by $h.c.$) and we can conclude that in this case the Majorana splitting ϵ is zero. We do not worried about the other Majorana operators γ_2 because they correspond to hight energies excitations.
After that we take a different local tunnelling: we suppose for that an amplitude

it_c, adding a complex term which break the effective time-reversal:

$$H_{\text{Tunneling}} = it_c a_B^\dagger a_A + h.c. \tag{3.43}$$

Again, rewriting $H_{\text{Tunneling}}$ in the Majorana representation we obtain:

$$H_{\text{Tunneling}} = i2t(\gamma_{1,B}\gamma_{1,A} + \gamma_{2,A}\gamma_{2,B}). \tag{3.44}$$

This coupling contains our low-energies degree of freedom$\gamma_{1,B}\gamma_{1,A}$ and comparing with H^{Eff} we find that a imaginary coupling correspond to a energy splitting $\epsilon = t_c$.

With this simple example we can se that when the Hamiltonian is purely real a coupling between MFs is forbidden. When we add an imaginary perturbation with strength t_c we lift the energy of MF form zero to $\epsilon \sim t_c$. Physically a complex term can be obtained by some disorder in the helical spin texture which we assumed as perfect.

In order to simulate disorder in the orientation, we can simply add a small random variation on the orientation of the magnetic moments of the impurities.The impurity spin can be parametrized by θ_n the angle between the z axis and the $x-y$ plane and ϕ_n the angle in the $x-y$plane. Then the disorder is made adding:

$$\begin{aligned}
&\theta_n = \frac{\pi}{2} + \delta\theta_n, \\
&\phi_n = k_H n a + \delta\phi_n, \\
&\cos(k_H a(m-n)) \to \cos(\theta_m)\cos(\theta_n)e^{i(\phi_m-\phi_n)} + \sin(\theta_m)\sin(\theta_n)e^{-i(\phi_m-\phi_n)}, \\
&\sin(k_H a(m-n)) \to -i(\cos(\theta_m)\sin(\theta_n)e^{i(\phi_m-\phi_n)} - \sin(\theta_m)\cos(\theta_n)e^{-i(\phi_m-\phi_n)}).
\end{aligned} \tag{3.45}$$

As we can see from the substitution the more relevant effect is the fact that a non perfect planar order with a finite $\delta\theta$, introduces a complex term in the Hamiltonian. This new term breaks the effective time-reversal $\mathcal{T}$. Then the system is no more in the class BDI but in class D, which has a $\mathbb{Z}_2$ invariant. In this case the topological invariant becomes $\mathcal{M}(H) = (-)^{w_{\mathbb{Z}}}$ and we cannot have multiple MFs. Any pairs of MFs will recombine in one ordinary electron. Then if we had an even number of MFs before the breaking of the symmetry we will have no Majorana Fermions. Otherwise if we had an odd number we will remain with only one Majorana

fermion.

3.5 Conclusions to the chapter

In this chapter, we describe a chain of magnetic atoms on top of a superconductor by taking into account the different impurity orbital degrees of freedom. These orbitals may play an important role in the intermediate regime between the dilute and the dense limit. Due to the impurity orbital overlap, one has a 1D conduction band on top of the superconductor (forming effectively a 1D conducting wire) . The band coexists with the magnetic moments which can create a 1D Shiba band into the superconductor. In this chapter we derive an effective Hamiltonian that describe the system as two coupled Kitaev-like channels (see section 3.4). This chapter represents the core of this thesis since this effective two channels Hamiltonian is still unprecedented in the literature.

In section 3.4, we discuss the symmetries and the topological class of the system. We show that if the helical spin texture is perfectly planar the effective Hamiltonian is invariant under complex conjugation, which acts as an effective time-reversal symmetry $\mathcal{T}$. If the effective Hamiltonian is invariant under $\mathcal{T}$, it posses a topological index in $\mathbb{Z}$ and can a-priori host multiple MFs. If $\mathcal{T}$-symmetry is broken, the topological index is a $\mathbb{Z}_2$ -index. In this case the system can host only a pair of MFs.

We remark that we have no reason to suppose a perfect helical spin texture in a realistic system. Then, we expect that this symmetry is broken in an experimental setup.

Finally, in subsection 3.4.1 we derive the effective Hamiltonian in the more generic case when the large magnetization limit $t_w \ll J'S$ is not taken.

Chapter 4

Phase diagram of Shiba chain and magnetic wire

In this chapter, we study the Shiba chain and the orbital (or wire) part as non coupled. These system does not have any physical meaning. However, this two uncoupled models are well studied in literature and the meaning of this chapter is to test our numerical tools and show that they are in agree with the result in literature. Furthermore before the studying of the full problem, it is useful to develop some intuition about this model. Most of the observations that are applicable here can been applied in the more general coupled system.

- **Momentum space study** : in the section 4.1, imposing periodic boundary condition, we are able to calculate (semi-analytically) the topological index w, which correspond to the number of MFs when we take open boundary condition. In the periodic system we are also able to calculate the spectrum analytically (or semi-analytically). Thanks to that we can show that the number of MF depends on the number of times that the energy band cross the Fermi level. We check that our result are in agree with literature [29, 31].

- **Real space**: in the section 4.2, we impose open boundary condition and we numerically calculate the local density of states LDOS. Another useful tool is Majorana polarization: a quantity C_j, depending on the wavefunction, that it is equal to one if the state is a Majorana excitation.
  After that we will discuss the role of the disorder, showing that multiple MFs are not robust against a variation in the orientation of the magnetic impurities.

About the scale of our parameters for the condition of low-energy $\epsilon \ll \Delta$, we have

to chose most of the parameters in order to stay consistently. In a real system the Superconducting gap has value of the order: $\Delta \sim 1meV$, then we set $\Delta = 1$ and we will chose most of the parameters in order of meV. The magnetic couplings J, J' in reality are in the order of eV. We will simply take $J, J' > \Delta$ because a larger value does not affect our conclusion, but it simply renormalizes some couplings.

4.1 Periodic boundary condition

In order to derive the phase diagram of the system we use the Bulk-Boundaries correspondence: we impose periodic boundary condition and we calculate the topological index w, the winding number, as an integral on the whole Brillouin zone. This index is equal to the number of edge states (MFs) [37] when open boundary condition is taken.

4.1.1 Winding number of Shiba chain

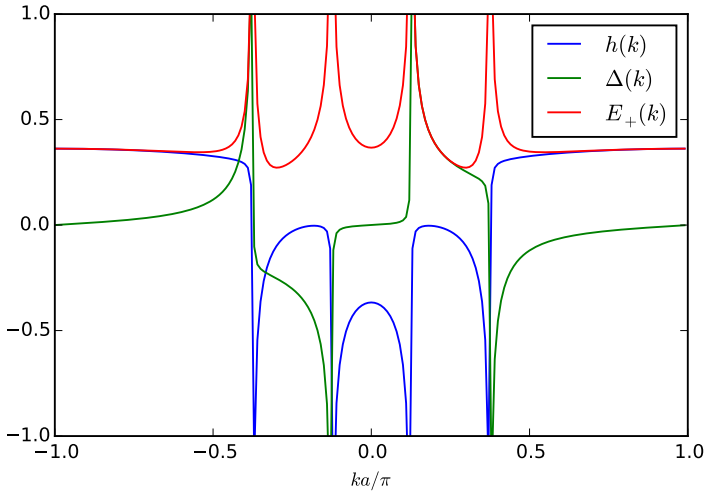

Figure 4.1: The spectrum of the Shiba chain: the energy $E(k)$, the normal coupling $h(k)$, and the superconducting pairing $\Delta(k)$, as a functions of the quasi-momentum k. The four peaks in the spectrum (in red) correspond to $|k_F + k_H|$, $|k_F - k_H|$, mod $(2\pi/a)$. Here we have $w = 1$. The parameters used are $\Delta = 1$, $\alpha = 0.9$, $k_H a/\pi = 1/8$, $k_F a/\pi = 4.25$ and $e^{-a/\xi} = 1$.

In order to study the topological properties of the system we consider the

Fourier transform of the Hamiltonian Eq:D.37: Given the two matrix elements:

$$\begin{aligned} h_{n,n} &= \epsilon_\alpha, \\ h_{m\neq n} &= -\Delta\sqrt{\frac{2}{\pi k_F r_{mn}}}\cos(k_F r_{mn} - \frac{\pi}{4})\cos(k_H(x_m - x_n))e^{-\frac{r_{mn}}{\xi}}, \\ \Delta_{m\neq n} &= -\Delta\sqrt{\frac{2}{\pi k_F r_{mn}}} i\sin(k_F r_{mn} - \frac{\pi}{4})\sin(k_H(x_m - x_n))e^{-\frac{r_{mn}}{\xi}}, \end{aligned} \tag{4.1}$$

where we restored the factor $e^{-\frac{r}{\xi}}$ for convergence manner. Due the translational invariance we have to calculate:

$$\begin{aligned} h(k) &= \sum_m e^{ikma} h_{m,0}, \\ \Delta(k) &= \sum_m e^{ikma} \Delta_{m,0}, \end{aligned} \tag{4.2}$$

See Appendix:H for explicit calculation. After that we have a BdG Hamiltonian:

$$\mathcal{H}(k) = \begin{pmatrix} h(k) & \Delta(k) \\ \Delta^*(k) & -h(-k) \end{pmatrix}. \tag{4.3}$$

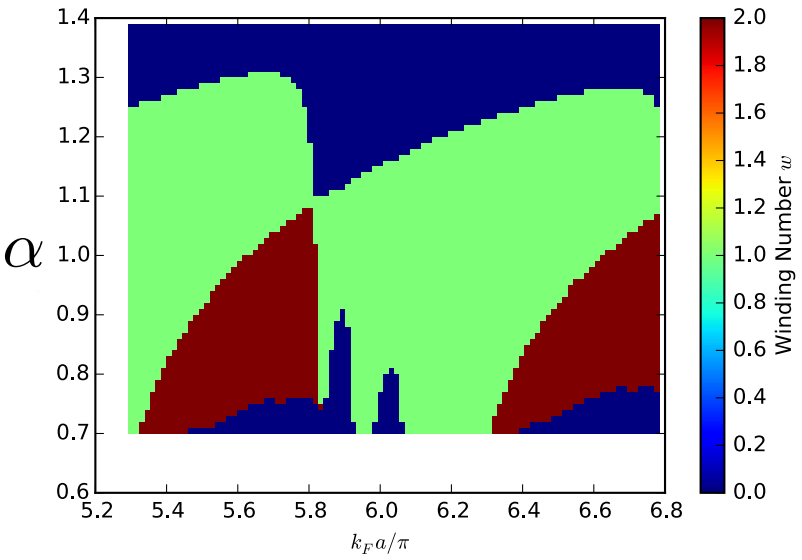

Figure 4.2: Phase diagram for the Shiba chain. The winding number w as a function of α and $k_F a/\pi$. This phase diagram is in agree with Figure 3.1 in [31]. The parameters we used are: $\Delta = 1$, $k_H a/\pi = 1/8$ and $a/\xi = 0.05$.

with the bulk spectrum $E_\pm^2(k) = h^2(k) + \Delta^2(k)$. The explicit expression of single elements is in appendix Eq: (H.9), (H.10). We also have $h(k) = h(-k)$ and

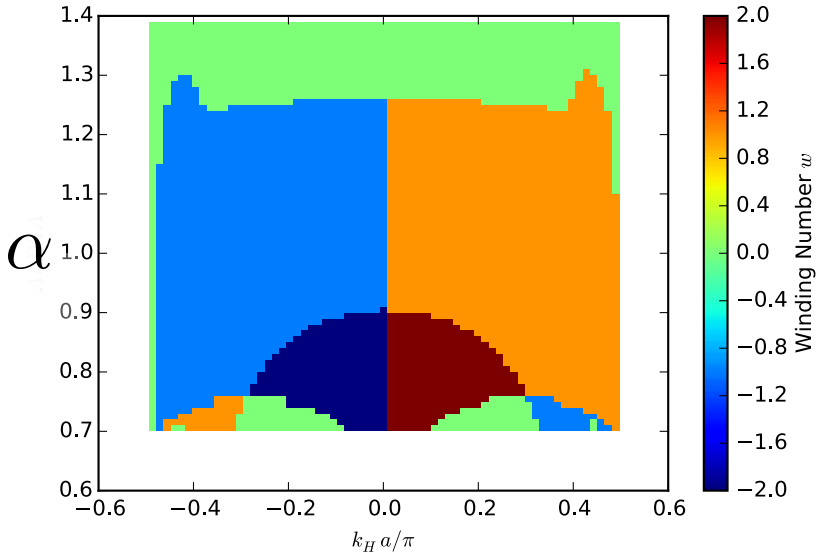

Figure 4.3: Phase diagram for the Shiba chain. The winding number w as a function of α and $k_H a/\pi$. The parameters we used are: $\Delta = 1$, $k_F a/\pi = 6.45$ and $a/\xi = 0.05$.

$\Delta(k) = \Delta^*(k)$.

In order to make the Hamiltonian explicitly time-reversal invariant we perform a unitary transformation: $c_k \longrightarrow e^{i\pi/4} c_k$.

Following [37] we can make $\mathcal{H}(k)$ purely off-diagonal performing a rotation in particle-hole space $U = e^{-i\tau_y \pi/4}$.

The transformed Hamiltonian $U\mathcal{H}(k)U^\dagger$ becomes:

$$\mathcal{H}'(k) = \begin{pmatrix} 0 & h(k) - i\Delta(k) \\ h(k) + i\Delta(k) & 0 \end{pmatrix} = \begin{pmatrix} 0 & A(k) \\ A^*(k) & 0 \end{pmatrix}. \tag{4.4}$$

We note that $\Delta(0/\pi) = 0$, it follows that $A(0/\pi)$ is purely real. Thus, we can define the angle $\theta(k)$ as $\frac{A(k)}{|A(k)|} = e^{-i\theta(k)}$. Calling $z(k) = e^{i\theta(k)}$.We can calculate the winding number w using the appendix formula I.7:

$$w = \frac{1}{i\pi} \int_0^{\frac{\pi}{a}} \frac{dz(k)}{z(k)} = \int \frac{d\theta(k)}{\pi} = \frac{\theta(\frac{\pi}{a}) - \theta(0)}{\pi}. \tag{4.5}$$

4.1.2 Discussion of phase diagram of the Shiba chain

In the previous Subsection we showed that the Shiba chain has a non-trivial phase diagram and that the topological phase can host one or two MFs,depending on the

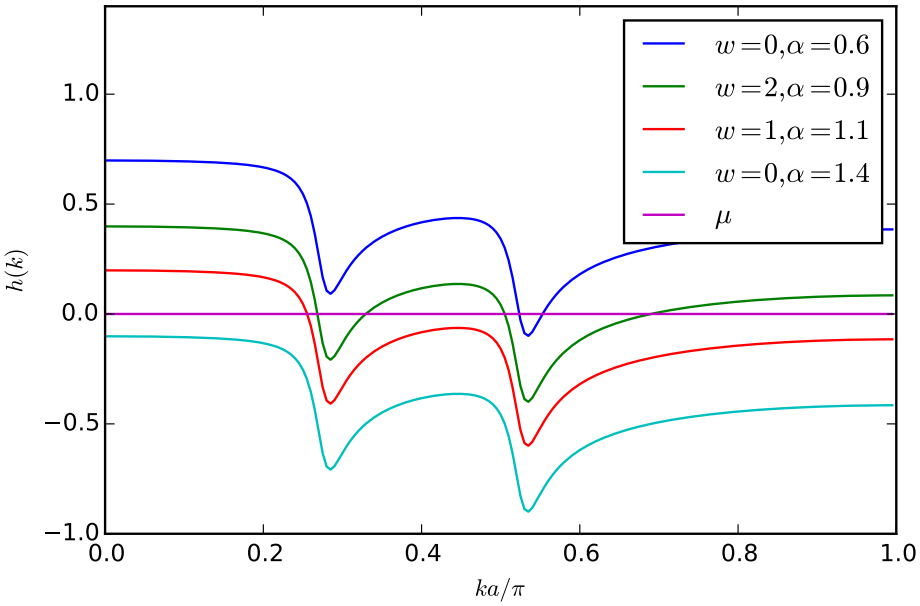

Figure 4.4: Shiba Chain: $h(k)$ as a function of the quasi-momentum k, for for different values of α (which correspond to different winding numers). The winding number changes when the number of intersection between $h(k)$ and the Fermi level μ changing. This can be understood by the parity $\mathcal{P} = (-1)^W = sign(h(0)h(\pi))$: even (odd) numbers of intersection correspond to even (odd) winding numbers and even (odd) MF. The parameters we used are: $\Delta = 1$, $k_H a/\pi = 1/8$,$k_F = 5.6$ and $a/\xi = 0.05$.

parameters. In the Figure 4.2 we show a phase diagram in good agreement with the results obtained in literature. In the Figure 4.4 we show that the number of times that the energy $h(k)$ cross the Fermi lever is related to the winding number.

4.1.3 Winding number of magnetic wire

In this section, we will study the phase diagram of wire,without any coupling with Shiba chain. We recall that the orbital (or wire) Hamiltonian can be expressed as

$$\begin{aligned} H^{\text{eff}}_{\text{Wire}} = &\sum_n \tilde{a}^\dagger_{n,\uparrow}\left(\epsilon_g + t_w - J'S - \frac{t_w^2\sin^2(k_H a)}{4J'S}\right)\tilde{a}_{n,\uparrow} \\ &+ \sum_n [\tilde{a}^\dagger_{n,\uparrow}\frac{t_w^2\sin^2(k_H a)}{8J'S}\tilde{a}_{n+2,\uparrow} - \tilde{a}^\dagger_{n,\uparrow}\frac{t_w}{2}\cos(k_H a)\tilde{a}_{n+1,\uparrow} \\ &-\left(\frac{1}{J'S}+\frac{1}{\epsilon_g}\right)\frac{\Delta' it\sin(k_H a)}{4}\tilde{a}^\dagger_{n,\uparrow}\tilde{a}^\dagger_{n+1,\uparrow} + h.c.]. \end{aligned} \tag{4.6}$$

taking the Fourier Transform in according with the notation defined in Appendix H we have:

$$\begin{aligned} h_w(k) =&\epsilon_w - \frac{t_w^2\sin^2(k_H a)}{4J'S} + t_w(1-\cos(ka)\cos(k_H a)) \\ &+ \frac{t_w^2\sin^2(k_H a)\cos(2ka)}{4J'S}, \end{aligned} \tag{4.7}$$

$$\Delta_w(k) = +\frac{1}{2}\left(\frac{1}{J'S}+\frac{1}{\epsilon_g}\right)\Delta' t_w\sin(k_H a)\sin(ka), \tag{4.8}$$

where $\epsilon_w = \epsilon_g - J'S \sim 0$ because we want that the wire band cross the Fermi energy. The Bulk Spectrum is $E^2_\pm(k) = (h^2(k) + \Delta^2(k))$. Thanks to the procedure of section 4.1.1, by performing the two unitary transformation: $a_k \longrightarrow e^{i\pi/4}a_k$ and $U = e^{-i\tau_y\pi/4}$ we obtain:

$$\mathcal{H}'(k) = \begin{pmatrix} 0 & h_w(k) - i\Delta_w(k) \\ h_w(k) + i\Delta_w(k) & 0 \end{pmatrix} = \begin{pmatrix} 0 & A(k) \\ A^*(k) & 0 \end{pmatrix}. \tag{4.9}$$

Another time we can define $\theta(k) = -\arg(A(k))$ and the winding number w as Eq: (4.5):

$$w = \frac{\theta(\frac{\pi}{a}) - \theta(0)}{\pi}, \tag{4.10}$$

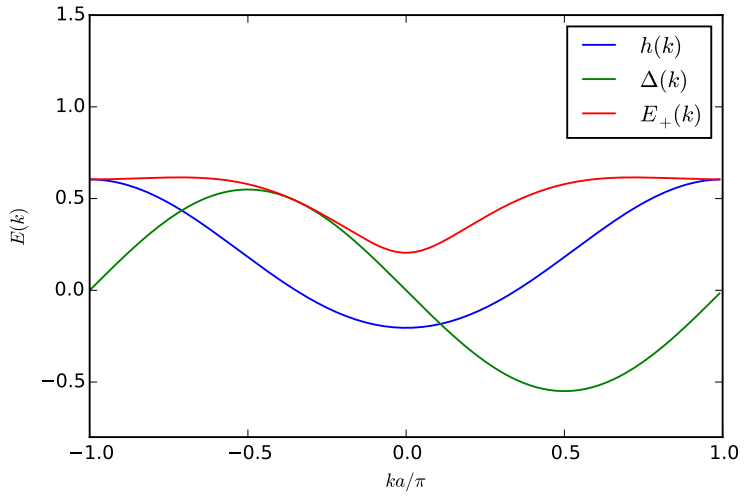

Figure 4.5: Wire Hamiltonian: The energy $E(k)$, the normal coupling $h(k)$, and the superconducting pairing $\Delta(k)$ as a functions of the quasi-momentum k. The parameters we used are: $\Delta' = 1$, $t_w = 0.5$, $J'S = 2.3$, $\epsilon_g = 2$ and $k_H = 0.2$.

Because $\Delta(0) = \Delta(\pi/a) = 0$ we have, [1]:

$$\mathcal{P} = (-1)^w = (-1)^{\frac{sign(h(0)) - sign(h(\frac{\pi}{a}))}{2}}, \tag{4.11}$$

Neglecting the t_w^2 terms we can simplify the previous formula. [2]

$$\mathcal{P} = (-1)^w = \approx (-1)^{\frac{sign(\epsilon_w) - sign(\epsilon_w + (1+\cos(k_H a))t_w)}{2}}. \tag{4.12}$$

4.1.4 Discussion of the phase diagram of magnetic wire

In the previous Subsection we showed that the magnetic (or Orbital) wire has a non-trivial phase diagram. This system can host only one edge state and the topological condition depends only on the crossing of the Fermi level.

4.2 Open boundary conditions

Now we study the system in the real space, imposing open boundary conditions. In this way we can reveal directly MFs, as edge states, looking at the local density of states.

[1] We use the Parity to avoid the fact that the phase, is defined less 2π, without the knowledge of $\Delta(k)$

[2] This is the same result of 2.10, but here the notation is different.

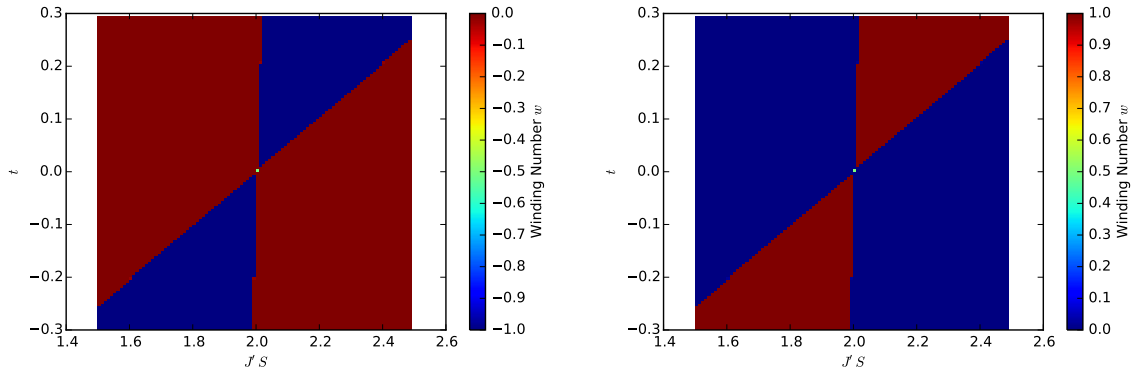

Figure 4.6: Phase diagram of the wire Hamiltonian. The winding number as a function of t and $J'S$. The rotation respect to Figure 2.2 is due to a different definition of parameter t_w. The parameters we used are: $\Delta' = 1$, $\epsilon_g = 2$, with $k_H = 0.1$ (left figure) and $k_H = -0.1$ (right figure).

In this section, we introduce two tools to reveal MFs:

- **LDOS**: to reveal MFs we can use the local density of state(LDOS, this is a direct measure of the wave function at given energy. The LDOS is experimentally accessible because it can measured with tunneling experiment. Now we expose our notation: in general we have a BdG Hamiltonian as:

$$H = \frac{1}{2}\sum_{m,n} \Psi_m^\dagger \mathcal{H}_{m,n} \Psi_n, \quad \Psi_n = \begin{pmatrix} a_n \\ a_n^\dagger \end{pmatrix}, \tag{4.13}$$

  where $n, m \in [0, N]$ are the site index. Diagonalising the Hamiltonian we can find the eigenvector $\Psi^{(j)}$ relatives to the eigenvalues $E^{(j)}$. Then we define the local density of states $\rho(n, E)$ as:

$$\rho(n, E) = \sum_j \Psi_n^{(j)\dagger} \left(\frac{1 + \tau_z}{2} \right) \Psi_n^{(j)} \delta(E - E^{(j)}). \tag{4.14}$$

- **Majorana polarization** The Majorana polarization (MP) is a numerical tool to reveal if an eigenvector is a Majorana mode or not. Unlike LDOS, Majorana polarization is not experimentally observable, it is just a numerical tool to analyse the wavefunction.

  A Majorana zero mode is invariant under the charge conjugation $\mathcal{C}\Psi^{(M)} = \Psi^{(M)}$, where $\mathcal{C} = \tau_x K$. Due this consideration we can define the Majorana

polarization [45]:

$$C^{(j)} = \frac{|\sum_{n\in\mathcal{R}} \langle\Psi^{(j)\dagger}|\mathcal{C}_n|\Psi^{(j)}\rangle|}{\sum_{n\in\mathcal{R}} \langle\Psi^{(j)\dagger}|r_n|\Psi^{(j)}\rangle} \tag{4.15}$$

Where r_n is the projection on the $n-$site, $\mathcal{C}_n = r_n\mathcal{C}$, and we can take $\mathcal{R}$ as half of the system. If Ψ is a Majorana zero mode, then $C^{(M)} = 1$

4.2.1 Shiba chain

In this section, we study the LDOS of the system. In the Figure: (4.2.1) we can see two MF (left figure) and one (right).The transition between the two phases happens when the number of intersection of $h(k)$ and the Fermi level changes. (Figure:(4.4)). After that we will see how the disorder affect the Majorana Modes.

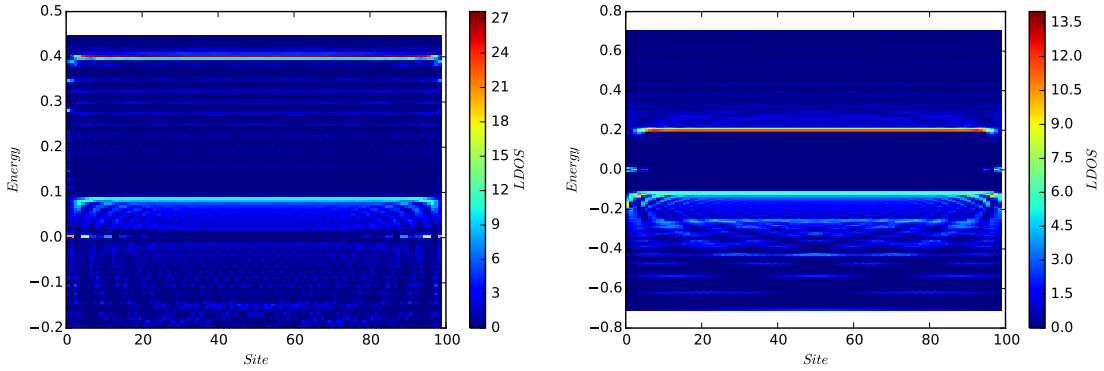

Figure 4.7: LDOS of Shiba chain. We show the LDOS as a function of the energy and the site index. There are two Majoranas in the left picture and one in the right, between the two situation the Shiba energy $\epsilon_\alpha = \Delta(1-\alpha)$ cross the Fermi Level. The parameters we used are: $N = 100$, $\Delta = 1$, $k_H a/\pi = 1/8$, $k_F = 5.6$, $a/\xi = 0.05$ and $\alpha = 0.9$ (w=2, on the left), $\alpha = 1.1$ (w=1, on the right).

We can see in the figure 4.2.1 that the two Majorana are in the same sites. Now we ask if they are robust against a moderate disorder. In order to do that we

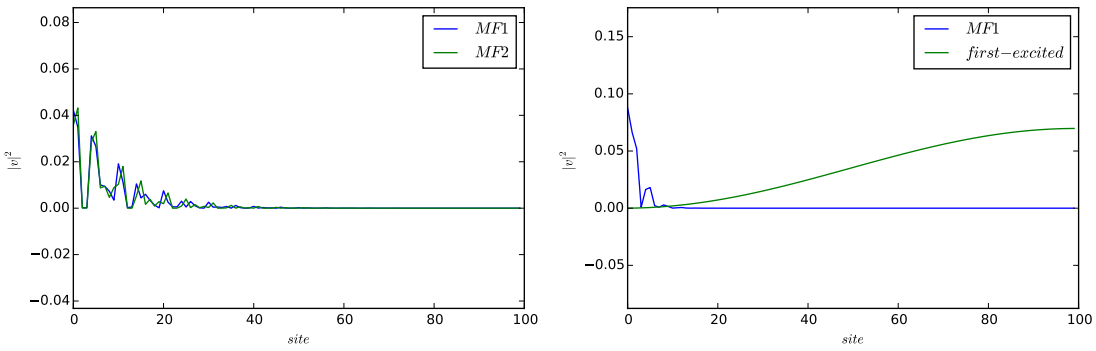

Figure 4.8: Shiba chain: The hole wavefunctions$|v|^2$ of the two first Bogoliubov quasiparticles in the half of system, as a function of the site index. In the left pictures there are two Majoranas, which are localized on the same sites. In the right there is only one Majorana and the first excited state is delocalized. The parameters we used are the same of Figure:(4.2.1) with $N = 200$.

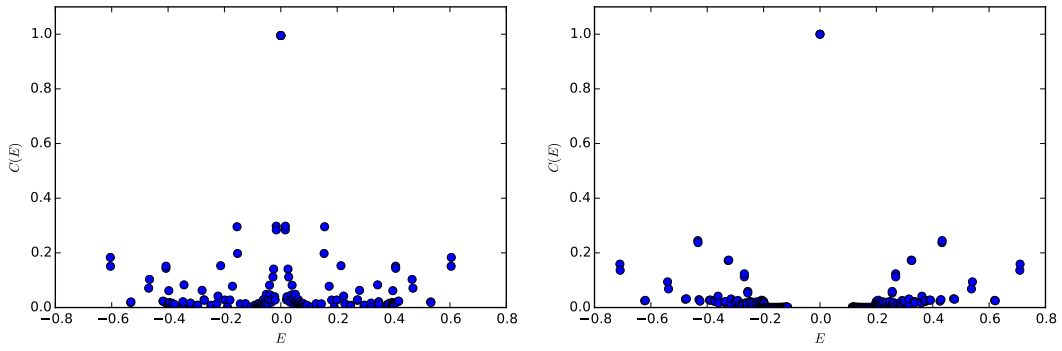

Figure 4.9: Shiba chain: The Majorana polarization as a function of the energy associated with an eigenfunction. In the Figure a MF has MP close to 1 and the other states have smaller values: the MP can be used to distinguish a MF to a normal mode. The parameters we used are the same of Figure:(4.2.1)

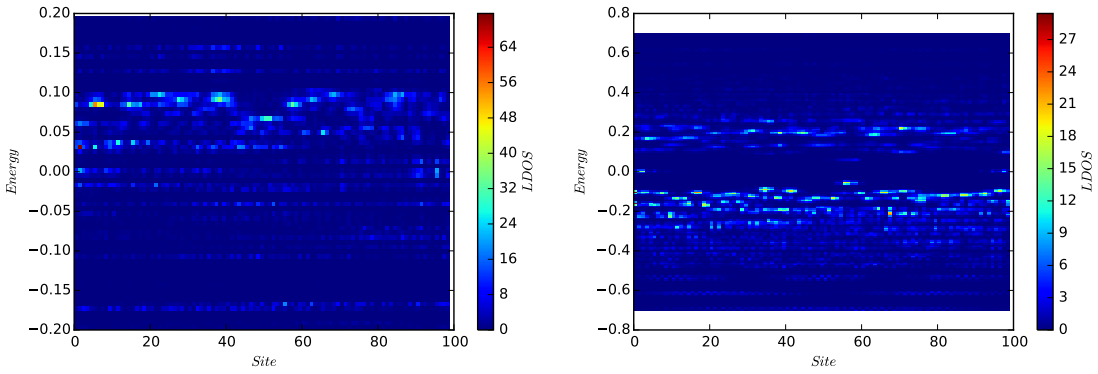

Figure 4.10: LDOS of disordered Shiba chain. The LDOS as a function of the energy and the site index. The disorder completely alter the spectrum above the gap. In the middle of the gap we can still see MFs. However, because the effective time-reversal symmetry is broken we can see in the left figure that the two MFs start to hybridize and to delocalize. The parameters we used are the same of Figure:(4.2.1), with small random variation $\delta\alpha \in [-0.05, 0.05]$, $\delta\theta, \delta\phi \in [-0.02, 0.02]$.

include in the Hamiltonian new parameters to mimic the disorder:

$$\begin{aligned}
&\alpha \to \alpha + \delta\alpha_n,\\
&\theta_n = \frac{\pi}{4} + \delta\theta_n,\\
&\phi_n = k_H n a + \delta\phi_n,\\
&\cos(k_H a(m-n)) \to \cos(\theta_m)\cos(\theta_n)e^{i(\phi_m-\phi_n)} + \sin(\theta_m)\sin(\theta_n)e^{-i(\phi_m-\phi_n)},\\
&\sin(k_H a(m-n)) \to -i(\cos(\theta_m)\sin(\theta_n)e^{i(\phi_m-\phi_n)} - \sin(\theta_m)\cos(\theta_n)e^{-i(\phi_m-\phi_n)}).
\end{aligned} \tag{4.16}$$

Where $\delta\alpha$ is a small random variation of Shiba Energy, and $\delta\phi_n, \delta\theta_n$ are small random variations of the orientation of the magnetic impurities. In the Figure:(4.10) we can see that multiple Majorana Modes are not robust against a weak complex disorder.[3] Because this substitution introduce a complex term, the Effective time-reversal symmetry $\mathcal{T} = K$ is broken and the system is no more in the class BDI but in class D, which has a $\mathbb{Z}_2$ invariant. [46] Thus, we expect that the two Majorana hybridize and become normal states.Because this process is continuous with small disorder we will have a Majorana Mode precursor,(see also [45]). On the contrary a single MF is not affected from the transition $\mathbb{Z} \longrightarrow \mathbb{Z}_2$, and so it is still robust against complex disorder.

[3]With complex disorder we mean disorder that add complex term to Hamiltonian, as the disorder in the orientation of the spin direction disorder.

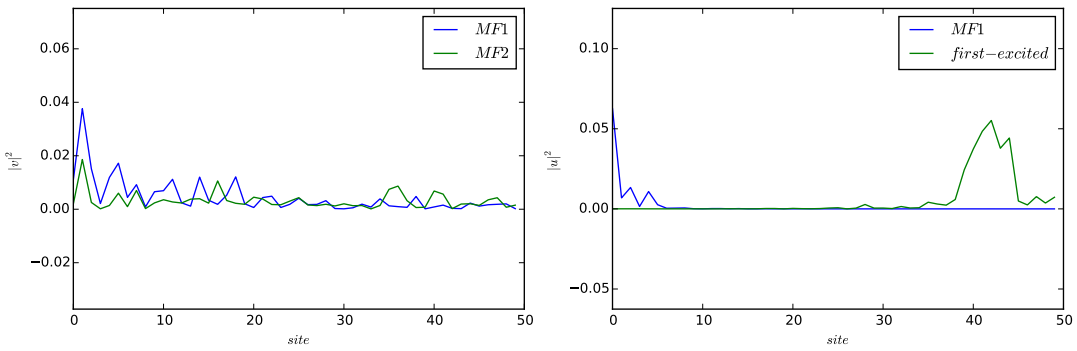

Figure 4.11: Shiba chain. The LDOS as a function of the energy and the site index. The electron wave function$|u|^2$ of the two first Bogoliubov quasiparticles in the half of system, as a function of the site index. In the right figure we can see an electron localized on a fluctuation of $\delta\alpha$ while the Majorana mode is localized in the edge of system. In the left figure the two MFs start to delocalize because here the time-reversal symmetry is broken, in the right figure we can see the only one MF is still protected against disorder. The parameters we used are the same of Figure:(4.10) .

4.2.2 Shiba chain: discussion of real space study

In the previous subsection, we computed the LDOS of the Shiba chain, showing that it is in a good agreement with the calculation in the k-space. After that we discussed the role of the disorder showing that multiple MFs are weak against complex disorder, whereas a single MF is still robust against complex disorder.

4.2.3 Magnetic wire

Here we simply report the LDOS for the wire Hamiltonian, showing the trivial and the topological phases. The LDOS is in good agreement with the calculation made in the k-space.

4.3 Conclusions to the chapter

In this chapter, we studied the Shiba chain and the magnetic wire, as uncoupled systems. These models are well-studied in the literature. This chapter aims at testing our numerical tools. Furthermore, before studying the full problem, this is useful to also develop some intuition about the physics at play.

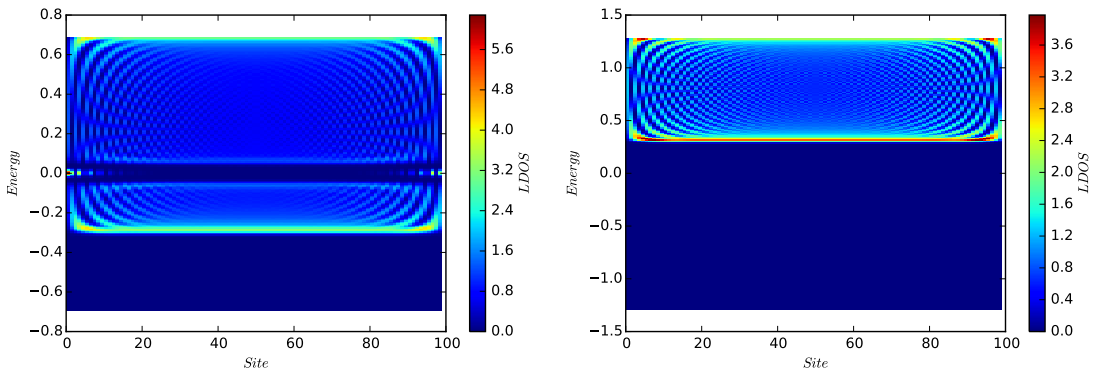

Figure 4.12: Magnetic wire. The LDOS as a function of the energy and the site index. In this situation the wire is topological (left) or trivial (right). In the topological phase (left figure) we can see the Majorana zero modes. The parameters we used are $\Delta' = 1$, $k_H a/\pi = 1/8$, $t = 1/2$, $\epsilon_g = 2$ and $J'S = 2.3$ (w=1, on the left), $J'S = 1.7$ (w=0, on the right).

Chapter 5

Phase diagram of Shiba chain with orbital degrees of freedom

In chapter 3, we derived the effective model for a low-energy description of the system. In the previous chapter 4 we introduced the main numerical tool to study the topological properties of the system. In this chapter, we use this tool to study our system. We derive the entire phase diagram and we discuss a simple criteria to infer the topology of the system.
This chapter, together with chapter 3, represents the main new result of this thesis. We will numerically explore the phase diagram of the Hamiltonian (3.36). Because this is an original model all the results are unprecedented. First of all we want to briefly introduce the tool that we will use to study the system:

- **Winding number**: we take the two Hamiltonians, the wire and the Shiba chain, coupled with small strength t. After the Fourier transform (see the appendix H, where the elements are expressed in detail) the Hamiltonian reads:

$$\begin{aligned} \mathcal{H}_{\alpha,\beta}(k) &= h_{\alpha,\beta}(k)\tau_x + \Delta_{\alpha,\beta}(k)\tau_y, \\ h_{\alpha,\beta}(k) &= \begin{pmatrix} h^a(k) & M(k) \\ M(k) & h^c(k) \end{pmatrix}, \\ \Delta_{\alpha,\beta}(k) &= \begin{pmatrix} \Delta^a(k) & N(k) \\ N(k) & \Delta^c(k) \end{pmatrix}. \end{aligned} \tag{5.1}$$

Then the winding number is defined by:

$$\begin{aligned} w &= \frac{1}{i\pi}\int_{k=0}^{k=\pi}\frac{dz(k)}{z(k)} = \frac{1}{\pi}(\theta(\pi)-\theta(0)), \\ \theta(k) &= \arg(\det[A(k)]), \qquad\qquad A_{\alpha,\beta}(k) = h_{\alpha,\beta}(k) + i\Delta_{\alpha,\beta}. \end{aligned} \tag{5.2}$$

- **Parity and Spectrum**: Another important criteria is parity $\mathcal{P}$. [1]. Because the terms $a^\dagger a^\dagger, aa$ does not change the parity if we have an Hamiltonian like $\mathcal{H}_{\alpha,\beta}(k) = h_{\alpha,\beta}(k)\tau_x + \Delta_{\alpha,\beta}(k)\tau_y$, we can neglect the superconducting part Δ to evaluate the parity.
  Diagonalising the electronic part of Hamiltonian $h_{\alpha,\beta}(k)$ we get two bands $E_+(k), E_-(k)$. We can define the parity on each band as $\mathcal{P}^\pm$. We have also $\mathcal{P}^\pm = sign(E_\pm(0)E_\pm(\pi))$. Thus, to have a single MF on one band the band has to cross the Fermi level μ. This is a single criteria to find the topological non-trivial phase but it is not possible to conclude that when the $\mathcal{P} = +$ we do not have Majorana. In fact this shows that we have an even number of MF. $w = 0, 2, 4 \ldots$. This is the same criteria used in Figure:(4.4).

- **Nambu wavefunction**: In the real space we define the Nambu spinor as:

$$\hat{\Psi}_n = \begin{pmatrix} a_n \\ a_n^\dagger \\ c_n \\ c_n^\dagger \end{pmatrix}. \tag{5.3}$$

  We define the Nambu wavefunction as:

$$\Psi_n = \begin{pmatrix} u_n^{(a)} \\ v_n^{(a)} \\ u_n^{(c)} \\ v_n^{(c)} \end{pmatrix}. \tag{5.4}$$

  Then the probability to find an electron (hole) in the system $S = a, c$, in the position n is $|u_n^{(S)}|^2$ ($|v_n^{(S)}|^2$).

[1] Let us recall that there is a relation between Parity and the winding number:$\mathcal{P} = (-)^W$

5.1 Scaling of parameters

Here we recall what are the relevant parameters of Hamiltonian (3.36).
We start by treating t as a small perturbation, we increase t starting from 0 and we see how the wire and the chain will coupled. We also remind that $\Delta' \sim t^2$, then when $t = 0$ the gap will be closed and we are not able to talk about topology. We call w_1 the winding number on the Shiba chain, and w_2 the winding on the wire when the two systems are decoupled ($t = 0$). We start with one MF on the Shiba, and zero on the wire. In order to have a clean relation between parameters we set $\pi\nu_0 = 1$. First of all we declare the important parameters:
On the wire we have the energy scale ϵ_W and the p-wave superconductivity $\Delta^{\text{p-wave}}$.

$$\begin{aligned} \epsilon_W &= \epsilon_g + t_w - J'S + t_w \hat{f}^{1-\text{neighbour}}(k_H r), \\ \Delta^{\text{p-wave}} &= (\frac{1}{\epsilon_g} + \frac{1}{J'S}) t^2 t_w \sin(k_H a). \end{aligned} \tag{5.5}$$

On the Shiba chain we have the shiba energy ϵ_α and a long-range potential:

$$\begin{aligned} \epsilon_\alpha &= \Delta(1-\alpha) = \Delta(1 - JS), \\ H^{\text{Shiba}} &= \epsilon_\alpha + \frac{\Delta}{\sqrt{kr}} \hat{h}(k_F r, k_H r), \end{aligned} \tag{5.6}$$

The scales of the coupling are:

$$H^{\text{Tunneling}} = t\sqrt{\frac{\Delta}{JS}} \hat{f}^{\text{local}} + t\sqrt{\frac{\Delta}{JS}} \frac{1}{\sqrt{kr}} \hat{f}^{\text{long-range}}(k_F r, k_H r). \tag{5.7}$$

5.2 Discussion of numerical result

Let us discuss the figures of this chapter: first we show the winding number when t is increasing from zero. Then we show that a change in the value of the winding number correspond of a change of the type of crossing between $h_\pm(k)$ and the Fermi Level. Finally studying the wavefunction we can infer the localisation of the MFs on one of the two system. After that we show the full phase diagram, calculated with the winding number.
Thanks to this analysis we can infer the following conclusions:

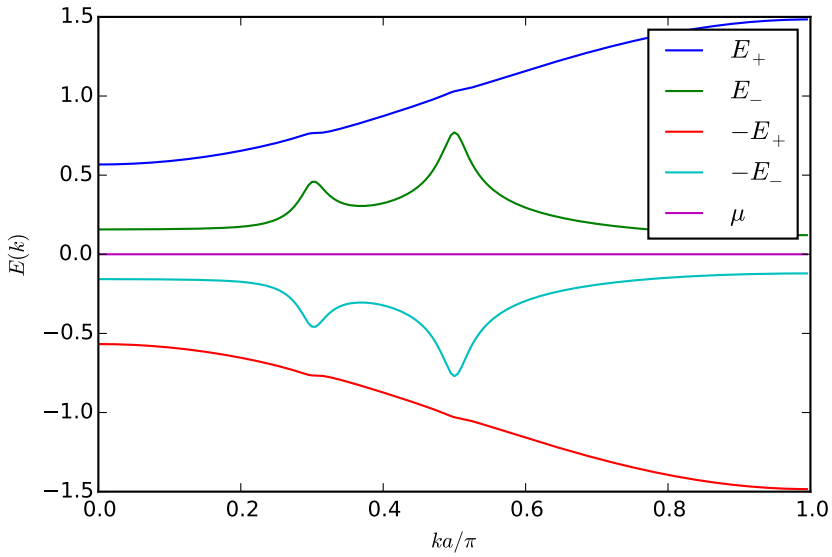

Figure 5.1: Plot of the energy spectrum and of the chemical potential. The two peaks in the spectrum correspond to $|k_F + k_H|$,$|k_F - k_H|$, mod $(2\pi/a)$. The parameters we used are: $\Delta = 1$, $k_H a/\pi = 0.1$, $k_F a/\pi = 5.6$,$t_w = 0.5$, $\epsilon_g = 2$, $a/\xi = 0.05$ and $J'S = 1.5$, $JS = 1.1$

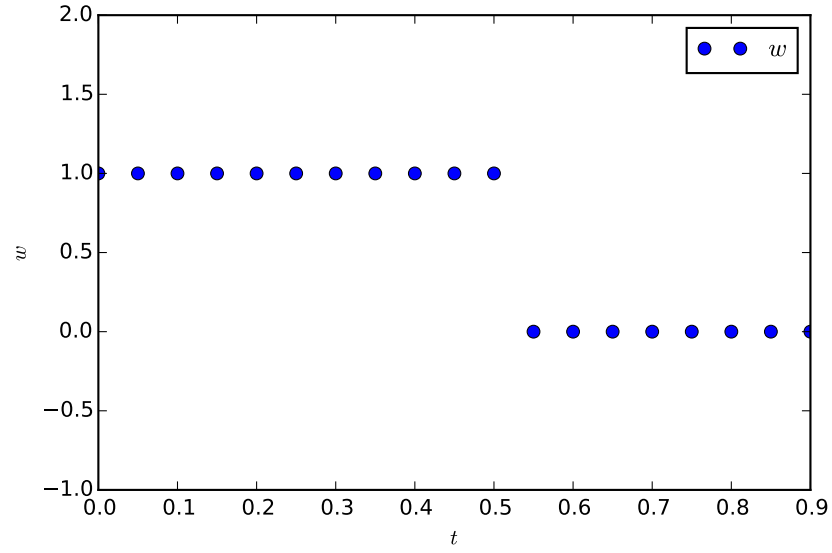

Figure 5.2: The winding number as a function of t. For small values of t the Shiba chain is topological. Increasing t we increase the splitting of the two bands. When the Shiba (hybridised) band does not cross the Fermi level μ anymore the system is topologically trivial. The parameters we used are: $\Delta = 1$, $k_H a/\pi = 0.1$, $k_F a/\pi = 5.6$,$t_w = 0.5$, $\epsilon_g = 2$, $a/\xi = 0.05$ and $J'S = 1.5$, $JS = 1.1$

- The system can be topological and can host multiple MFs. It can accommodate up to three Majorana excitation: two localized on the chain and one on the wire.
- All the phase transitions are characterized by the gap closing and by the change of the number of crossing between the Fermi level and $h(k)$. Looking at this function it is possible to establish the topology of the system.

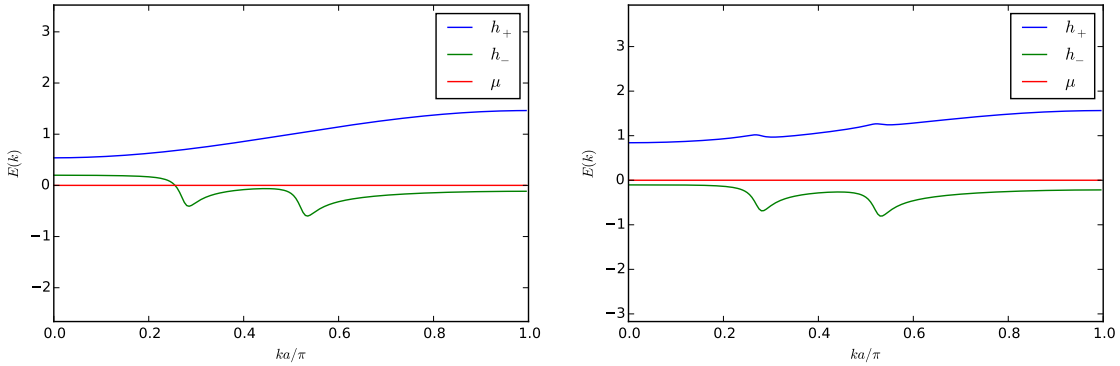

Figure 5.3: The energy $h_{\pm}(k)$ as a function of the quasi-momentum k. Neglecting the superconducting part we can see that the condition for the system to be topologically non-trivial is the crossing of the Fermi level (right). Here the Shiba (hybridized) band is topological $w = 1$. The parameters we used are the same of precedent Figure :(5.2) with $t = 0$ (right) and $t = 0.7$ (left).

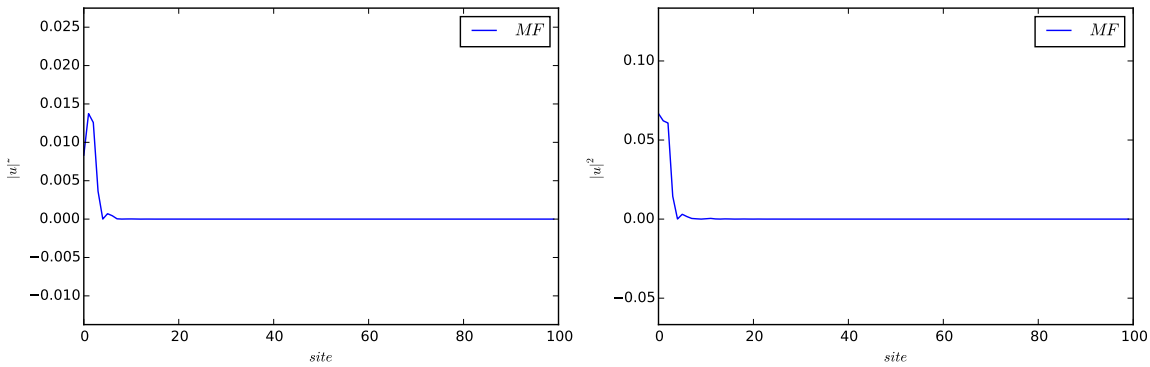

Figure 5.4: The electron wave function $|u|^2$ of the MF as a function of the sites index, on the wire (right) and on the chain (left). The MF is localized on the Shiba chain with a small hopping in the wire part. The parameters we used are the same of precedent figure (Figure :(5.2)) with $t = 0.4$ and $N = 200$).

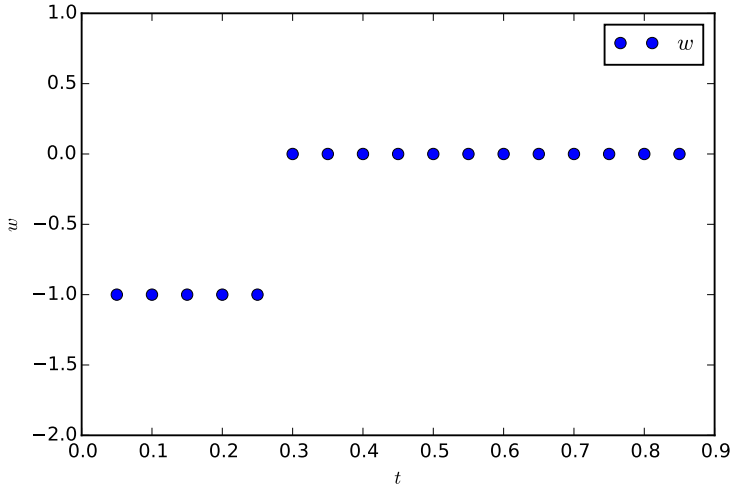

Figure 5.5: The winding number as a function of t. For small values of t the wire is topological ($t = 0$ is a special case, because the wire is gapless). Increasing t we increase the splitting of the two bands. When the (hybridized) wire band does not cross the Fermi level μ anymore the system becomes topologically trivial. The parameters we used are: $\Delta = 1$, $k_H a/\pi = 0.1$, $k_F a/\pi = 5.6$, $t_w = 0.5$, $\epsilon_g = 2$, $a/\xi = 0.05$ and $J'S = 2.3$, $JS = 1.4$

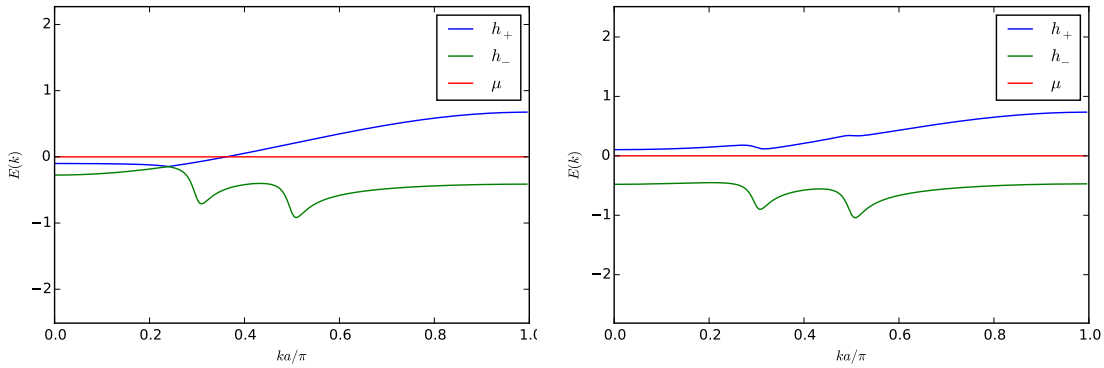

Figure 5.6: The energy $h_{\pm}(k)$ as a function of the quasi-momentum k. Neglecting the superconducting part we can see that the condition to be topologically non-trivial is the crossing of the Fermi level (right). Here the wire (hybridized) band is topological $w = 1$. The parameters we used are the same of precedent figure (Figure :(5.5)) with $t = 0$ (right) and $t = 0.5$ (left).

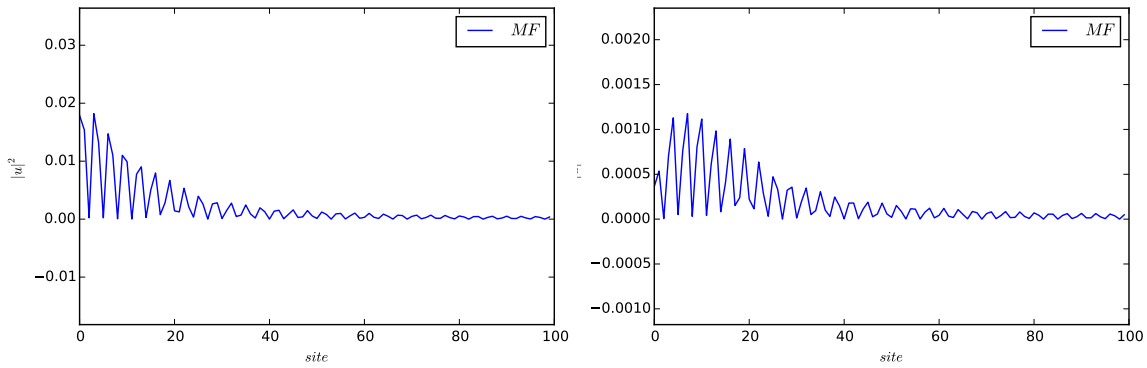

Figure 5.7: The electron wave function $|u|^2$ of the MF, on the wire (right) and on the chain (left), as a function of the site index. The MF is localized on the wire with a small hopping in the wire part. The parameters we used are: the same of precedent figure (Figure :(5.5)) with $t = 0.2$.

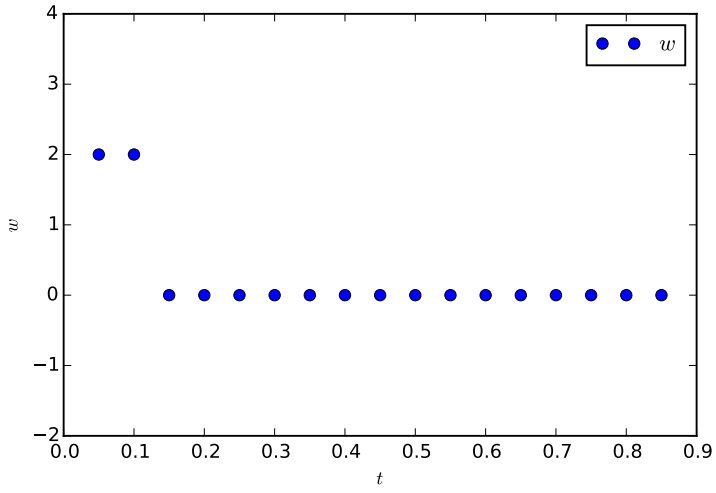

Figure 5.8: The winding number as a function of t. Here at the start t both wire and chain cross the Fermi level and host a MF, then both are topological. Increasing t there is a energy splitting $\delta E \sim t$ without the superconductivity, and the system becomes like a gapped semi-conductor, without any MF. The parameters we used are: $\Delta = 1$, $k_H a/\pi = 0.1$, $k_F a/\pi = 5.6$,$t_w = 0.5$, $\epsilon_g = 2$, $a/\xi = 0.05$ and $J'S = 2.3$, $JS = 1.1$

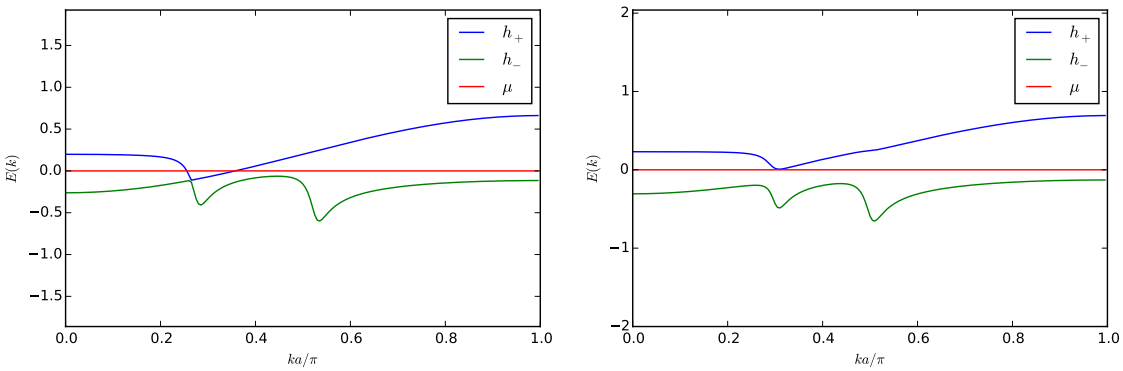

Figure 5.9: The energy $h_{\pm}(k)$ in function of k. Neglecting the superconducting part we can see that the condition to be topologically non-trivial is the crossing of the Fermi level (right). In the right figure both bands cross the Fermi level and there are 2 MF. Increasing t only the upper band will cross the Fermi level two times, hosting 2 MF. The system becomes trivial when there is not any crossing. The parameters we used are: the same of precedent figure (Figure :(5.8)) with $t = 0$ (right) and $t = 0.2$ (left).

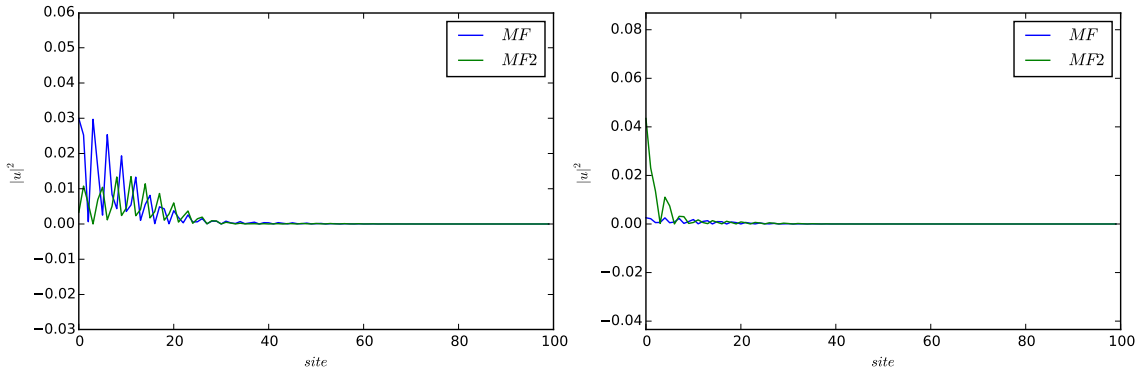

Figure 5.10: The electron wave function $|u|^2$ of the MF on the wire (right) and on the chain (left), as a function of the site index. One MF is mostly localized on the wire. The other MF is shared between the two systems. The parameters we used are: the same of precedent Figure :(5.8) with $t = 0.1$ and $N = 200$).

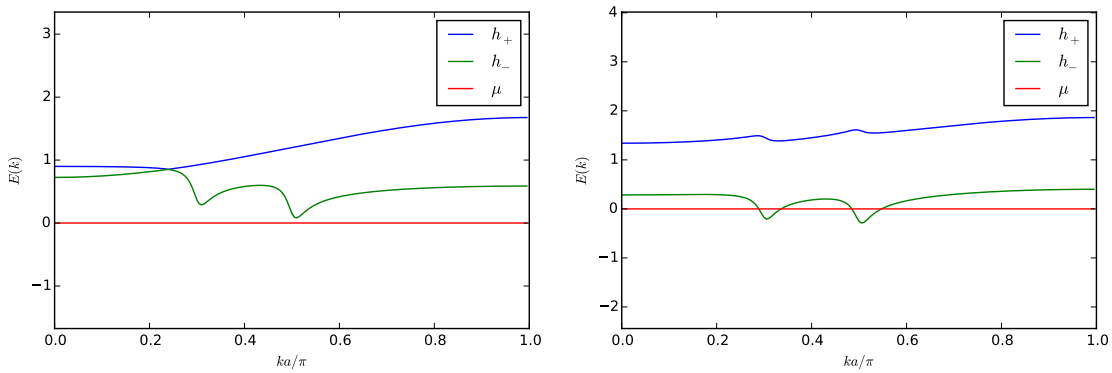

Figure 5.11: The energy $h_{\pm}(k)$ in function of the quasi-momentum k. For small values of t there is not any crossing of the Femi level and $w = 0$. As t increases, the lower band moves down until there are 2 crossing with the Fermi level, which means an even winding number w. An explicit numerical calculation shows that we have $w = 2$, with 2 MF. The parameters we used are: $\Delta = 1$, $k_H a/\pi = 0.1$, $k_F a/\pi = 5.6$,$t_w = 0.5$, $\epsilon_g = 2$, $a/\xi = 0.05$ and $J'S = 1.3$, $JS = 0.4$ with $t = 0$ (right) and $t = 0.5$ (left).

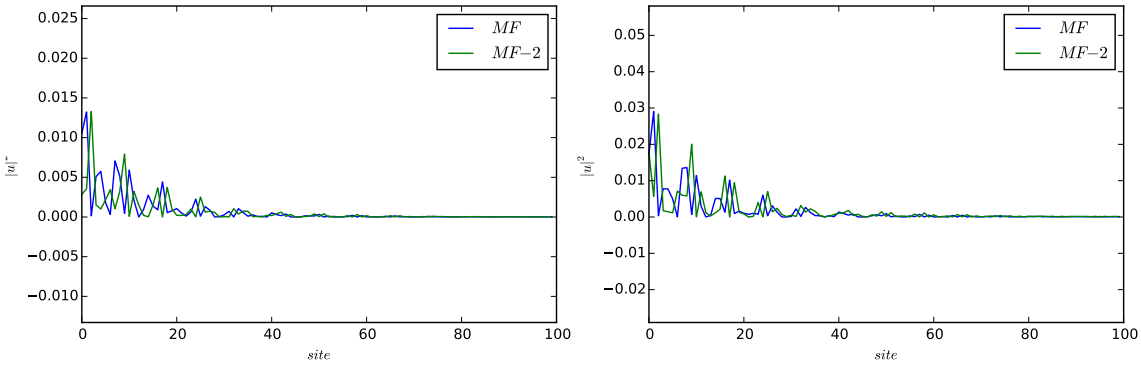

Figure 5.12: The electron wave function $|u|^2$ of the MF on the wire (right) and on the chain (left), as a function of the site index. The two MF are mostly localized on the chain. The parameters we used are the same of precedent figure (Figure :(5.2)) with $t = 0.5$ and $N = 200$).

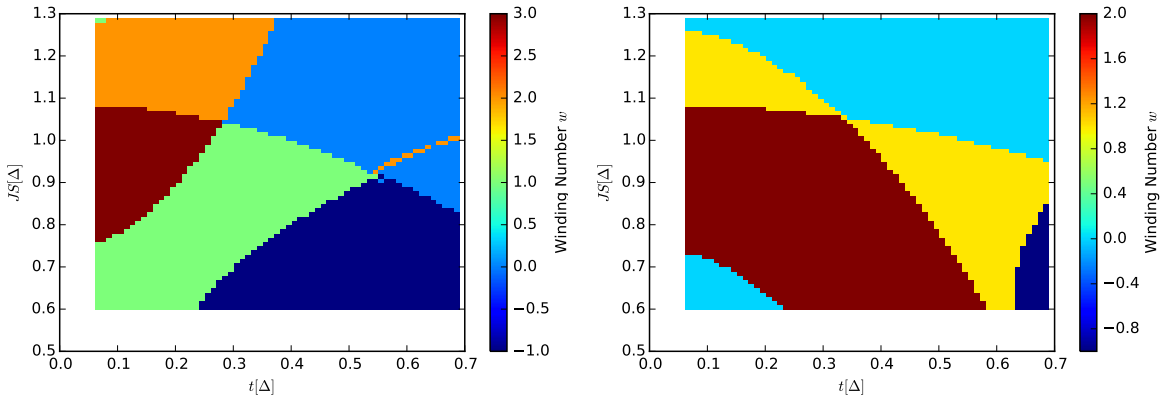

Figure 5.13: Phase diagram. The winding number w as a function of JS and t. In this situation the decoupled wire is topological (left) or trivial (right). The parameters we used are $\Delta = 1$, $k_H a/\pi = 1/8$, $k_F a/\pi = 5.8$,$t_w = 0.5$, $\epsilon_g = 2$, $a/\xi = 0.05$ and $J'S = 2.3$ (on the left), $J'S = 1.7$ (on the right).

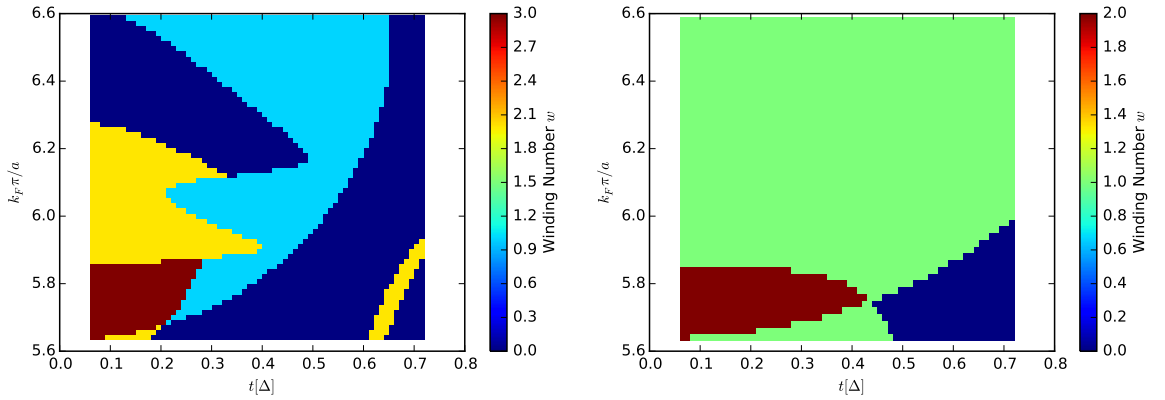

Figure 5.14: Phase diagram. The winding number w as a function of k_F and t. In this situation the decoupled wire is topological (left) or trivial (right). The parameters we used are: $\Delta = JS = 1$, $k_H a/\pi = 1/8$,$t_w = 0.5$, $\epsilon_g = 2$, $a/\xi = 0.05$ and $J'S = 2.3$ (on the left), $J'S = 1.7$ (on the right).

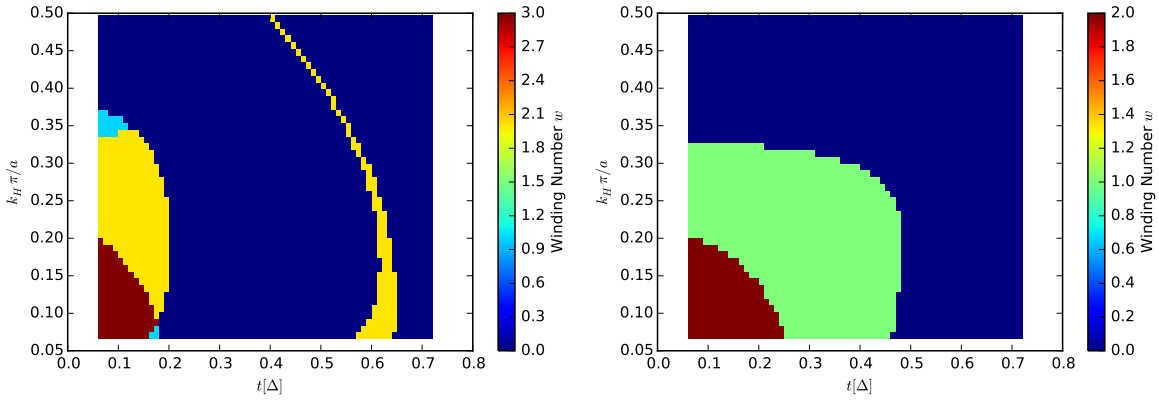

Figure 5.15: Phase diagram. The winding number w as a function of k_H and t. Let's recall that we arbitrary set $w = 0$ when the gap is (nearly) closed. The parameters we used are: $\Delta = \Delta' = JS = \alpha = 1$, $k_F a/\pi = 6.45$, $t = 0.5$, $\epsilon_g = 2$, $a/\xi = 0.05$ and $J'S = 2.3$ (on the left), $J'S = 1.7$ (on the right).

5.3 Conclusions to the chapter

This chapter, together with chapter 3, represents the main new result of this thesis. We numerically explored the phase diagram of the Hamiltonian (3.36). Because this is an original model all the results are unprecedented.

The phase diagram shows that the system can host multiple MFs. We find $w = 0, 1, 2, 3$ as allowed number for the winding number.

We numerically computed the phase diagram of the system, assuming a perfect planar helical spin texture. The more generic case when the spin order is not perfectly helical or perfectly planar can be inferred by our result as a transition $\mathbb{Z} \longrightarrow \mathbb{Z}_2$: each pairs of Majorana couple to each other and form normal quais-particles.

Therefore, we can conclude that, in a realistic disordered system, we have either zero or one pair of MFs.

Chapter 6

Spinful case of Shiba chain with orbital degrees of freedom

In this chapter, we discuss the case (less realistic) of the small magnetization $J'S \ll t_w$. In this case we cannot consider the orbital conduction band as a spinless band. We explore the phase diagram of the system, showing that small coupling t does not change the topological property of the Shiba chain.
Now we want to discuss what happens if we don't take the large magnetization limit $J'S \gg t_w$ for the orbital electron. This limit is realistic because in experiment we have J' larger than the other parameter [1] but we want to explore the opposite case. In this chapter, we take $J' = 0$.
We are studying the Shiba chain, coupled with a spinful conducting band.This system is described by the Hamiltonian with the spinful tunneling Eq.(3.38) and the full orbital Hamiltonian Eq.(3.23). In this case, the orbital band is a spinful band. Then, the usual proximity effect provides an induced s-wave superconductivity with the strength $\Delta^{\text{Prox}} \sim \nu_0 \pi t^2$. In the limit of small coupling the orbital electron can virtually visit the continuum with strength Δ^{Prox}, but also the Shiba chain. This effect provides a spinless p-wave superconductivity $\Delta^{\text{P-wave}} \sim t^2\Delta/(JSk_F a\delta\epsilon)$. Where $\delta\epsilon = \epsilon_w - \epsilon_\alpha$ is the energy difference between the Shiba states and the orbital state, due to perturbation theory formula. We are thinking about a self

[1] The exact scale of J, J' is debate. In the Yazdany article [17] they assume $J \sim 1eV$. In [20] the magnetic exchange J is estimate in the order of meV, with a difference of two order of magnitude.

energy of the form:

$$\begin{aligned}\Sigma_W = \sum_k \Big(& \Delta^{\text{Prox}}(k) a^\dagger_\uparrow(k) a^\dagger_\downarrow(-k) \\ & + \Delta^{\text{P-wave}}(k)(a^\dagger_\downarrow(k) a^\dagger_\downarrow(-k) + a^\dagger_\uparrow(k) a^\dagger_\uparrow(-k)) + h.c \Big).\end{aligned} \tag{6.1}$$

Due the scale of $J \sim 1eV$, in a realistic case we can take $\Delta^{\text{Prox}} \gg \Delta^{\text{P-wave}}$. The ordinary s-wave gap then is larger than the induced p-wave. In this case we can expect that the conducting bands of orbital electron does not have any topological features. The s-wave gap protects the system against any gap inversion.

For this reason, (in the weak coupling) we are expecting that coupling a Shiba chain with a spinful system does not add any MFs. In the next section, we try to confirm this expectation with a numerical calculation.

Numerical analysis

In this section, we use numerical calculation to confirm our expectation. Showing the LDOS and the Majorana polarization we try to support the previous argument. Diagonalizing the BdG Hamiltonian we find the eigenvectors:

$$\Psi_n = \begin{pmatrix} u_\uparrow(n) \\ v_\uparrow(n) \\ u_\downarrow(n) \\ v_\downarrow(n) \\ u_{\text{Shiba}}(n) \\ v_{\text{Shiba}}(n) \end{pmatrix}, \tag{6.2}$$

where $u(v)$ is the particle (hole) wavefunction, we report the spin index $\uparrow\downarrow$ for the orbitals electrons. We use the LDOS, projected on the orbital part and on the Shiba:

$$\begin{aligned}\rho_{\text{Orbital}}(n, E) &= \sum_{j,\alpha} |u_\alpha(n, j)|^2 \delta(E - E^{(j)}), \\ \rho_{\text{Shiba}}(n, E) &= \sum_j |u_{\text{Shiba}}(n, j)|^2 \delta(E - E^{(j)}),\end{aligned} \tag{6.3}$$

where j is the energy index and α is the spin index. We also remember that Majorana polarization Eq.(4.15) is a numerical tool that gives $C(E) \simeq 1$ when a quasiparticle is a Majorana excitation. Now we put ourselves in the condition when both system cross the Fermi level. In the spinless case this condition is sufficient to have multiple MFs, but here we do not add any topological features for the Shiba system.

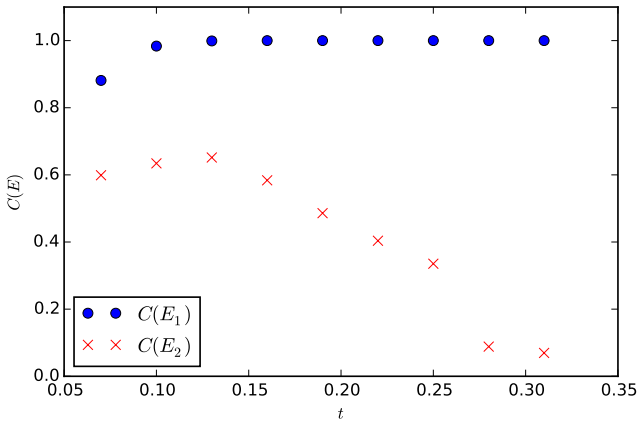

Figure 6.1: The Majorana polarization of the first 2 excited states, as a function of t. We can see that a small coupling does not change the topology of the Shiba chain. With this parameters we have one MF in the decoupled case, and one in the coupled. In this case, we can say that the conducting band does not change the Shiba Physics. The parameters used are $\Delta = 1$, $k_H a/\pi = 0.3$, $k_F a/\pi = 5.6$, $t_w = 0.5$, $\epsilon_g = 2$, $a/\xi = 0.05$, $\alpha = 1.1$ and $t = 0.2$. We used a number of site $N = 200$.

With numerics we have seen that in the spinful case the orbital part cannot host MFs, due the spin degeneracy and the s-wave gap. The Shiba part however can host MFs as in decoupled case. We also showed that the coupling t can induces a phase transition and destroy MFs in the Shiba chain.

6.1 Conclusions to the chapter

In this chapter, we discuss the case of the small magnetization $J'S \ll t_w$. In this case we cannot consider the orbital conduction band as a spinless band. We explore the phase diagram of the system, showing that small coupling t does not change the topological properties of the Shiba chain.
The orbital conducting band is spinful. Therefore, it is affected by the procimity of the s-wave superconductor. This s-wave gap protects the system to have any

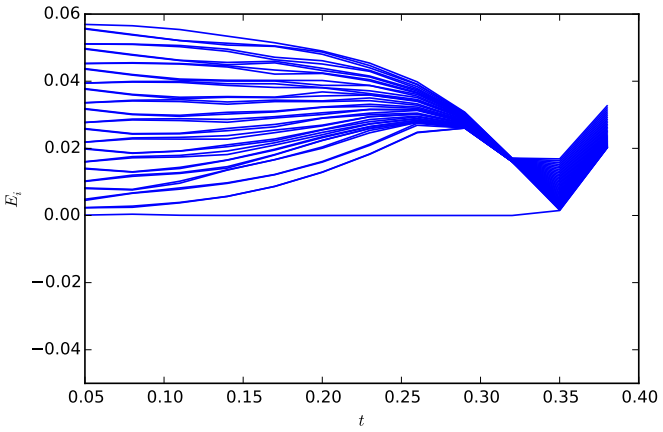

Figure 6.2: The energy E_i as a function of t of the first 40 excited states. At $t \sim 0.35$ the gap is close and we have a phase transition. The parameters we used are: $\Delta = 1$, $k_H a/\pi = 0.3$, $k_F a/\pi = 5.6$,$t_w = 0.5$, $\epsilon_g = -0.5$, $a/\xi = 0.05$ and $\alpha = 1.1$. We used a number of site $N = 300$.

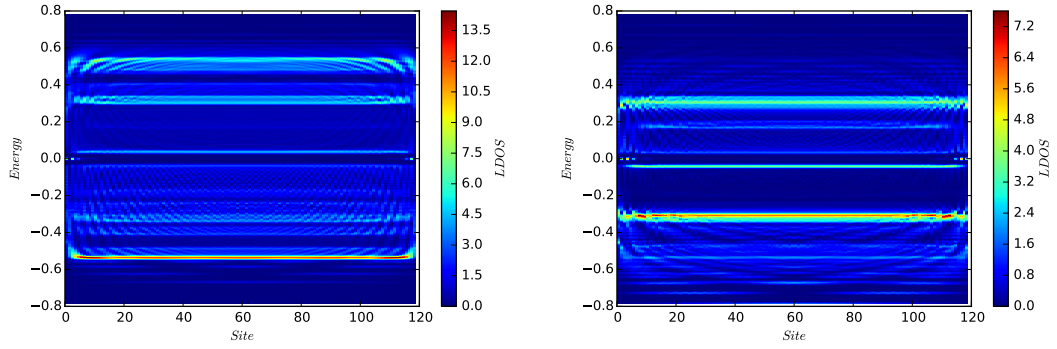

Figure 6.3: $\rho_{\text{Orbital}}(n, E)$ as a function of the site n and the energy E on the left and $\rho_{\text{Shiba}}(n, E)$ on the right. The parameters we used are: $\Delta = 1$, $k_H a/\pi = 0.3$, $k_F a/\pi = 5.6$,$t_w = 0.5$, $\epsilon_g = 2$, $a/\xi = 0.05$ and , $JS = 1.1$ and $t = 0.25$. We used a number of site $N = 200$

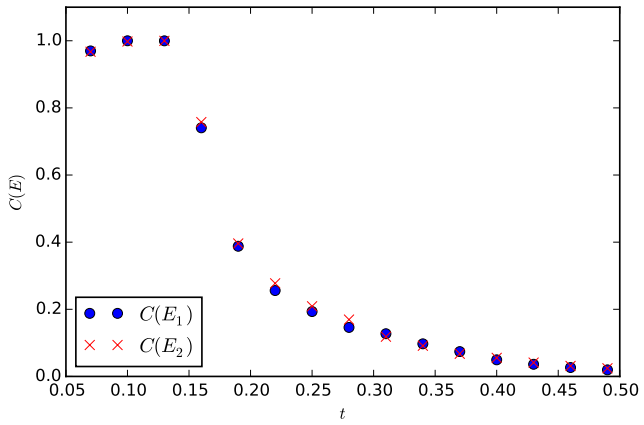

Figure 6.4: The Majorana polarization (MP) of the first two excited states, as a function of t. We can see that the increasing of the coupling destroys the two MFs: a $t \sim 1.16$, the gap is close and we have a phase transition between $w = 2$ and $w = 0$. This case is representative and we do not find any case where the coupling increase the number of MFs. The parameters we used are: $\Delta = 1$, $k_H a/\pi = 0.3$, $k_F a/\pi = 5.6$, $t_w = 0.5$, $\epsilon_g = 2$, $a/\xi = 0.05$ and $JS = 0.9$. We used a number of site $N = 200$.

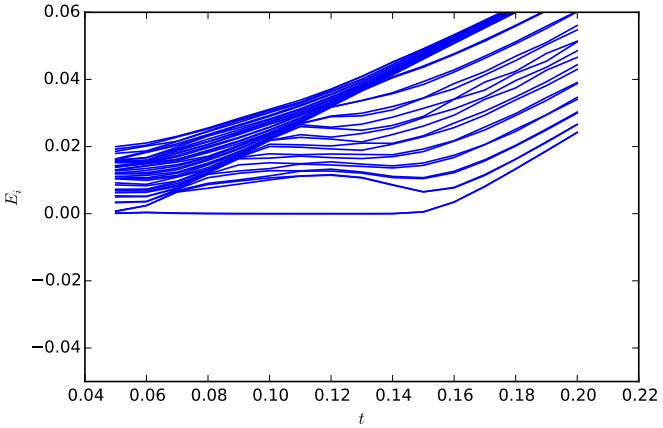

Figure 6.5: The energy E_i of the first 40 excited states, as a function of t. At $t \sim 0.16$ there is a gap closing, however is not clearly visible in the figure due the level spacing. The parameters we used are: $\Delta = 1$, $k_H a/\pi = 0.3$, $k_F a/\pi = 5.6$,$t_w = 0.5$, $\epsilon_g = -0.5$, $a/\xi = 0.05$ and $\alpha = 0.9$. We used a number of site $N = 300$

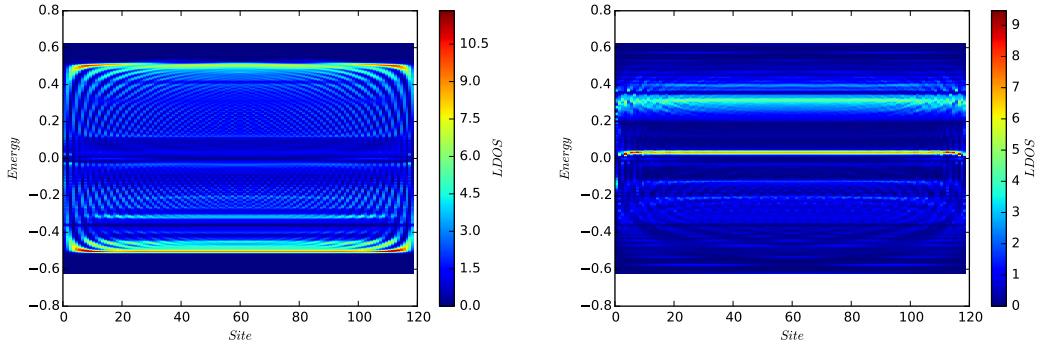

Figure 6.6: $\rho_{\text{Orbital}}(n, E)$ as a function of the site n and the energy E on the left and $\rho_{\text{Shiba}}(n, E)$ on the right. The parameters we used are: $\Delta = 1$, $k_H a/\pi = 0.3$, $k_F a/\pi = 5.6$, $t_w = 0.5$, $\epsilon_g = -0.5$, $a/\xi = 0.05$ and $\alpha = 0.9$ and $t = 0.1$. We used a number of site $N = 200$

gap inversion and the conduction band on top of the superconductor remains trivial.

Chapter 7

Conclusions

In conclusion we consider an array of helical magnetic Impurities, taking also in account the orbital degree of freedom. Due the overlap t_w between these orbitals, electrons belonging to these orbitals form a proximitized conduction band which can be topologically non-trivial. In parallel to that, the magnetic impurities try to break Cooper pairs in the bulk superconductor which creates a one-dimensional band of bound states called a Shiba band. Our system description is new in the sense that a dilute chain of magnetic adatoms is usually described by the Shiba chain model [26], or by the wire model [20] in the dense case. In this thesis, we described an intermediate case where the hopping of the impurity orbital degrees of freedom can strongly affect the phase diagram of the system. In this thesis, we successfully derived an effective Hamiltonian that captures this intermediate situation (see Eq:2.54) . Our system is new in the literature: usually a *chain of magnetic adatom* is described by the *Shiba chain* model, in the dilute case, or by the wire model, in the dense case. In this thesis, we described an intermediate case where the hopping of the orbital degree of freedom can affect heavily the phase diagram of the system. We successfully derived a model that can describe an intermediate situation.
Thanks to this low-energy model, we answered to some of the questions we raised in the introduction, namlely:

- In which parameter space can such system be topological and thus support Majorana fermions?
  In the chapter 5, we numerically computed the phase diagram of the system, showing that the system can be topological.

- Can this system support pairs of Majorana fermions at its edge?

The system can host multiple Majorana if the effective time-reversal $\mathcal{T}$ is present. Breaking this symmetry would couple two MFs in a single normal electron. Because the non-planar helical texture breaks this symmetry it seems that multiple Majorana are not very robust in a realistic system, while a perfect planar order may be difficult to achieve. We also note that today there is not any clear experimental way to distinguish two localized MFs in the same site to only one. In a realistic system, where the disorder is present there is not any reason to suppose a perfect planar helical texture. In this situation, our main conclusion is that the two MFs which are predicted in both subsystems will hybridize and therefore destroy each other. Therefore, we are expecting that MFs are not present at all in this intermediate regime.

- What is the role of the tunneling coupling t? For $t = 0$ the gap is closed and we cannot speak about topology. For $t \ll \Delta$ we can have MFs if the energy bands cross the Fermi level. For $t \sim \Delta$ the two bands of the system can be lifted out the gap and the systems is topologically trivial, without any MFs. For this reason our work is focused on the weak coupling case.

- What is the role of magnetic coupling J'?
  For strong magnetic coupling (see chapter 6) we are dealing with a spinless conduction band. Than we have two coupled potentially topological systems and we can have multiple MFs. In the case of weak magnetization $J'S \ll t_w$ the Zeeman splitting is negligible and we are dealing with a spin degenerate system. The s-wave superconducting gap prevents any gap inversion and than the orbital system remains topologically trivial.

We described the phases of the system with a low-energy model. Finally we discuss how the relaxation of the some key hypothesis affects the topology of the system.

Appendices

Appendix A

Proximity effect

If a 1D system is in good electrical contact with a superconductor, Cooper pairs can tunnel from superconductor to normal system inducing a superconductivity on that. The superconductivity parameter of normal system Δ' is largely controlled by the parent bulk superconductor.We follow [25] for a simple treatment of proximity effect.

Using the BdG formalism, we start considering a 1D generic system:

$$H_{\mathrm{1D}} = \int dx \Phi^{\dagger}(x) \mathcal{H}(x) \Phi(x), \tag{A.1}$$

where $\Phi(x)$ is the Nabu's spinor of the electrons of the system. And a 3D bulk superconductors:

$$H_{\mathrm{SC}} = V \int \frac{d\mathbf{k}}{(2\pi)^3} \Big(\psi^{\dagger}_{\sigma}(\mathbf{k}) \epsilon(k) \psi_{\sigma}(\mathbf{k}) + \Delta(\psi^{\dagger}_{\uparrow}(\mathbf{k}) \psi_{\downarrow}(-\mathbf{k}) + h.c.) \Big), \tag{A.2}$$

where $psi^{\dagger}_{\sigma}$ creates an electron with spin σ. We add then a Tunneling coupling, which describe a possibility for one electron to tunneling from one system to the other.

$$H_t = t \int d\mathbf{r} \Phi^{\dagger}(x) \delta(y) \Psi(\mathbf{r}) + h.c. \tag{A.3}$$

We deduce crudely the hybridization effect of H_t using perturbative arguments an dimensional analysis. In the experimental relevant setup $\mu_{\mathrm{SC}} \gg \mu_{\mathrm{1D}}$, in this case the hybridization is controlled by t and proprieties of superconductors.

When $k_F^{\mathrm{SC}} t \ll \Delta$ we can treat H_t pertubatively because the tunnelling is suppressed by the large superconducting gap Δ. At the second order of perturbation theory we describe a possibility for a cooper pair (two electrons) to tunnel between the

two systems. This term, using dimensional analysis takes the form:

$$H_{\Delta'} \sim \frac{t^2}{\Delta k_F^{\mathrm{SC}}} \int dx \phi_\uparrow(x)\phi_\downarrow(x)\psi_\downarrow^\dagger(x)\psi_\uparrow^\dagger(x) + h.c. \tag{A.4}$$

For low-energies we can replace $\psi_\downarrow^\dagger(x)\psi_\uparrow^\dagger(x) \to \langle\psi_\downarrow^\dagger(x)\psi_\uparrow^\dagger(x)\rangle \sim \Delta\rho_{\mathrm{SC}}$ where ρ_{SC} is the density of states at Fermi energy. We have derived a low-energy effective Hamiltonian:

$$\begin{aligned} H_{\mathrm{eff}} &= H_{\mathrm{1D}} + H_{\Delta'}, \\ H_{\Delta'} &\sim \Delta' \int dx(\phi_\uparrow(x)\phi_\downarrow(x) + h.c.), \end{aligned} \tag{A.5}$$

where $\Delta' \sim \frac{t^2}{\Delta k_F^{\mathrm{SC}}}\Delta\rho_{\mathrm{SC}} = t^2\rho_{\mathrm{SC}}/k_F^{\mathrm{SC}}$. The proximity effect is one of the main ingredient for engineering effective p-wave superconductivity. See also [27, 28] for experimental discussion.

In all the thesis the proximity effect will represent the best way (for an experimental purpose) to induce superconductivity in a system.

Appendix B

Anderson model of magnetic impurity

Starting form the Anderson model we derive the so-called Kondo model, that describes a classical magnetic impurity, with fixed spin. The Anderson model describes a magnetic impurity embedded in a normal metal. The impurity here is simply taken as a two level Hamiltonian, with Coulomb repulsion U on site:

$$H_{\text{Impurity}} = \epsilon_d(n_{d,\uparrow} + n_{d,\downarrow}) + U n_{d,\uparrow} n_{d,\downarrow}. \tag{B.1}$$

Now we consider another state in the system: one itinerant orbital $c_k^\dagger$ coupled with the two level system via an hopping parameter t:

$$H = H_{\text{Impurity}} + \epsilon_k(c_{k,\uparrow}^\dagger c_{k,\uparrow} + c_{k,\downarrow}^\dagger c_{k,\downarrow}) + \sum_\sigma t(c_{d,\sigma}^\dagger c_{k,\sigma} + h.c). \tag{B.2}$$

We can consider the case where the correlation are very important taking the simple limit $U = \infty$, which prevent the double occupation of the orbital c_d. It can be shown (see [43])that we can derive the Kondo Hamiltonian as effective interacting Hamiltonian:

$$H_{\text{Kondo}} = -2J\mathbf{s}_1\mathbf{s}_2, \tag{B.3}$$

where J is related with the microscopic parameters as $J = -t^2/(\epsilon_k - \epsilon_d)$. For the following we are interested only on the scaling $J \sim t^2$. There is a general relation between the Anderson model and the Kondo Hamiltonian (appendix:**??**,see below), obtained by Shrieffer-Wolf transformations which keeps the scaling $J \sim t^2$.
In the main text we will treat the magnetic impurities only with the Kondo model,

treating the impurity spin as a classical fixed variable, supposing that the core provide a large spin $S \gg 1$.

$$H_{\text{Kondo}} = -J\mathbf{S}\boldsymbol{\sigma}\delta(\mathbf{r}). \tag{B.4}$$

Appendix C

Schrieffer-Wolff transformation

In this chapter, we consider the well known calculation of Schrieffer-Wolff transformation because they are used some times in the main text. We follow [43] where there is a more detailed discussion. Considering a generic Hamiltonian H, one can always perform a unitary transformation which preserves the same spectrum.

$$\tilde{H} = e^{-S} H e^{S} = H + [H, S] + \frac{1}{2!}[[H, S]S] + ... \tag{C.1}$$

We separate H in two terms, with smallλ:

$$H = H_0 + \lambda H_1. \tag{C.2}$$

Keeping up to the second order in λ we have:

$$\tilde{H} = H_0 + \lambda H_1 + [H_0, S] + \frac{1}{2!}[[H, S]S] + ... \tag{C.3}$$

Now we use the arbitrariness of S to eliminate the first order in λ:

$$\lambda H_1 + [H_0, S] = 0. \tag{C.4}$$

Our Hamiltonian at second order (put $\lambda = 1$) reads :

$$\tilde{H} = H_0 + \frac{1}{2}[H_1, S] + O(\lambda^3). \tag{C.5}$$

We can rewrite Eq:(C.5)as:

$$\begin{aligned} \tilde{H} &= H_0 + H_{\text{indirect}}, \\ H_{\text{indirect}} &= \frac{1}{2}[H_1, S]. \end{aligned} \tag{C.6}$$

From Eq:(C.4) in the diagonal basis for H_0 we find:

$$\langle n|S|m\rangle = \frac{\langle n|H_1|m\rangle}{E_m - E_n}. \tag{C.7}$$

Now we can express H_{indirect} in the basis of H_0:

$$\langle f|H_{\text{indirect}}|i\rangle = \frac{1}{2}\sum_{\alpha} \langle f|H_1|\alpha\rangle \langle \alpha|H_1|i\rangle \left(\frac{1}{E_i - E_\alpha} + \frac{1}{E_f - E_\alpha}\right). \tag{C.8}$$

We can note that this is the usual second order correction given by perturbation theory. It is also possible to derive this formula by Eq:(3.15). This formula can be used to connect Anderson and Kondo Hamiltonians: starting from an interacting Hamiltonian of a metal c_k and a single impurities d:

$$H = \sum_{k,\sigma}[\epsilon_k c^\dagger_{k,\sigma} c_{k,\sigma} + (V_k d^\dagger_\sigma c_{k,\sigma} + h.c).] + \sum_{\sigma}[\epsilon_\sigma n_{d,\sigma} + U n_{d,\uparrow} n_{d,\downarrow}]. \tag{C.9}$$

Using the formula C.8 after some calculation we have:

$$H = \sum_{k,\sigma} \epsilon_k c^\dagger_{k,\sigma} c_{k,\sigma} + \sum_{k,k'}[2J_{k,k'}\boldsymbol{\sigma}_{k,k'}\mathbf{S}_d + K_{k,k'}\sum_{\sigma} c^\dagger_{k,\sigma} c_{k,\sigma}], \tag{C.10}$$

with:

$$\begin{aligned} J_{k,k'} &= V^*_{k'} V_k [\frac{1}{U + \epsilon_d - \epsilon_{k'}} + \frac{1}{\epsilon_k - \epsilon_d}] \\ K_{k,k'} &= \frac{V^*_{k'} V_k}{2} [\frac{1}{\epsilon_k - \epsilon_d} - \frac{1}{U + \epsilon_d - \epsilon_{k'}}]. \end{aligned} \tag{C.11}$$

If both $U + \epsilon_d$and ϵ_d greatly excess of the typical excitation energy scales, one may safely neglect the particular energy dependence of the parameters $J_{k,k'}$ and$K_{k,k'}$. In this case, the exchange interaction $J_{k,k'}$ can be treated as local, the scattering term $K_{k,k'}$ can be absorbed into a shift of the single-particle energy of the itinerant band.

Appendix D

Detailed derivation of Shiba chain model

This chapter is the detailed derivation of Shiba chain and it can be read independently of the main text.

D.0.1 Shiba state

We start analysing only one magnetic impurities on a 2D superconductors. We will derive the allowed energies ϵ_α for a state bound to the impurity, the so-called Shiba state [24], this will be useful to derive a new energy scale α which tell us how deep is bound state [1] respect to gap Δ.
Our system is described by the follow BdG Hamiltonian:

$$\begin{aligned} \mathcal{H} &= \Big(\xi_p \tau_z - J\mathbf{S}\boldsymbol{\sigma}\delta(\mathbf{r}) + \Delta\tau_x\Big), \\ \Psi(\mathbf{r})^\dagger &= \Big(\psi_\uparrow^\dagger(\mathbf{r}), \psi_\downarrow^\dagger(\mathbf{r}), \psi_\downarrow(\mathbf{r}), -\psi_\uparrow(\mathbf{r})\Big)\,. \end{aligned} \tag{D.1}$$

We can choose the classical impurity spin along z-axis $\mathbf{S} = S\hat{\mathbf{z}}$. In this case the Hamiltonian (4×4) (D.1) is separable in 2 decoupled Hamiltonians (2×2).

$$\mathcal{H}_\pm = \Big(\xi_p \tau_z \mp JS\delta(r) + \Delta\tau_x\Big). \tag{D.2}$$

[1] When we speak about bound states, in this context we mean $|E| < |\Delta|$, with this constrain the wave function of this state is localized on the impurities and has a $e^{-r/\xi(E)}/\sqrt{k_F r}$ tail. In this thesis, we only consider the case $r \ll \xi$ and with $e^{-r/\xi(E)} \approx 1$ we cannot see explicitly the difference between a bound states and a continuum state.

We solve for Nambu wave function:

$$\Big(E - \xi_{\mathbf{p}}\tau_z - \Delta\tau_x\Big)\Psi(\mathbf{r}) = \mp JS\delta(\mathbf{r})\Psi(0). \tag{D.3}$$

Taken the Fourier transform we obtain:

$$\Big(E - \xi_{\mathbf{p}}\tau_z - \Delta\tau_x\Big)\hat{\Psi}(\mathbf{p}) = \mp JS\Psi(0), \tag{D.4}$$

where $\hat{\Psi}(\mathbf{p}) = \int d\mathbf{r}e^{-i\mathbf{pr}}\Psi(\mathbf{r})$, now we can rewrite as:

$$\hat{\Psi}(\mathbf{p}) = \mp\frac{JS}{E^2 - \xi_{\mathbf{p}}^2 - \Delta^2}\Big(E + \xi_{\mathbf{p}}\tau_z + \Delta\tau_x\Big)\Psi(0), \tag{D.5}$$

and taking Fourier antitrasfom:

$$\Psi(0) = \mp\int\frac{Vd\mathbf{p}}{(2\pi)^2}\frac{JS}{E^2 - \xi_{\mathbf{p}}^2 - \Delta^2}\Big(E + \xi_{\mathbf{p}}\tau_z + \Delta\tau_x\Big)\Psi(0). \tag{D.6}$$

After the evaluation of integral (see appendix Eq. G.1) we have an equation to determine the allowed energies:

$$\Big(1 \mp \alpha\frac{E + \Delta\tau_x}{\sqrt{\Delta^2 - E^2}}\Big)\Psi(0) = 0, \tag{D.7}$$

where $\alpha = \pi\nu_0 JS$. The allowed energies with constrain $|E| < |\Delta|$and correspondent eigenvectors are:

$$\begin{aligned}
\epsilon_{\pm} &= \pm\Delta\frac{1-\alpha^2}{1+\alpha^2}, \\
\tau_x\Psi_+ &= \Psi_+ \qquad \sigma_x\Psi_+ = \Psi_+, \\
\tau_x\Psi_- &= -\Psi_- \quad \sigma_x\Psi_- = -\Psi_-.
\end{aligned} \tag{D.8}$$

We write explicitly the eigenvectors:

$$\Psi_+(0) = \frac{1}{\sqrt{2\mathcal{N}}}\begin{pmatrix}1\\0\\1\\0\end{pmatrix}, \Psi_-(0) = \frac{1}{\sqrt{2\mathcal{N}}}\begin{pmatrix}0\\1\\0\\-1\end{pmatrix}. \tag{D.9}$$

The normalization factors $\mathcal{N}$ is determined by normalization $\int d\mathbf{x}|\Psi|^2 = 1$. We also note that particle-hole symmetry $\mathfrak{C} = \tau_y\sigma_y K$ [2]relates the two eigenvectors: $\mathfrak{C}\Psi_+ = \Psi_-$.
For the later is useful express the eigenvectors of generic orientation of spin $\mathbf{S} = S\hat{\mathbf{S}}$:

$$\Psi_+(0) = \frac{1}{\sqrt{2\mathcal{N}}}\begin{pmatrix}|\uparrow\rangle_{\hat{\mathbf{S}}}\\ |\uparrow\rangle_{\hat{\mathbf{S}}}\end{pmatrix}\Psi_-(0) = \frac{1}{\sqrt{2\mathcal{N}}}\begin{pmatrix}|\downarrow\rangle_{\hat{\mathbf{S}}}\\ -|\downarrow\rangle_{\hat{\mathbf{S}}}\end{pmatrix}. \tag{D.10}$$

For a generic direction:

$$\begin{aligned}&\hat{\mathbf{S}} = \Big(\sin(\theta)\cos(\phi),\quad \sin(\theta)\sin(\phi),\quad \cos(\theta)\Big),\\ &|\uparrow\rangle_{\hat{\mathbf{S}}} = \begin{pmatrix}\cos(\theta/2)\\ e^{i\phi}\sin(\theta/2)\end{pmatrix}, \qquad |\downarrow\rangle_{\hat{\mathbf{S}}} = \begin{pmatrix}e^{-i\phi}\sin(\theta/2)\\ -\cos(\theta/2)\end{pmatrix}.\end{aligned} \tag{D.11}$$

D.0.2 Shiba state's wavefunction

We just obtained the allowed energies for a bound state in a Shiba system, and the form of the Spinorial solution at the position of the impurity $\mathbf{r} = 0$. Now we want to derive the solution in a generic position $\mathbf{r}$, we can do that simply evaluating the free Propagator.
Our system is described by the follow BdG Hamiltonian:

$$\mathcal{H} = \Big(\xi_p\tau_z - J\mathbf{S}\boldsymbol{\sigma}\delta(\mathbf{r}) + \Delta\tau_x\Big) = \mathcal{H}_0 - J\mathbf{S}\boldsymbol{\sigma}\delta(\mathbf{r}). \tag{D.12}$$

Inverting the Shrodinger equation we can show that the Spinors solution only depends on the free Propagator $\mathcal{G}^0_E(\mathbf{r}) = (E - \mathcal{H}_0)^{-1}$:

$$\Psi(\mathbf{r}) = -\mathcal{G}^0_E(\mathbf{r})J\mathbf{S}\boldsymbol{\sigma}\Psi(0), \tag{D.13}$$

where the Propagator is given by:

$$\mathcal{G}^0_E(\mathbf{r}) = \int \frac{Vd\mathbf{p}}{(2\pi)^2}\left(\frac{E + \xi_{\mathbf{p}}\tau_z + \Delta\tau_x}{E^2 - \xi^2_{\mathbf{p}} - \Delta^2}\right)e^{-i\mathbf{pr}}. \tag{D.14}$$

With this we can value the asymptotic wave function $k_F r \gg 1$, knowing the asymptotic expansion of the Resolvent $\mathcal{G}_E(\mathbf{r})$ (D.27). For positive energy ϵ_+ we

[2]This representation of $\mathfrak{C}$ is little bit different than 2.25 because we are dealing explicitly with spin.

have:

$$\Psi^+(\mathbf{r}) = -JS\mathcal{G}^0_{\epsilon_+}(\mathbf{r})\sigma_z\Psi^+(\mathbf{0}),$$
$$\Psi^+(\mathbf{r})_{k_Fr\gg 1} = -\alpha\sqrt{\frac{2}{\pi k_Fr}}\left(\frac{-\cos(k_Fr-\frac{\pi}{4})}{\sqrt{\Delta^2-{\epsilon_+}^2}}(\epsilon_+ + \Delta\tau_x) + \sin(k_Fr-\frac{\pi}{4})\tau_z\right)\Psi^+(\mathbf{0}). \tag{D.15}$$

At the first order in the deep limit $\alpha \approx 1$ the wave function reads:

$$\Psi^+(\mathbf{r})_{k_Fr\gg 1} = \sqrt{\frac{2}{\pi\mathcal{N}k_Fr}}\begin{pmatrix}\cos(k_Fr)\\0\\\sin(k_Fr)\\0\end{pmatrix}, \tag{D.16}$$

end $\Psi^-(\mathbf{r})_{k_Fr\gg 1}$ is the relative PHS conjugate. We want to emphasise the long range decay $\frac{1}{\sqrt{k_Fr}}$ and the different phase shift $\delta_\pm$ for electron $(+)$ and hole $(-)$ component. More detailed calculation without deep limit [32] shows:

$$\tan(\delta_\pm) = \pm\alpha. \tag{D.17}$$

Now we try to determine the normalization factor $\mathcal{N}$, using:

$$\int d\mathbf{r}|\Psi(\mathbf{r})|^2 = \int \frac{Vd\mathbf{k}}{(2\pi)^2}|\Psi(\mathbf{k})|^2 = 1. \tag{D.18}$$

Then we have, using D.5:

$$\int \frac{Vd\mathbf{k}}{(2\pi)^2}|\Psi^+(\mathbf{k})|^2 = \nu_0(JS)^2\int d\xi\Psi^\dagger_+(\mathbf{0})\left(\frac{\epsilon_+ + \xi\tau_z + \Delta\tau_x}{\epsilon_+^2-\Delta^2-\xi^2}\right)^2\Psi_+(\mathbf{0}). \tag{D.19}$$

After the calculation (see appendix A Eq:(G.7)) we have:

$$\mathcal{N} = \frac{JS(1+\alpha^2)^2}{4\Delta\alpha^2} \approx_{\text{deep limit}} \frac{JS}{\Delta} + O(\eta^2), \tag{D.20}$$

where $\eta = 1-\alpha = \epsilon_\alpha/\Delta$ is the small parameter of deep limit. After that in the

deep limit we obtain:

$$\begin{aligned}\Psi_+(0) &= \sqrt{\frac{\Delta}{2JS}}\begin{pmatrix}|\uparrow\rangle_{\hat{\mathbf{S}}}\\ |\uparrow\rangle_{\hat{\mathbf{S}}}\end{pmatrix}\\ \Psi_+(\mathbf{r})_{k_F r\gg 1} &= \sqrt{\frac{2\Delta}{\pi JSk_F r}}e^{-r/\xi}\begin{pmatrix}\cos(k_F r)\,|\uparrow\rangle_{\hat{\mathbf{S}}}\\ \sin(k_F r)\,|\uparrow\rangle_{\hat{\mathbf{S}}}\end{pmatrix}\end{aligned} \tag{D.21}$$

Now we know the energies ϵ_α and the wave function of the so-called Shiba bound state in presence of a single magnetic impurity.

D.0.3 Shiba chain

We just treated a single magnetic impurity in the classical limit, now we want to treat the more complex situation of a chain of impurities $\mathbf{S}_j$ at site r_j. A single impurity creates a bound state below the gap Δ, we show following [26] that a 1D chain creates an entire band below the gap, with a reference energy ϵ_α and a band with $\Delta/\sqrt{k_F a}$.
We start considering the BdG Hamiltonian:

$$\mathcal{H} = \left(\xi_p\tau_z - J\sum_n \mathbf{S}_n\boldsymbol{\sigma}\delta(\mathbf{r}-\mathbf{r}_n) + \Delta\tau_x\right). \tag{D.22}$$

First we separate the impurity terms from the rest:

$$\left(E - \xi_{\mathbf{p}}\tau_z - \Delta\tau_x\right)\Psi(\mathbf{r}) = -J\sum_n \mathbf{S}_n\boldsymbol{\sigma}\delta(\mathbf{r}-\mathbf{r}_n)\Psi(\mathbf{r}_n), \tag{D.23}$$

Now we take the Fourier Transform:

$$\hat{\Psi}(\mathbf{p}) = -J\sum_n \mathbf{S}_n\boldsymbol{\sigma}\left(\frac{E+\xi_{\mathbf{p}}\tau_z+\Delta\tau_x}{E^2-\xi_{\mathbf{p}}^2-\Delta^2}\right)e^{-i\mathbf{p}\mathbf{r}_n}\Psi(\mathbf{r}_n). \tag{D.24}$$

Note that we can commute $\left(E - \xi_{\mathbf{p}}\tau_z - \Delta\tau_x\right)^{-1}$ and $\boldsymbol{\sigma}$ because they act on different space. Now we antitrasfom and evaluate Ψ in the position of a generic impurities $\mathbf{r}_m$:

$$\Psi(\mathbf{r_m}) = -J\sum_n \mathbf{S}_n\boldsymbol{\sigma}\int\frac{Vd\mathbf{p}}{(2\pi)^2}\left(\frac{E+\xi_{\mathbf{p}}\tau_z+\Delta\tau_x}{E^2-\xi_{\mathbf{p}}^2-\Delta^2}\right)e^{-i\mathbf{p}(\mathbf{r}_n-\mathbf{r}_m)}\Psi(\mathbf{r}_n). \tag{D.25}$$

Defying the free resolvent $\mathcal{G}^0_E(\mathbf{r}) = \int \frac{Vd\mathbf{p}}{(2\pi)^2}\left(\frac{E+\xi_{\mathbf{p}}\tau_z+\Delta\tau_x}{E^2-\xi^2_{\mathbf{p}}-\Delta^2}\right)e^{-i\mathbf{pr}}$ and calculating that in appendix (Eq. G.8), we have:

$$\Psi(\mathbf{r_m}) = -JS\sum_n \mathcal{G}^0_E(\mathbf{r}_m-\mathbf{r}_n)\hat{\mathbf{S}}_n\boldsymbol{\sigma}\Psi(\mathbf{r}_n). \tag{D.26}$$

In the approximation $\xi_0 \gg r$, $J_E(\mathbf{r})$ reads:

$$\begin{aligned}
&\mathcal{G}^0_E(\mathbf{0}) = -\nu_0\pi\frac{E+\Delta\tau_x}{\sqrt{\Delta^2-E^2}},\\
&\mathcal{G}^0_E(\mathbf{r})_{k_Fr\gg1} = \nu_0\pi\sqrt{\frac{2}{\pi k_Fr}}\left(\frac{-\cos(k_Fr-\frac{\pi}{4})}{\sqrt{\Delta^2-E^2}}(E+\Delta\tau_x)+\sin(k_Fr-\frac{\pi}{4})\tau_z\right).
\end{aligned} \tag{D.27}$$

D.0.4 Tight-binding model for deep impurities

Taking the so-called deep limit $\epsilon_\alpha \ll \Delta$ and the dilute limit $k_Fa \gg 1$ we can derive a Tight-binding effective Hamiltonian for the states below the gap, this systems form an energy band which can have some topological superconductivity, hosting MF. So we specialise to the case of deep impurities with α close to the unity, so the energy $\epsilon_\alpha = \Delta(1-\alpha)$of single Shiba state is close to the center of the gap. We approximate the Eq. (D.26) expanding in terms of $(1-\alpha)$,E/Δ and $1/\sqrt{k_Fr}$, keeping only the terms up to linear order in all three. We note that in Eq. (D.27) all terms are linear in $1/\sqrt{k_Fr}$ so for $m \neq n$ we can set $E = 0$ and $\alpha = 1$. The linearized Eq. (D.26) reads:

$$\begin{aligned}
&\left(1-\left[\alpha\tau_x+\frac{E}{\Delta}\right]\hat{\mathbf{S}}_m\boldsymbol{\sigma}\right)\Psi(\mathbf{r}_m) =\\
&\sum_{n\neq m}\sqrt{\frac{2}{\pi k_Fr_{mn}}}\left(\cos(k_Fr_{mn}-\frac{\pi}{4})\tau_x-\sin(k_Fr_{mn}-\frac{\pi}{4})\tau_z\right)\hat{\mathbf{S}}_n\boldsymbol{\sigma}\Psi(\mathbf{r}_n),
\end{aligned} \tag{D.28}$$

where $r_{mn} = |\mathbf{r_n}-\mathbf{r_m}|$ is the distance between two impurities.Multiplying by $\hat{\mathbf{S}}_m\boldsymbol{\sigma}$ and using that $(\hat{\mathbf{S}}_m\boldsymbol{\sigma})(\hat{\mathbf{S}}_m\boldsymbol{\sigma}) = 1$ we have:

$$\begin{aligned}
&\left(\hat{\mathbf{S}}_m\boldsymbol{\sigma}-\left[\alpha\tau_x+\frac{E}{\Delta}\right]\right)\Psi(\mathbf{r}_m) =\\
&\sum_{n\neq m}\sqrt{\frac{2}{\pi k_Fr_{mn}}}\left(\cos(k_Fr_{mn}-\frac{\pi}{4})\tau_x-\sin(k_Fr_{mn}-\frac{\pi}{4})\tau_z\right)(\hat{\mathbf{S}}_m\boldsymbol{\sigma})(\hat{\mathbf{S}}_n\boldsymbol{\sigma})\Psi(\mathbf{r}_n).
\end{aligned} \tag{D.29}$$

Now we project this equation on the set of Shiba states in Eq. D.9 with N impurities, this yields an effective Hamiltonian $\tilde{\mathcal{H}}^{\text{eff}}$ $2N \times 2N$. We define:

$$|\uparrow, n\rangle = |\uparrow\rangle_{\hat{\mathbf{S}}_n} \, |\downarrow, n\rangle = |\downarrow\rangle_{\hat{\mathbf{S}}_n} \,, \tag{D.30}$$

and also we note that time-reversal symmetry $\mathcal{T} = i\sigma_y K$ relates the two states $\mathcal{T}\,|\uparrow, n\rangle = |\downarrow, n\rangle$. We can express $\mathcal{H}_{\text{eff}}$ as:

$$\tilde{\mathcal{H}}^{\text{eff}}\Phi = E\Phi, \quad \Phi^T = \Big(\psi_+, \quad \psi_-\Big)\,, \tag{D.31}$$

where $\tilde{\mathcal{H}}^{\text{eff}}$ reads:

$$\begin{aligned}
\tilde{\mathcal{H}}^{\text{eff}}_{m,m} &= \begin{pmatrix} \Delta(1-\alpha) & 0 \\ 0 & -\Delta(1-\alpha) \end{pmatrix} = \begin{pmatrix} \epsilon_\alpha & 0 \\ 0 & -\epsilon_\alpha \end{pmatrix}, \\
\tilde{\mathcal{H}}^{\text{eff}}_{m\neq n} &= \Delta\sqrt{\frac{2}{\pi k_F r_{mn}}} \begin{pmatrix} -\cos(k_F r_{mn} - \frac{\pi}{4})\,\langle\uparrow, m|\uparrow, n\rangle & -\sin(k_F r_{mn} - \frac{\pi}{4})\,\langle\uparrow, m|\downarrow, n\rangle \\ -\sin(k_F r_{mn} - \frac{\pi}{4})\,\langle\downarrow, m|\uparrow, n\rangle & \cos(k_F r_{mn} - \frac{\pi}{4})\,\langle\downarrow, m|\downarrow, n\rangle \end{pmatrix}.
\end{aligned} \tag{D.32}$$

We have to evaluate the products of spins in different sites, to do this we specialise to a 1D chain of magnetic impurities with helical field:

$$\hat{\mathbf{S}}_n = \Big(\cos(2k_H x_n)\sin(\theta), \quad \sin(2k_H x_n)\sin(\theta), \quad \cos(\theta)\Big)\,, \tag{D.33}$$

$$\begin{aligned}
\langle\uparrow, m|\uparrow, n\rangle &= \cos^2(\theta/2) + \sin^2(\theta/2)e^{-2ik_H(x_m - x_n)} \\
\langle\uparrow, m|\downarrow, n\rangle &= i\sin(\theta/2)\sin(k_H(x_m - x_n))e^{-ik_H(x_n + x_m)}
\end{aligned} \tag{D.34}$$

This Hamiltonian is not translational invariant but this can be restored by an unitary transformation $U = \exp(ik_H\sigma_z \boldsymbol{X})$, the same in 2.39 , where $\boldsymbol{X}_{mn} = \delta_{mn}x_n$:

$$\mathcal{H}_{\text{eff}} = U\tilde{\mathcal{H}}_{\text{eff}}U^\dagger. \tag{D.35}$$

For planar field $\theta = \pi/2$ we have:

$$\begin{aligned}
\langle\uparrow, m|'\uparrow, n\rangle' &= \cos(k_H(x_m - x_n)), \\
\langle\uparrow, m|'\downarrow, n\rangle' &= i\sin(k_H(x_m - x_n)),
\end{aligned} \tag{D.36}$$

$$\mathcal{H}^{\text{eff}}_{m\neq n} = \Delta\sqrt{\frac{2}{\pi k_F r_{mn}}}$$
$$\times \begin{pmatrix} -\cos(k_F r_{mn} - \frac{\pi}{4})\cos(k_H(x_m - x_n)) & -i\sin(k_F r_{mn} - \frac{\pi}{4})\sin(k_H(x_m - x_n)) \\ -i\sin(k_F r_{mn} - \frac{\pi}{4})\sin(k_H(x_m - x_n)) & \cos(k_F r_{mn} - \frac{\pi}{4})\cos(k_H(x_m - x_n)) \end{pmatrix}. \tag{D.37}$$

Appendix E

Derivation of BdG equation and projection

In this appendix first we introduce the BdG equation [42] for the particle-hole components of a BdG excitation, showing that it is possible write down a "single particle" equation for the excitation wave function, despite the many body characters of Superconducting ground states.
After that we show how is possible to derive the effective Tight-binding Hamiltonian D.32 of Shiba chain as a projection on Shiba state of a single Impurity. We can do that thanks to the "single particle" characters of the BdG equation.
We start from a mean field superconducting Hamiltonian:

$$H = \frac{1}{2}\sum_{i,j}\Big(h_{i,j}c_i^\dagger c_j - h_{i,j}c_j c_i^\dagger + \Delta_{i,j}c_i^\dagger c_j^\dagger + \Delta_{i,j}^* c_j^\dagger c_i^\dagger\Big), \tag{E.1}$$

where i, j are generic index as site, spin. We can rewrite the previous equation introducing a spinor $\boldsymbol{c} = \begin{pmatrix} c^\dagger \\ c \end{pmatrix}$ and labelling the spinorial index with α. The BdG Hamiltonian reads:

$$H = \frac{1}{2}\sum_{i,j,\alpha,\beta} \boldsymbol{c}_{i,\alpha}^\dagger \mathcal{H}_{i,j}^{\alpha,\beta} \boldsymbol{c}_{j,\beta}. \tag{E.2}$$

Because the matrix $\mathcal{H}_{i,j}^{\alpha,\beta}$ is Hermitian, we can diagonalize the Hamiltonian with the trasformation:

$$\begin{aligned} \boldsymbol{c}_{j,\beta}^{\dagger} &= \sum_{n,\alpha} \Psi_{j,\beta}^{(n)} \gamma_n^{\dagger}, \\ \sum_{j,\beta} \mathcal{H}_{i,j}^{\alpha,\beta} \Psi_{j,\beta}^{(n)} &= \epsilon_n \Psi_{i,\alpha}^{(n)}. \end{aligned} \tag{E.3}$$

After this transformation the diagonalized Hamiltonian reads[1]:

$$H = \frac{1}{2} \sum_n \epsilon_n \gamma_n^{\dagger} \gamma_n \tag{E.4}$$

This is nothing else that usual Bogoliubov transformation. What is very useful in this treatment is the condition in the Eq.E.3. Renaming $\Psi_{j,1} = u_j$ and $\Psi_{j,2} = v_j$ we obtain the BdG equation:

$$\begin{pmatrix} h_{i,j} & \Delta_{i,j} \\ \Delta_{i,j}^* & -h_{i,j} \end{pmatrix} \begin{pmatrix} u_j \\ v_j \end{pmatrix} = \epsilon \begin{pmatrix} u_i \\ v_i \end{pmatrix} \tag{E.5}$$

This is a one particle Shrodinger equation for the component of the Bogoliubov excitation. Despite the many-body characters of the Superconductivity in this way we obtained a formal one particle description for the excitation. This can be rewrite in the "Shroedinger" form: $\mathcal{H}\boldsymbol{\Psi} = \epsilon\boldsymbol{\Psi}$,with $\boldsymbol{\Psi} = \begin{pmatrix} u \\ v \end{pmatrix}$.
Because this is a single particle Hamiltonian that describe the excitation we can work on that as every one particle quadratic Hamiltonian.

E.0.1 Tight-binding Shiba chain from projection

In the following we derive the effective tight-binding Hamiltonian D.32 of Shiba chain as a projection on Shiba state of a single Impurity. Instead linearizing the equation D.28 we project the BdG Hamiltonian on the wave function of single Shiba state $\Psi_+^{(n)}, \Psi_-^{(n)}$ placed on the impurities $\mathbf{r}_n$. See Eq:D.16.
The BdG Hamiltonian is:

$$\mathcal{H}_{SC} = \left(\xi_p \tau_z - J \sum_n \mathbf{S}_l \boldsymbol{\sigma} \delta(\mathbf{r} - \mathbf{r}_l) + \Delta \tau_x \right). \tag{E.6}$$

[1] This spectrum can be unfamiliar because we are not using explicitly the PHS that relates different energy: $\gamma_n^{\dagger} = \gamma_{-n}$ and $\epsilon_n = -\epsilon_{-n}$

We want to project this Hamiltonian on the Shiba state placed on the single impurity, this state is the bound state discussed in the chapter D.0.1, projecting on this kind of state we are neglecting the state of continuum above the gap, this seems a good approximation only if our energy are very small compared to energy gap $E \ll \Delta$. Because the reference energy of the Shiba state is given by ϵ_α, we take the deep Shiba limit $\epsilon_\alpha \ll \Delta$, because we expect a band with of $\Delta/\sqrt{k_F a}$, we have to suppose $\sqrt{k_F a} \gg 1$, the dilute limit. This is the same approximation of chapter D.0.1 but they arise more naturally asking the low energy limit$\epsilon_\alpha \ll \Delta$. We define the States as:

$$\begin{aligned} |m,\pm\rangle &= \Psi_\pm(\mathbf{r}-\mathbf{r}_m), \\ |m,+\rangle_{\text{Spin}} = \begin{pmatrix} |\uparrow\rangle_{\hat{\mathbf{S}}_\mathbf{m}} \\ |\uparrow\rangle_{\hat{\mathbf{S}}_\mathbf{m}} \end{pmatrix}, &\quad |m,-\rangle_{\text{Spin}} = \begin{pmatrix} |\downarrow\rangle_{\hat{\mathbf{S}}_\mathbf{m}} \\ -|\downarrow\rangle_{\hat{\mathbf{S}}_\mathbf{m}} \end{pmatrix}. \end{aligned} \tag{E.7}$$

Defined the states for projection we rewrite the Hamiltonian as:

$$\mathcal{H}_{SC} = \mathcal{H}^{(n)}_{\text{1Impurity}} - J\sum_{l\neq m} \mathbf{S}_l \boldsymbol{\sigma}\delta(\mathbf{r}-\mathbf{r}_l). \tag{E.8}$$

Finally we project on the states $|m,\pm\rangle$:

$$\langle n,\pm|\mathcal{H}|m,\pm\rangle = \pm\epsilon_\alpha\delta_{m,n} - J\langle n,\pm|\mathbf{S}_n\boldsymbol{\sigma}\delta(\mathbf{r}-\mathbf{r}_n)|m,\pm\rangle - J\langle n,\pm|\sum_{l\neq m,n}\mathbf{S}_l\boldsymbol{\sigma}\delta(\mathbf{r}-\mathbf{r}_l)|m,\pm\rangle\,. \tag{E.9}$$

It's easy to see that $\langle n,\pm|\sum_{l\neq m,n}\mathbf{S}_l\boldsymbol{\sigma}\delta(\mathbf{r}-\mathbf{r}_l)|m,\pm\rangle \sim 1/\sqrt{k_F r_{lm} k_F r_{ln}}$, so this is a second order in $1/\sqrt{k_F r}$ and we can neglect this term in the dilute limit. Our Projected Hamiltonian reads:

$$\begin{aligned} &\langle n,\pm|\mathcal{H}|m,\pm\rangle = \\ &\pm\epsilon_\alpha\delta_{m,n} - (\pm)_n\frac{\Delta}{\sqrt{2\pi k_F r}}\langle n,\pm|_{\text{Spin}}\left(\cos(k_F r_{mn}-\frac{\pi}{4})\tau_x - \sin(k_F r_{mn}-\frac{\pi}{4})\tau_z\right)|m,\pm\rangle_{\text{Spin}}\,. \end{aligned} \tag{E.10}$$

Now we have only to calculate the scalar product obtaining:

$$\tilde{\mathcal{H}}^{\text{eff}}_{m,m} = \begin{pmatrix} \Delta(1-\alpha) & 0 \\ 0 & -\Delta(1-\alpha) \end{pmatrix} = \begin{pmatrix} \epsilon_\alpha & 0 \\ 0 & -\epsilon_\alpha \end{pmatrix}$$
$$\tilde{\mathcal{H}}^{\text{eff}}_{m\neq n} = \Delta\sqrt{\frac{2}{\pi k_F r_{mn}}} \begin{pmatrix} -\cos(k_F r_{mn} - \frac{\pi}{4}) \langle\uparrow, m| \uparrow, n\rangle & -\sin(k_F r_{mn} - \frac{\pi}{4}) \langle\uparrow, m| \downarrow, n\rangle \\ -\sin(k_F r_{mn} - \frac{\pi}{4}) \langle\downarrow, m| \uparrow, n\rangle & \cos(k_F r_{mn} - \frac{\pi}{4}) \langle\downarrow, m| \downarrow, n\rangle \end{pmatrix}. \tag{E.11}$$

This is nothing else that Effective Hamiltonian $\mathcal{H}_{\text{eff}}$Eq: (D.32). Also the overlap matrix $S_{n,m} = \langle n, \pm | m, \pm \rangle$ is not strictly diagonal but at the first order we can neglect the overlap.

This derivation has the value of shows that linearized Eq:(D.28)is equivalent to project of wave function of single Shiba state, the Shiba chain is made by hybridization of single Shiba states.

Appendix F

Effective Hamiltonian

In this appendix, we report the entire effective Hamiltonian. In this brief section, we summarize the effective Hamiltonian after the projection, in Nambu formalism the total Hamiltonian is:

$$\mathcal{H}^{\text{eff}} = \mathcal{H}_{\text{Shiba}} + \mathcal{H}_{\text{Wire}} + \mathcal{H}_{\text{Tunneling}}. \tag{F.1}$$

Neglecting the t_w^2 terms which does not affect the topological features we can rewrite $\mathcal{H}_{\text{Wire}}$ in Nambu formalism:

$$\begin{aligned} H_{\text{Wire}}^{\text{eff}} = &\sum_n A_n^\dagger \left(\epsilon_g + t_w - J'S\right)\tau_z A_n \\ &+ \sum_n [-A_n^\dagger \frac{t_w}{2}\cos(k_H a)\tau_z A_{n+1} - \left(\frac{1}{J'S} + \frac{1}{\epsilon_g}\right)\frac{\Delta' t_w \sin(k_H a)}{4} A_n^\dagger \begin{pmatrix} 0 & i \\ i & 0 \end{pmatrix} A_{n+1} + h.c.] \end{aligned} \tag{F.2}$$

Where $A_n = \begin{pmatrix} \tilde{a}_{n,\uparrow} \\ \tilde{a}_{n,\uparrow}^\dagger \end{pmatrix}$, is the spinor on the wire. $\epsilon_W = \epsilon_g - J'S$ is the mean energy of the band,which has a width t_w. Δ'-term is the p-wave superconductivity on the wire. This is exactly the Kiteav model, but the coupling terms are in relation with the realistic case of the magnetic nano-wire. We had recover the spinless model in the limit of big magnetic field $J'S \gg t_w$, which is induced by magnetic moments of the impurities. The large magnetic field is required to project

out the upper bands.

$$\begin{aligned} H^{\text{Shiba}} =& C_n^\dagger \Delta(1-\alpha)\tau_z C_n - \Delta\sqrt{\frac{2}{\pi k_F r_{mn}}} \\ & \times \sum_{m\neq n} C_m^\dagger \Bigg(\cos(k_F r_{m,n} - \frac{\pi}{4}) \cos(k_H(x_m - x_n))\tau_z \\ & + \sin(k_F r_{mn} - \frac{\pi}{4}) \sin(k_H(x_m - x_n)) \begin{pmatrix} 0 & i \\ i & 0 \end{pmatrix} \Bigg) C_n. \end{aligned} \tag{F.3}$$

Where $C_n = \begin{pmatrix} c_n & c_n^\dagger \end{pmatrix}$, creates or destroy a Shiba state on Superconductors, $c_n^\dagger = \Psi^\dagger_{\text{Shiba}}(\mathbf{r} - \mathbf{r}_m)$. This is a band made by Shiba wave function Eq:(D.16) on every sites, which forms a spinless band with long-range p-wave superconductivity. Each states has an energy on site $\epsilon_\alpha \approx \Delta(1-\alpha)$, and a long-range hopping $\sim 1/k_F r$ with the others Shiba States. We take the deep limit, e.g. the Shiba Energy lies in the gap $\alpha \sim 1$ and the dilute limit $k_F a \gg 1$. This limits are necessary to deal with a linear equation which can be interpretate as a tight-binding Hamiltonian. The original result of this chapter is the derivation of the tunnelling term between the Shiba chain and the magnetic wire:

$$\begin{aligned} H_{\text{Tunneling}} =& -t\sqrt{\frac{\Delta}{2JS}} \sum_n A_n^\dagger \tau_z C_n - t\sqrt{\frac{\Delta}{2JS\pi k_F r_{mn}}} \\ & \times \sum_{m\neq n} A_m^\dagger \Bigg(\cos(k_F r_{mn}) \cos(k_H(x_m - x_n))\tau_z \\ & + \sin(k_F r_{mn}) \sin(k_H(x_m - x_n)) \begin{pmatrix} 0 & i \\ i & 0 \end{pmatrix} \Bigg) \Bigg) C_n + h.c. \end{aligned} \tag{F.4}$$

The first term is the usual local tunnelling, the second term is a long-range tunneling due to extension of Shiba wave function.

Appendix G

Integrals for derivation of the free propagator

In this appendix we evaluate some integrals in order to calculate the free propagator $\mathcal{G}_E^0(\mathbf{r})$.

1. From Eq:(D.6) we have to calculate:

$$\begin{aligned} I_1 &= \int \frac{V d\mathbf{p}}{(2\pi)^2} \frac{1}{E^2 - \xi_{\mathbf{p}}^2 - \Delta^2}, \\ I_2 &= \int \frac{V d\mathbf{p}}{(2\pi)^2} \frac{\xi_{\mathbf{p}}}{E^2 - \xi_{\mathbf{p}}^2 - \Delta^2}. \end{aligned} \tag{G.1}$$

   Remember that we are searching sub-gap energies $E < |\Delta|$. We change variable to ϕ and ξ, and we can integrate trivially on the angle ϕ, due the denominators both integrals are peaked on $\xi_{\mathbf{p}} = 0$, so we can extend the variable $\xi \in [-\mu, \infty]$ to the interval $[-\infty, \infty]$. Under this approximation I_2 vanish for the antisymmetry of the integrands . For I_1 we have:

$$I_1 = \frac{Vm}{(2\pi)} \int_{-\infty}^{+\infty} d\xi \frac{1}{E^2 - \xi^2 - \Delta^2}. \tag{G.2}$$

   Evaluating that with Residue Theorem we have:

$$I_1 = \frac{-\pi\nu_0}{\sqrt{\Delta^2 - E^2}}, \tag{G.3}$$

   where $\nu_0 = \frac{mV}{2\pi}$ is two dimensional density of states of free electrons.

2. From Eq:(D.19) to determine the normalization we have to calculate:

$$1 = \int \frac{Vd\mathbf{k}}{(2\pi)^2}|\Psi^+(\mathbf{k})|^2 = \nu_0(JS)^2 \int d\xi \Psi_+^\dagger(\mathbf{0})\left(\frac{\epsilon_+ + \xi\tau_z + \Delta\tau_x}{\epsilon_+^2 - \Delta^2 - \xi^2}\right)^2 \Psi_+(\mathbf{0}) = \frac{\nu_0(JS)^2}{\mathcal{N}} \int d\xi \frac{(\epsilon_+ + \Delta)^2 + \xi^2}{(\epsilon_+^2 - \Delta^2 - \xi^2)^2} \tag{G.4}$$

For evaluating we use residuum theorem:

$$\int dz f(z) = 2\pi i \mathrm{Res}_{z_0}(f(z_0)), \tag{G.5}$$

If f is in the form $f(z) = h(z)/(z - z_0)^2$, expanding $h(z)$ around $z_0$we have:

$$\mathrm{Res}_{z_0}(f(z_0)) = \frac{d}{dz}h(z)|_{z=z_0}, \tag{G.6}$$

at the end we find:

$$1 = \frac{JS(1+\alpha^2)^2}{4\Delta\alpha^2\mathcal{N}}. \tag{G.7}$$

3. We have defined $\mathcal{G}_E(\mathbf{r})$ in (D.26) as:

$$\mathcal{G}_E(\mathbf{r}) = \Big(I_1(\mathbf{r})(E + \Delta\tau_x) + I_2(\mathbf{r})\tau_z\Big). \tag{G.8}$$

We have to calculate:

$$\begin{aligned} I_1(\mathbf{r}) &= \int \frac{Vd\mathbf{p}}{(2\pi)^2} \frac{e^{-i\mathbf{pr}}}{E^2 - \xi_\mathbf{p}^2 - \Delta^2}, \\ I_2(\mathbf{r}) &= \int \frac{Vd\mathbf{p}}{(2\pi)^2} \frac{e^{-i\mathbf{pr}}\xi_\mathbf{p}}{E^2 - \xi_\mathbf{p}^2 - \Delta^2}. \end{aligned} \tag{G.9}$$

We note $I_k(0) = I_k$. Another time we change variables to ϕ and ξ and we extend ξ-integral to $-\infty$:

$$\begin{aligned} I_1(\mathbf{r}) &= \frac{Vm}{(2\pi)^2} \int_0^{2\pi} d\phi \int d\xi \frac{e^{-ip(\xi)r\cos(\phi)}}{E^2 - \xi^2 - \Delta^2}, \\ I_2(\mathbf{r}) &= \frac{Vm}{(2\pi)^2} \int_0^{2\pi} d\phi \int d\xi \frac{e^{-ip(\xi)r\cos(\phi)}\xi}{E^2 - \xi^2 - \Delta^2}, \end{aligned} \tag{G.10}$$

Because the integrals are peaked on $\xi = 0$ or equivalently on $p = k_F$ we can expand $p(\xi) = k_F + \xi/v_F + \dots$, where $v_F = k_F/m$. First we perform the integral on ξ, we have to close the integral of $e^{-i\alpha z}$ on the upper part of complex plane if $\alpha < 0$ ($e^{-i\alpha z} \sim e^{\alpha|y|}$) and on the lower if $\alpha > 0$ ($e^{-i\alpha z} \sim e^{-\alpha|y|}$) so we have to split the integral in two parts $cos(\theta) < 0$ and $cos(\theta) > 0$:

$$\begin{aligned} I_1(\mathbf{r}) &= \frac{Vm}{(2\pi)^2}\int_0^{2\pi} d\phi \int d\xi \frac{e^{-i(k_F+\xi/v_F)r\cos(\phi)}}{E^2-\xi^2-\Delta^2} \\ &= \frac{Vm}{(2\pi)^2}\int_{-\pi/2}^{\pi/2} d\phi \int d\xi \frac{e^{-i(k_F+\xi/v_F)r\cos(\phi)}}{E^2-\xi^2-\Delta^2} \\ &+ \frac{Vm}{(2\pi)^2}\int_{\pi/2}^{\frac{3}{2}\pi} d\phi \int d\xi \frac{e^{-i(k_F+\xi/v_F)r\cos(\phi)}}{E^2-\xi^2-\Delta^2} \\ &= \frac{-\nu_0}{2\sqrt{\Delta^2-E^2}}\left(\int_{-\pi/2}^{\pi/2} d\phi e^{-i(k_F-1/\xi_E)r\cos(\phi)} + \int_{\pi/2}^{\frac{3}{2}\pi} d\phi e^{-i(k_F+1/\xi_E)r\cos(\phi)}\right). \end{aligned} \tag{G.11}$$

We have introduced $\xi_E = v_F/\sqrt{\Delta^2 - E^2}$, we note that $\xi_0 = v_F/\Delta$ which is the proper coherence length of superconductors. Because we are interested at deep Shiba chain $E \ll \Delta$ we can assume $\xi_E \approx \xi_0$, also in experimental situation we have $r \ll \xi_0$.In this limit we have:

$$I_1(\mathbf{r}) \approx \frac{-\nu_0}{2\sqrt{\Delta^2-E^2}}\int_0^{2\pi} d\phi e^{-ik_F r\cos(\phi)} = \frac{-\nu_0}{\sqrt{\Delta^2-E^2}}\pi J_0(k_F r). \tag{G.12}$$

Where J_0 is the 0-Bessel of First Kind, we know also an asymptotic form:

$$\begin{aligned} J_0(z) &= \frac{1}{\pi}\int_0^{\pi} d\phi e^{iz\cos(\phi)}, \\ J_0(z \gg 1) &\approx \sqrt{\frac{2}{\pi z}}\cos(z - \frac{\pi}{4}). \end{aligned} \tag{G.13}$$

We also assume $k_F r \gg 1$, then:

$$I_1(\mathbf{r}) = \frac{-\nu_0}{\sqrt{\Delta^2-E^2}}\sqrt{\frac{2\pi}{k_F r}}\cos(k_F r - \frac{\pi}{4}). \tag{G.14}$$

Now we redo the same steps for $I_2(r)$ obtaining:

$$I_2(\mathbf{r}) = \frac{i\nu_0}{2}\left(\int_{-\pi/2}^{\pi/2} d\phi e^{-i(k_F - 1/\xi_E)r\cos(\phi)} - \int_{\pi/2}^{\frac{3}{2}\pi} d\phi e^{-i(k_F+1/\xi_E)r\cos(\phi)}\right)$$
$$= \frac{i\nu_0\pi}{2}\Big(J_0((k_F - 1/\xi_E)r) - iH_0((k_F - 1/\xi_E)r) - J_0((k_F + 1/\xi_E)r) - iH_0((k_F + 1/\xi_E)r)\Big). \tag{G.15}$$

Where $H_0(r)$ is Struve function, with asymptotic form:

$$H_0(z \gg 1) \approx \sqrt{\frac{2}{\pi z}}\sin(z - \frac{\pi}{4}). \tag{G.16}$$

Than for $r \ll \xi_0$, $rk_F \gg 1$:

$$I_2(\mathbf{r}) = \nu_0\pi H_0(k_F r) \approx \sqrt{\frac{2\pi}{k_F r}}\nu_0 \sin(k_F r - \frac{\pi}{4}). \tag{G.17}$$

After the evaluating of integrals we can rewrite $\mathcal{G}_E(\mathbf{r})$ as:

$$\mathcal{G}_E(\mathbf{0}) = -\nu_0\pi\frac{E + \Delta\tau_x}{\sqrt{\Delta^2 - E^2}},$$
$$\mathcal{G}_E(\mathbf{r})_{k_F r \gg 1} = \nu_0\pi\sqrt{\frac{2}{\pi k_F r}}\left(\frac{-\cos(k_F r - \frac{\pi}{4})}{\sqrt{\Delta^2 - E^2}}(E + \Delta\tau_x) + \sin(k_F r - \frac{\pi}{4})\tau_z\right)e^{-\frac{r}{\xi_E}}. \tag{G.18}$$

A more detailed calculation(see [44]) introduces also the factor $e^{-\frac{r}{\xi_E}}$, which will ignore in the main text because we work with $\xi \gg r$.

Appendix H

Details of Bogoliubov-de Gennes Hamiltonian in k space

In this chapter we have to calculate some Fourier transform, but first of all we settle the notation about Fourier Transform. We start with an usual translational invariant Hamiltonian in second quantization:

$$H = \sum_{l,m} c_l^\dagger h(l-m) c_m, \tag{H.1}$$

where $c_l^\dagger$ creates an electron in the site l. We define the Fourier transform and antitrasfom as:

$$c_k = \frac{1}{\sqrt{N}} \sum_m e^{ikma} c_m \quad c_m = \frac{1}{\sqrt{N}} \sum_k e^{-ikma} c_k. \tag{H.2}$$

Also we remind the completeness rules:

$$\sum_k e^{ikma} = N\delta_{m,0}, \quad \sum_m e^{ikma} = N\delta_{k,0}. \tag{H.3}$$

These trasformation is unitary and preserves anti-commutation rules:

$$\{\, c_l^\dagger, c_m \,\} = \delta_{l,m}, \quad \{\, c_k^\dagger, c_q \,\} = \delta_{k,q}. \tag{H.4}$$

We can rewrite the Hamiltonian Eq:H.1 as:

$$\begin{aligned} H &= \sum_k c_k^\dagger \hat{h}(k) c_k, \\ \hat{h}(k) &= \sum_h h(h) e^{ikha}, \end{aligned} \tag{H.5}$$

where $h = l - m$. When we add a Cooper pairing term we have:

$$H_\Delta = \frac{1}{2} \sum_{l,m} \Big(c_l^\dagger \Delta(l-m) c_m^\dagger + c_m \Delta^*(l-m) c_l \Big). \tag{H.6}$$

Taking the Fourier Transform we obtain:

$$\begin{aligned} H_\Delta = \frac{1}{2} \sum_k \Big(c_k^\dagger \hat{\Delta}(k) c_{-k}^\dagger + c_{-k} \hat{\Delta}^*(k) c_k \Big), \\ \hat{\Delta}(k) = \sum_h e^{ikha} \Delta(h), \end{aligned} \tag{H.7}$$

where $h = i - j$.Now we can rewrite the Hamiltonian with Nambu spinors:

$$H = \sum_{k>0} \begin{pmatrix} c_k^\dagger & c_{-k} \end{pmatrix} \begin{pmatrix} \hat{h}(k) & \hat{\Delta}(k) \\ \hat{\Delta}^*(k) & -\hat{h}(-k) \end{pmatrix} \begin{pmatrix} c_k \\ c_{-k}^\dagger \end{pmatrix}. \tag{H.8}$$

From 4.1 we have to calculate:

1.

$$\begin{aligned} &h(k) = \epsilon_\alpha + \sum_{m \neq 0} e^{ikma} h_{m,0} = \\ &\epsilon_\alpha - \Delta \sqrt{\frac{2}{\pi k_F a}} \sum_{m>0} \frac{1}{\sqrt{m}} \cos(k_F m a - \frac{\pi}{4}) 2 \cos(k_H m a) \cos(kma) e^{-\frac{ma}{\xi}} \\ &= \epsilon_\alpha + f_1(k). \end{aligned} \tag{H.9}$$

Where we have rearranged the sum to have only positive m.

2.

$$\begin{aligned} \Delta(k) = -i\Delta \sqrt{\frac{2}{\pi k_F a}} \sum_{m \neq 0} \frac{1}{\sqrt{m}} e^{ikma} \sin(k_F |m| a - \frac{\pi}{4}) \sin(k_H m a) e^{-\frac{|m|a}{\xi}} = \\ +\Delta \sqrt{\frac{2}{\pi k_F a}} \sum_{m>0} \frac{2}{\sqrt{m}} \sin(kma) \sin(k_F m a - \frac{\pi}{4}) \sin(k_H m a) e^{-\frac{ma}{\xi}} = g_1(k). \end{aligned} \tag{H.10}$$

Now we take two type of electron on the same site c_m and a_l, if they are decoupled we have two block Hamiltonian:H^c and H^a. If we want describe the coupling between the two systems we add:

$$H_{\text{Tunneling}} = \sum_{l,m} \left(a_l^\dagger M_{l,m} c_m + c_m^\dagger M_{l,m}^* a_l \right). \tag{H.11}$$

Taking the Fourier Transform we have:

$$\begin{aligned} H_{\text{Tunneling}} &= \sum_{k} \left(a_k^\dagger M(k) c_k + c_k^\dagger M^*(k) a_k \right), \\ M(k) &= \sum_{h} M(h) e^{ikha}. \end{aligned} \tag{H.12}$$

We can also add a pairing coupling:

$$H_\Delta = \sum_{l,m} \left(a_l^\dagger N_{l,m} c_m^\dagger + c_m N_{l,m}^* a_l \right). \tag{H.13}$$

Taking the Fourier transform:

$$H_\Delta = \sum_{k} \left(a_k^\dagger N(k) c_{-k}^\dagger + c_{-k} N^*(k) a_k. \right) \tag{H.14}$$

Defining the Nambu spinor as:

$$\phi(k) = \begin{pmatrix} a_k \\ c_k \\ a_{-k}^\dagger \\ c_{-k}^\dagger \end{pmatrix}. \tag{H.15}$$

We can rewrite the Hamiltonian as:

$$H = \sum_{k>0} \phi^\dagger(k) \begin{pmatrix} h^a(k) & M(k) & \Delta^a(k) & N(k) \\ M^*(k) & h^c(k) & -N(-k) & \Delta^c(k) \\ \Delta^a(k) & -N^*(-k) & -h^a(-k) & -M^*(-k) \\ N^*(k) & \Delta^c(k) & -M(-k) & -h^c(-k) \end{pmatrix} \phi(k). \tag{H.16}$$

From Eq:(3.34) we have:

$$\begin{aligned} M(k) &= -t\sqrt{\frac{\Delta}{2JS}}\left(1+\frac{2}{\sqrt{\pi k_F a}}\sum_{m>0}\frac{1}{\sqrt{m}}\cos(k_F ma)\cos(k_H ma)\cos(kma)e^{-ma/\xi}\right) \\ &= f_2(k), \\ N(k) &= t\sqrt{\frac{2\Delta}{JS}}\frac{1}{\sqrt{\pi k_F a}}\sum_{m>0}\frac{1}{\sqrt{m}}\sin(k_F ma)\sin(k_H ma)\sin(kma)e^{-ma/\xi} \\ &= g_2(k), \end{aligned} \tag{H.17}$$

with $M(k) = M(-k)$ and $N(k) = -N(-k)$. The Hamiltonian is in the form:

$$\begin{aligned} \mathcal{H}_{\alpha,\beta}(k) &= h_{\alpha,\beta}(k)\tau_z + \Delta_{\alpha,\beta}(k)\tau_x \\ h_{\alpha,\beta}(k) &= \begin{pmatrix} h^a(k) & M(k) \\ M(k) & h^c(k) \end{pmatrix}, \\ \Delta_{\alpha,\beta}(k) &= \begin{pmatrix} \Delta^a(k) & N(k) \\ N(k) & \Delta^c(k) \end{pmatrix}. \end{aligned} \tag{H.18}$$

Performing a unitary transformation $a_k \longrightarrow e^{i\pi/4}a_k$. and $c_k \longrightarrow e^{i\pi/4}c_k$ we make the Hamiltonian in the form of Eq:(I.4).

Appendix I

Winding number

In this chapter we treat the topological invariant w, the so-called winding number, following [37] we show how to evauate w for an Hamiltonian in the BDI class 1.

A BdG Hamiltonian invariant under the PSH and time-reversal anticommutes with τ_x:

$$\{\,\mathcal{H}(k), \tau_x\,\} = 0. \tag{I.1}$$

Then the winding number is:

$$w = \int_0^\pi \frac{dk}{2\pi i} tr[\tau_x \mathcal{H}(k) \partial_k \mathcal{H}^{-1}(k)]. \tag{I.2}$$

In general if an Hamiltonian anticommutes with a matrix Σ, with $\Sigma^2 = 1$ we have:

$$w = \int_0^\pi \frac{dk}{2\pi i} tr[\Sigma \mathcal{H}(k) \partial_k \mathcal{H}^{-1}(k)]. \tag{I.3}$$

Now we take an Hamiltonian invarian under PHS and TRS:

$$\mathcal{H}_{\alpha,\beta}(k) = h_{\alpha,\beta}(k)\tau_z + \Delta_{\alpha,\beta}(k)\tau_y, \tag{I.4}$$

where tau acts on particle-hole space, and α, β are referred on the other quantum numbers. Now we perform a unitary transformation $U = e^{-i\tau_y \pi/4}$, the new Hamiltonian reads:

$$\mathcal{H}'_{\alpha,\beta}(k) = h_{\alpha,\beta}(k)\tau_x + \Delta_{\alpha,\beta}(k)\tau_y = \begin{pmatrix} 0 & A(k) \\ A^\dagger(k) & 0 \end{pmatrix}. \tag{I.5}$$

For this Hamiltonian $\Sigma = \tau_z$, in fact $\{ \mathcal{H}', \tau_z \}$ so the winding number is:

$$\begin{aligned} w &= \int_0^\pi \frac{dk}{2\pi i} tr[\tau_z \mathcal{H}(k) \partial_k \mathcal{H}^{-1}(k)] \\ &= \int_0^\pi \frac{dk}{\pi} \Im(tr[A(k)\partial_k A^{-1}(k)]). \end{aligned} \tag{I.6}$$

Defining $z(k) = \frac{1}{\det A(k)}$ we have:

$$w = \int_0^\pi \frac{dk}{\pi} \Im(\partial_k \log(z(k))) = \int_0^\pi \frac{dk}{\pi} \partial_k \arg(z(k)) = \frac{1}{i\pi} \int_{k=0}^{k=\pi} \frac{dz(k)}{z(k)}. \tag{I.7}$$

Where $\theta(k) = \arg(z(k)) = \arg(\det[A^\dagger(k)])$.By this formula is very easy to understand that two independent system 1 and 2 have a winding number which is the sum of two single winding number of the independent systems:

$$\begin{aligned} &\det A(k) = e^{-i\theta_1} e^{-i\theta_2}, \\ &w = \frac{[\theta(k)]_0^\pi}{\pi} = \frac{[\theta_1(k) + \theta_2(k)]_0^\pi}{\pi} = w_1 + w_2. \end{aligned} \tag{I.8}$$

Bibliography

[1] M. Z. Hasan and C. L. Kane,
Colloquium: Topological insulators,
Rev. Mod. Phys. 82, 3045 (2010).

[2] D. J. Thouless, M. Kohmoto, M. P. Nightingale and M. den Nijs,
Quantized Hall conductance in a two-dimensional periodic potential,
Phys. Rev. Lett. 49, 405 (1982).

[3] M.B. Hastings,
JSTAT, P08024 (2007)

[4] X. Chen, Z.-C. Gu and X.-G. Wen,
Classification of gapped symmetric phases in one-dimensional spin systems,
Phys. Rev. B 83, 035107 (2011).

[5] A. P. Schnyder, S. Ryu, A. Furusaki and A. W. W. Ludwig,
Classification of topological insulators and superconductors in three spatial dimensions,
Phys. Rev. B 78, 195125 (2008).

[6] M. R. Zirnbauer,
Riemannian symmetric superspaces and their origin in random-matrix theory,
J. Math. Phys. 37, 4986 (1996).

[7] A. Altland and M. R. Zirnbauer,
Nonstandard symmetry classes in mesoscopic normal-superconducting hybrid structures,
Phys. Rev. B 55, 1142 (1997).

[8] Ettore Majorana,
A symmetric theory of electrons and positrons, Nuovo Cimento 5, 171,184 (1937).

[9] A. Y. Kitaev,
Unpaired Majorana fermions in quantum wires,
Physics Uspekhi 44, 131 (2001) arXiv:cond- mat/0010440

[10] Jason Alicea,
New directions in the pursuit of Majorana fermions in solid state systems,
Reports on Progress in Physics, Volume 75, Number 7 (2012).

[11] M. H. Freedman, A. Kitaev, M. J. Larsen, and Z. Wang
Topological quantum computation,
MathSciNet review: 1943131 (2003).

[12] V. Mourik, K. Zuo, S. M. Frolov, S. R. Plissard, E. P. A. M. Bakkers, L. P. Kouwenhoven,
Signatures of Majorana Fermions in Hybrid Superconductor-Semiconductor Nanowire Devices,
Science 336, 1003,1007 (2012).

[13] E. J. H. Lee, X. Jiang, R. Aguado, G. Katsaros, C. M. Lieber, and S. De Franceschi,
Zero-bias anomaly in a nanowire quantum dot coupled to superconductors,
Phys. Rev. Lett. 109, 186802 (2012).

[14] H. O. H. Churchill, V. Fatemi, K. Grove-Rasmussen, M. T. Deng, P. Caroff, H.Q. Xu, C. M. Marcus,
Superconductor-nanowire devices from tunneling to the multichannel regime: Zero-bias oscillations and magnetoconductance crossover,
Phys. Rev. B 87, 241401 (2013).

[15] D. I. Pikulin, J. P. Dahlhaus, M. Wimmer, H. Schomerus and C. W. J. Beenakker,
A zero-voltage conductance peak from weak antilocalization in a Majorana nanowire,
New J. Phys. 14, 125011 (2012).

[16] J. Liu, A. C. Potter, K. T. Law, and P. A. Lee,
Zero-bias peaks in the tunneling conductance of spin-orbit coupled superconducting wires with and without Majorana end-states,
Phys. Rev. Lett. 109, 267002 (2012).

[17] S. Nadj-Perge, I. K. Drozdov, J. Li, H. Chen, S. Jeon, J. Seo, A. H. MacDonald, B. A. Bernevig and A. Yazdani,
Observation of Majorana fermions in ferromagnetic atomic chains on a superconducto,
Science 346, 602 (2014).

[18] C.H. Lin, J. D. Sau, and S. Das Sarma,
Zero-bias conductance peak in Majorana wires made of semiconductor/superconductor hybrid structures,
Phys. Rev. B 86, 224511 (2012).

[19] G. Kells, D. Meidan, and P. W. Brouwer.
Near-zero-energy end states in topologically trivial spin-orbit coupled superconducting nanowires with a smooth confinement,
Phys. Rev. B 86, 100503 (2012).

[20] Remy Pawlak, Marcin Kisiel, Jelena Klinovaja, Tobias Meier, Shigeki Kawai, Thilo Glatzel, Daniel Loss, Ernst Meyer,
Probing atomic structure and majorana wavefunctions in mono-atomic Fe-chains on superconducting Pb-surface,
arXiv:1505.06078 (2015).

[21] Martin Leijnse and Karsten Flensberg,
Introduction to topological superconductivity and Majorana fermions,
Semicond. Sci. Technol. 27, 124003 (2012) arXiv:1206.1736.

[22] Jan Carl Budich and Eddy Ardonne,
Equivalent topological invariants for one-dimensional Majorana wires in symmetry class,
PhysRevB.88.075419 (2013).

[23] Steven R. Elliott and Marcel Franz,
Colloquium: Majorana fermions in nuclear, particle and solid-state Physics,
Rev. Mod. Phys. 87, 137 (2015) .

[24] Shiba, Hiroyuki,
Classical spins in superconductors,
1968, Progress of Theoretical Physics 40(3), 435 (1968).

[25] Jason Alicea,
New directions in the pursuit of Majorana fermions in solid state systems,
Rep. Prog. Phys. 75, 076501 (2012).

[26] Falko Pientka, Leonid I. Glazman, and Felix von Oppen,
Topological superconducting phase in helical Shiba chains ,
PhysRevB.88.155420 (2013).

[27] Y. J. Doh, J. A. van Dam, A. L. Roest, E. P. A. M. Bakkers, L. P. Kouwenhoven, and S. De Franceschi,
Tunable supercurrent through semiconductor nanowires,
Science, 309:272 (2015).

[28] J. A. van Dam, Yu. V. Nazarov, E. P. A. M. Bakkers, S. De Franceschi, and L. P. Kouwenhoven,
Supercurrent reversal in quantum dots,
Nature, 442:667,(2006).

[29] Doru C. Sticlet,
Edge States in Chern Insulators and Majorana Fermions in topological superconductors,
PhD Thesis (2012), Université Paris-Sud XI, Supervisor: Prof.Pascal Simon.

[30] Alex Weststrom,
Topological properties of helical Shiba chains,
Master Thesis (2015), University of Helsinki, Supervisor: Dr. Teemu Ojanen.

[31] Kim Poyonen,
Majorana states in ferromagnetic Shiba chains,
Master Thesis (2015), University of Helsinki, Supervisor: Dr. Teemu Ojanen.

[32] Gerbold C. Ménard, Sébastien Guissart, Christophe Brun, Stéphane Pons, Vasily S. Stolyarov, Francois Debontridder, Matthieu V. Leclerc, Etienne Janod, Laurent Cario, Dimitri Roditchev, Pascal Simon and Tristan Cren,
Coherent long-range magnetic bound states in a superconductor,
Nature Physics 11, 1013−1016 (2015).

[33] D. Chevallier, P. Simon, and C. Bena,
From Andreev bound states to Majorana fermions in topological wires on superconducting substrates: a story of mutation,
Phys. Rev. B 88, 165401 (2013).

[34] Bernd Braunecker, George I. Japaridze, Jelena Klinovaja, Daniel Loss,
Spin-selective Peierls transition in interacting one-dimensional conductors with spin-orbit interaction,
Phys.Rev.B.82,045127 (2010).

[35] M.A. Ruderman and C. Kittel,
Indirect exchange coupling of nuclear magnetic moments by conduction electrons,
Phys. Rev. 96, 99 (1954).

[36] Jelena Klinovaja, Peter Stano, Ali Yazdani, and Daniel Loss,
Topological superconductivity and Majorana fermions in RKKY systems,
Phys. Rev. Lett. 111, 186805 (2013).

[37] Sumanta Tewari and Jay D. Sau,
Topological invariants for spin-orbit coupled superconductor nanowires,
Phys. Rev. Lett. 109, 150408 (2012).

[38] Wei Chen and Andreas P. Schnyder,
Majorana edge states in superconductor/noncollinear magnet interfaces,
Phys. Rev. B 92, 214502 (2015).

[39] T.P. Choy, J. M. Edge, A. R. Akhmerov, and C. W. J. Beenakker,
Majorana fermions emerging from magnetic nanoparticles on a superconductor without spin-orbit coupling,
Phys. Rev. B 84, 195442 (2011).

[40] J. Bardeen, L. N. Cooper, and J. R. Schrieffer,
Theory of superconductivity,
Phys. Rev. 108, 1175 (1957).

[41] L. N. Cooper,
Bound electron pairs in a degenerate Fermi gas,
Phys. Rev. 104, 1189 (1956).

[42] P. G. de Gennes,
Superconductivity of metals and alloys,
West- view Press, Boulder (1999).

[43] Giuseppe Grosso, Giuseppe Parravicini,
Solid State Physics
Accademic Press, 1 edition (March 20, 2000).

[44] P. M. R. Brydon, S. Das Sarma, Hoi-Yin Hui, and Jay D. Sau,
Topological Yu-Shiba-Rusinov chain from spin-orbit coupling,
Phys.Rev.W B 91, 064505 (2015).

[45] N. Sedlmayr, and C. Bena,
Visualizing Majorana bound states in 1D and 2D using the generalized Majorana polarization,
Phys. Rev. B 92, 115115 (2015).

[46] Motohiko Ezawa, Yukio Tanaka and Naoto Nagaosa,
Topological phase transition without gap closing,
Arxiv:1307.7347 (2014).